# Generation and evaluation of universal influenza vaccine candidates

Dissertation

Zur Erlangung des Grades

Doktor der Naturwissenschaften

Am Fachbereich Biologie

Der Johannes Gutenberg-Universität Mainz

vorgelegt von

Lisa Walz

geboren am 04.10.1988 in Alsfeld

Mainz, Juli 2018

Dekan:

1. Berichterstatter:

2. Berichterstatter:

Tag der mündlichen Prüfung:

*You know the sound of two hands clapping;*
*tell me, what is the sound of one hand?*
— Hakuin Ekaku —

# CONTENTS

# ZUSAMMENFASSUNG

Trotz Grippeimpfung sterben jährlich 250.000 bis 500.000 Menschen weltweit an den Folgen saisonaler Influenzaepidemien. Der saisonale Influenza-Impfstoff richtet sich hauptsächlich gegen die immundominante, aber auch hochvariable Kopfregion des Oberflächenproteins Hämagglutinin (HA), was den Impfstoff stark stamm-spezifisch macht und bei Auftreten einer Driftvariante eine Anpassung des jeweiligen Impfstamms erfordert. Ein „universeller“ Influenza-Impfstoff würde eine langfristige Grundimmunität gegen alle saisonalen und pandemischen Stämme induzieren und dadurch eine jährliche Anpassung und Auffrischung ersetzen. In dieser Arbeit wurden zwei komplementäre Ansätze zur Entwicklung eines solchen Impfstoffes untersucht, einer basierend auf dem höher konservierten Oberflächenprotein Neuraminidase (NA) und ein weiterer, gerichtet gegen die ebenfalls konservierte Stammregion des HA.

Vesikuläre Stomatitis-Viren (VSV) wurden verwendet, um eine Reihe an NA Proteinen prototypischer saisonaler und pandemischer H1N1 Stämme, sowie humaner H5N1 und H7N9 Isolate zu exprimieren. Immunisierung von Mäusen und Frettchen führte zu humoralen und zellulären Immunantworten und vermittelte einen Schutz vor Infektion mit dem homologen Virus, der vergleichbar mit der durch das HA Protein desselben Stammes induzierten Immunität war. Der Schutz gegen heterologe Infektion innerhalb der N1 Proteine korrelierte mit dem Level an kreuzreaktiven, die NA hemmenden Antikörpern. Die Bedeutung dieser funktionellen Antikörper im Zusammenhang mit der Kreuzprotektivität konnte durch einen passiven Serumtransfer in Mäusen bestätigt werden. Des Weiteren wurden Mäuse mit inaktivierten Influenza-Impftstoffen (IIV) und Adeno-assoziierten Virus (AAV)-basierten Vektoren immunisiert, welche entweder ein Wildtyp HA Protein oder chimäre HA Proteine mit identischer Stammregion, aber irrelevanten divergenten Kopf-Domänen, exprimierten. Durch die von AAV-basierten Impfstoffkandidaten induzierten Antikörperantworten konnten die Mäuse vor heterologer Infektion geschützt werden. In dieser Arbeit wurden darauf aufbauend Frettchen mit den entsprechenden AAV Impfstoffkandidaten immunisiert und wir konnten bestätigen, dass alle Kandidaten eine Antikörperantwort, jedoch keine nachweisbare zelluläre Immunantwort, induzierten. Entsprechend des vorherigen Experiments korrelierten auch hier die nachgewiesenen Antikörperantworten mit dem Schutz gegen eine Influenza-Infektion, so dass AAV-HA als vielversprechende Influenza Impfstoffplattform angesehen werden kann. Diese Ergebnisse zeigen, dass beide getesteten Antigene eine breite und multifunktionale Antikörperantwort induzieren, welche mit dem Schutz vor einer Infektion korreliert und damit eine vielversprechende Basis für die Entwicklung eines breit schützenden Influenza-Impfstoffs darstellen.

# ABSTRACT

Despite the availability of vaccines, annual influenza epidemics cause 250,000 to 500,000 deaths worldwide. Currently licensed influenza vaccines are mainly directed against the immunodominant but variable hemagglutinin (HA) head domain, which makes them highly strain-specific and requires updating of the vaccine as soon as antigenic drift variants emerge. A “universal” influenza virus vaccine that induces long-term protection against all strains would abolish the need for annual re-vaccination and would significantly enhance our pandemic preparedness. In this thesis, two complementary approaches based on the more conserved neuraminidase (NA) and HA stalk domain were chosen as target towards such a broadly protective vaccine.

Vesicular stomatitis virus (VSV)-based replicons expressing a panel of N1 proteins from prototypic seasonal and pandemic H1N1 strains and human H5N1 and H7N9 isolates were generated. Immunization of mice and ferrets with the replicon carrying the matched N1 protein resulted in robust humoral and cellular immune responses and protected against challenge with the homologous influenza virus with similar efficacy as the matched HA protein, illustrating the potential of the NA protein as vaccine antigen. The extent of protection after immunization with mismatched N1 proteins correlated with the level of cross-reactive neuraminidase-inhibiting antibody titers. Passive serum transfer experiments in mice confirmed that these functional antibodies determine subtype-specific cross-protection. Vaccination of mice with adeno-associated virus (AAV)-based vectors expressing the wild type HA protein or chimeric HA proteins, which contain identical stalk but irrelevant divergent head domains, induced broadly reactive antibodies against a variety of influenza A subtypes and protected mice against heterologous challenge. Here, we immunized ferrets with the respective vaccine candidates and confirmed that vaccination with AAV-HA resulted in high antibody responses against matched virus, whereas no cellular immune response was detectable in any of the vaccinated groups. Antibody titers correlated with protection from challenge infection, illustrating the potential of AAV vectors as influenza vaccine platform. Taken together, the work presented here demonstrates that both influenza virus surface glycoproteins can induce a broadly specific and multifunctional antibody response, which correlates with protection and thus constitute a promising basis for the development of a broadly protective influenza vaccine.

# 1. INTRODUCTION

## 1.1. Influenza Biology

Influenza, commonly known as "the flu", is a viral infection caused by the influenza virus. Humans are regularly infected by three types of influenza, A, B and C. Influenza C causes clinical signs of a common cold, while influenza A and B lead to a more severe respiratory disease, including symptoms such as fever, headache, cough, sore throat, nasal congestion, sneezing, and body aches (Palese and Shaw, 2007). Influenza viruses are among the most common and significant causes of human respiratory infections, causing high morbidity and mortality, and influenza A viruses (IAV) have the additional potential to cause pandemics, as they occurred in 1918, 1957, 1968 and most recently in 2009 with the swine-origin pandemic H1N1 (pdmH1N1) influenza virus. Both seasonal and pandemic influenza are a major problem for human health. In 2017/18, there were four predominant seasonal strains circulating globally, two of each of influenza A and B. These strains are classified based on similarity to prototype strains previously identified by the World Health Organization (WHO).

IAV strains are classified according to the antigenic reactivity of their hemagglutinin (HA/H) and neuraminidase (NA/N) surface glycoproteins as HxNy; where x and y are numbers in various combinations up to 18 and 11, respectively. The currently circulating seasonal IAV strains belong to the H3N2 and H1N1 subtypes, whereby the H1N1 strains represent derivates of pandemic 2009 strain pdmH1N1. IAV strains are named according to their type, the species from which the strain was isolated, if not human, location of isolation, isolate number, the year of isolation, and their HA and NA subtypes. For example, the 4$^{th}$ isolate of an H1N1 subtype virus isolated from humans in 2009 in California is designated: influenza A/California/04/2009 (H1N1) virus. Although influenza B viruses contain the same proteins as IAV, there are no equivalent surface protein designations for influenza B. The current circulating strains of influenza B originate from either the Yamagata or Victoria lineages (Wright, Neumann and Kawaoka, 2007).

Seasonal influenza spreads effectively between humans, with rapid transmission in crowded areas such as schools and nursing homes. Wild aquatic bird populations are the natural IAV reservoir from which virus is transmitted to other avian and mammalian hosts, such as humans, horses, swine and other mammals. While most evidence still supports this hypothesis, recent detection of influenza sequences in bats suggest that other reservoir species may also exist (Tong *et al.*, 2012, 2013; Wu *et al.*, 2014; Freidl *et al.*, 2015). Sixteen HA and nine NA subtypes have so far been isolated from aquatic birds (Webster *et al.*, 1992; Fouchier *et al.*, 2005), and two HA and two NA have been

detected in bats (Tong *et al.*, 2012, 2013). The influenza viruses of domestic poultry and mammals including humans, have all evolved directly or indirectly from influenza viruses found in the aquatic bird reservoirs. Thus, there is a reasonable probability for an antigenically shifted virus from an animal reservoir causing the next pandemic, which due to the unpredictability of its HA and NA composition represents a formidable challenge for current influenza vaccines. Recent sporadic but recurrent human cases of H5N1 and H7N9 IAV infections in South-East Asia illustrate this risk (Bridges *et al.*, 2000; Ungchusak *et al.*, 2005; Li *et al.*, 2014).

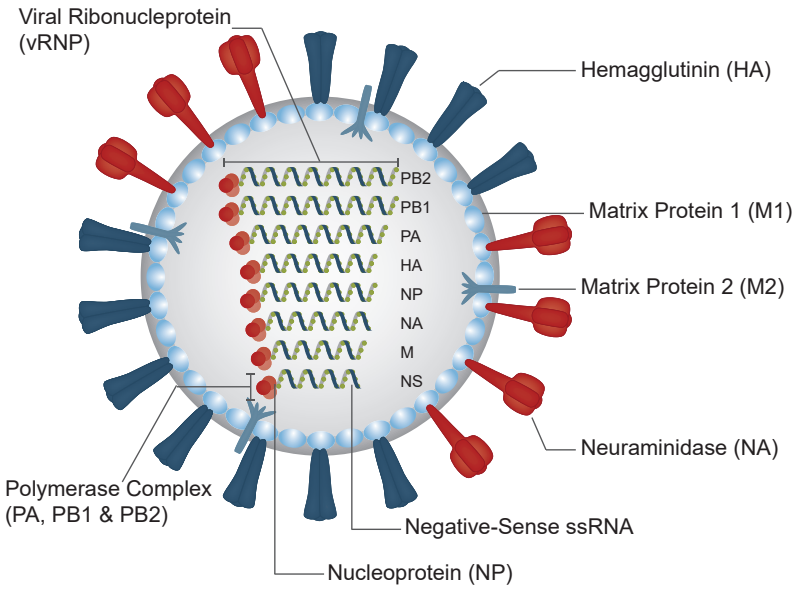


**Fig. 1 | Schematic structure of the influenza A virus particle.** The viral envelope is derived from the host cell membrane. Three envelope proteins hemagglutinin (HA) (blue), neuraminidase (NA) (red) and the ion channel protein (matrix protein 2, M2) are embedded in the lipid bilayer. The Matrix protein 1 (M1) lines the viral envelope from the inside and associates with the ribonucleoprotein (RNP) complex. Inside the virion are eight single-stranded RNA molecules of negative sense that are encapsidated by the nucleoprotein (NP) and associated with three RNA polymerase proteins polymerase basic protein 1 and 2 (PB1/2) and polymerase acidic protein (PA) to form the vRNP complex. Adapted from (Subbarao and Joseph, 2007).

## 1.2. Influenza Structure and Particle Composition

IAVs are spherical particles with a diameter of approximately 100 nm that are enveloped by a host cell-derived lipid membrane. Integrated in this envelope are the NA, HA and matrix protein 2 (M2) surface glycoproteins. The matrix 1 (M1) protein is located on the inside of the lipid membrane. It also forms a matrix holding the viral ribonucleoproteins (vRNPs) (Fig. 1) (Subbarao and Joseph, 2007). The genome of influenza viruses consists of 8 negative-sense RNA segments that encode for 11 proteins, with one or two proteins encoded on each segment. The RNA is encapsidated by the nucleoprotein (NP), and together with the polymerase basic 1 (PB1), polymerase basic 2 (PB2), and polymerase acid (PA) proteins forms the vRNP complex, which represents the minimal replicative unit. In addition, IAV also expresses the non-structural proteins NS1 and NS2, also

known as the nuclear export protein (NEP), in infected cells (Palese and Shaw, 2007; Wright, Neumann and Kawaoka, 2007).

Electron microscopic images of IAVs reveal spikes at the surface of the spherical virion, identified as the glycoproteins HA and NA at a length of 10 to 14 nm (Fujiyoshi *et al.*, 1994). The HA:NA ratio is strain-specific. However, HA is the most abundant surface protein at about 80 %, whereas NA only accounts for approximately 17 % (Palese and Shaw, 2007). HA forms homotrimers and mediates binding of the virion to host cell receptors and subsequent pH-dependent fusion of the viral envelope and endosomal membranes. Following virus replication, the receptor-destroying enzyme, NA, removes terminal sialic acids (SAs) of glycoproteins to facilitate release of the virion and infection of new cells (Liu *et al.*, 1995).

### 1.2.1. Hemagglutinin (HA)

The HA glycoprotein is a type I integral membrane protein. The trimer consists of a large membrane-distal, globular domain formed only by HA1 and an elongated membrane-proximal stem domain comprised of HA2 and the N- and C-terminal segments of HA1 (Fig. 2A). HA1 mediates virus binding to cell surface SA receptors to initiate viral entry through endocytosis. Virions are then taken up into endosomes, and upon acidification, HAs are activated to fuse the viral and endosomal membranes. Towards this, the fusion peptide at the HA2 N terminus is released from an interior pocket within the HA trimer.

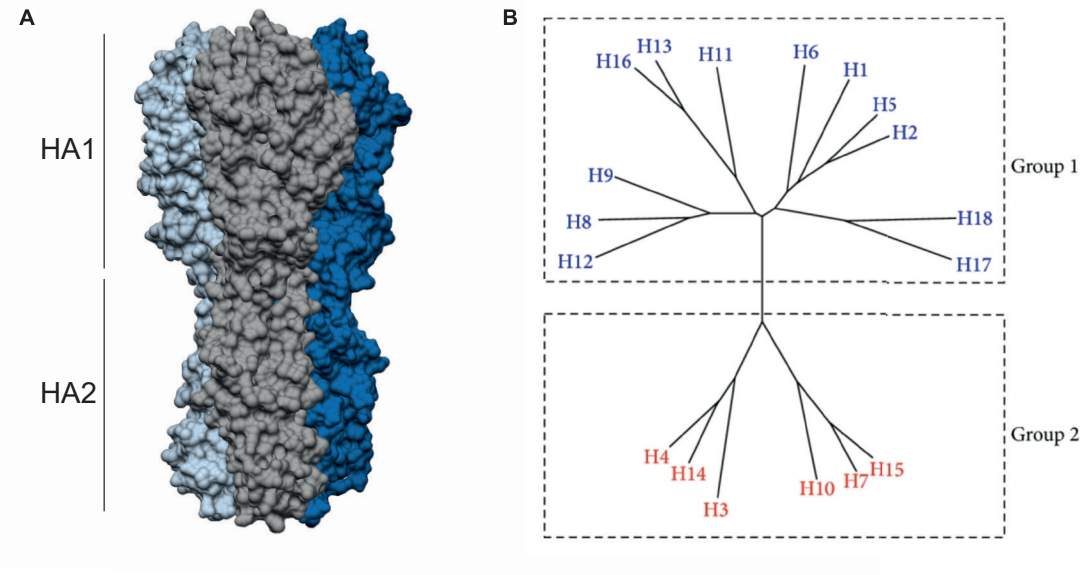


**Fig. 2 | Influenza virus hemagglutinin structure and phylogeny. A** | Side view of the HA trimer (PDB number: 3UBE) with each monomer depicted in dark blue, light blue and grey. Each monomer is composed of the globular head domain (HA1) and the stalk domain (HA2). **B** | Phylogenetic tree of known influenza virus HAs. Influenza HAs cluster into group 1 (H1, H2, H5, H6, H8, H9, H11, H13, H16, H17 and H18) and group 2 HAs (H3, H4, H7, H10, H14, and H15). Representative HA protein sequences were selected for each subtype from viruses belonging to following subtypes (H1N1, H2N2, H3N2, H4N6, H5N1, H6N2, H7N3, H8N4, H9N2, H10N7, H11N6, H12N5, H13N6, H14N5, H15N9, H16N3, H17N10, and H18N11). The phylogenetic tree was made with Geneious version 7.0. Adapted from (Hashem, 2015).

The subsequent insertion of the fusion peptide into the endosomal membrane initiates fusion of viral and endosomal membranes and uncoating (Skehel and Wiley, 2000; Lazniewski *et al.*, 2017). Phylogenetic and serological analyses reveal two groups of HA proteins: group 1 (H1, H2, H5, H6, H8, H9, H11, H13, H16, H17 and H18), and group 2 (H3, H4, H7, H10, H14, and H15) (Fig. 2B) (Russell *et al.*, 2004; Hashem, 2015). This indicates a certain sequence similarity between the H1 and H5 IAVs independent of their serological characteristics.

Whereas human seasonal influenza viruses bind to receptors containing α(2,6)-linked SA, avian influenza viruses predominantly bind to receptors containing α(2,3)-linked SA (Rogers *et al.*, 1983; Matrosovich *et al.*, 1997). Highly pathogenic avian influenza (HPAI) viruses cause a systemic disease that rapidly leads to death. Low pathogenic avian influenza (LPAI) viruses cause a localized infection with little or no disease unless exacerbated by other pathogens (Swayne and Suarez, 2000). The main difference between HPAI and LPAI lies in the cleavage site of the HA0 protein. As a result of an insertion or substitution of amino acids in the cleavage site, the HA0 precursor of HPAI is cleavable by ubiquitous host proteases (Bosch *et al.*, 1981), whereas LPAI viruses are limited to cleavage by host proteases such as trypsin-like enzymes and are thus restricted to tissues where such enzymes are found, such as the respiratory and intestinal tract (Swayne, 2007; Remacle *et al.*, 2008). As a result, HPAI viruses are able to replicate systemically, damaging vital organs and tissues, which results in severe disease and death.

### 1.2.2. Neuraminidase (NA)

The second major surface glycoprotein NA is a type II integral membrane protein composed of four identical mushroom-shaped tetramers at the surface of the virion and infected cells. Each subunit contains a *N*-terminal cytoplasmic domain, a hydrophobic transmembrane region, a thin hypervariable stalk, and a globular head domain that includes the enzymatic active site acting as a receptor-destroying enzyme, which assists in binding and release of the virion (Fig. 3A) (Air, 2012; Krammer *et al.*, 2018). Although the enzymatic active site of each individual NA monomer appears to be independently localized in the crystal structure, isolated monomeric forms of the protein lack enzymatic activity (Bucher and Kilbourne, 1972; Paterson and Lamb, 1990; Wohlbold and Krammer, 2014). Whereas the NA stalk region can readily accommodate mutations, the enzymatic active site is extremely conserved among the majority of subtypes (Sylte D. L., 2009). NA enzymatically cleaves α(2,6)- and α(2,3)-linked SAs and is thereby thought to aid in the detachment of nascent viral particles by cleaving SA residues from HA molecules on the surface of host cells (Marcelin, Sandbulte and Webby, 2012). In the absence of NA activity, influenza viruses can infect host cells and carry out a complete

replication cycle, but progeny viruses remain aggregated on the host cell surface and consequently fail to infect naïve cells (Palese et al., 1974)]. The enzymatic activity of NA is also thought to facilitate influenza virus infection by penetrating respiratory tract mucins and removing decoy receptors from epithelial cells (Matrosovich *et al.*, 2004b). This phenomenon, however, remains unconfirmed *in vivo* (Cohen et al., 2013).

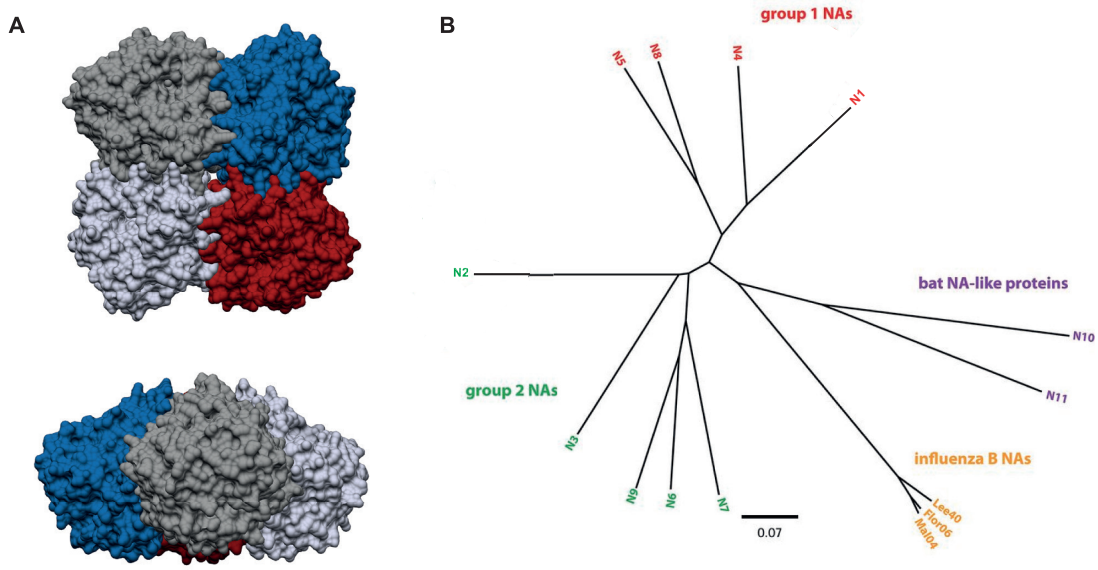


**Fig. 3 | Influenza virus neuraminidase structure and phylogeny. A** | Top and side view of the NA tetramer of an H5N1 virus (PDB number: 2HTY), with each monomer depicted in dark blue, light blue, red or grey, respectively. The structure of the variable stalk domain is not characterized. **B** | Phylogenetic tree of known influenza virus NAs and NA-like proteins (N10 and N11). Influenza NAs cluster into group 1 (N1, N4, N5, N8) and group 2 NAs (N2, N3, N6, N7, N9). Influenza B NAs as well as the NA-like proteins (from sequences found in bats) form their own clusters. The tree was generated using Clustal Omega and was visualized in FigTree. Adapted from (Krammer *et al.*, 2018).

NA proteins from IAV also form two phylogenic groups: group 1 contains N1, N4, N5, N8 and group 2 N2, N3, N6, N7, and N9 (Fig. 3B), illustrating that NA subtypes found in humans are not necessarily genetically more similar than NA subtypes found in other species. The novel NA subtypes recently isolated in bats (N10 and N11) seem to be much more distantly related to existing subtypes, forming a separate influenza-like group 3 and displaying no apparent sialidase activity (Tong *et al.*, 2013; Krammer *et al.*, 2018).

## 1.3. Influenza Virus Life Cycle

The IAV life cycle is divided into several different stages (Fig. 4). NA aids in the penetration of mucins on the surface of respiratory epithelial cells by removing decoy receptors and SAs of the host cell, which allows the virus to reach the cell surface. IAV then binds via its HA to SAs at the terminal ends of complex carbohydrates, found at the host cell surface (Skehel and Wiley, 2000; Matrosovich *et al.*, 2004a; Shi *et al.*, 2014).

Upon binding to SA residues, receptor-mediated endocytosis occurs, and the low pH in the endosome induces conformational changes in the HA that lead to exposure

of the fusion peptide (Wiley, 1987; Skehel and Wiley, 2000). After fusion of the viral and endosomal membranes, the M2 ion channel opens up, leading to acidification of the viral core and release of the vRNPs into the cytoplasm. Subsequently, the vRNP complexes are transported into the nucleus, where viral transcription and replication takes place (Palese and Shaw, 2007).

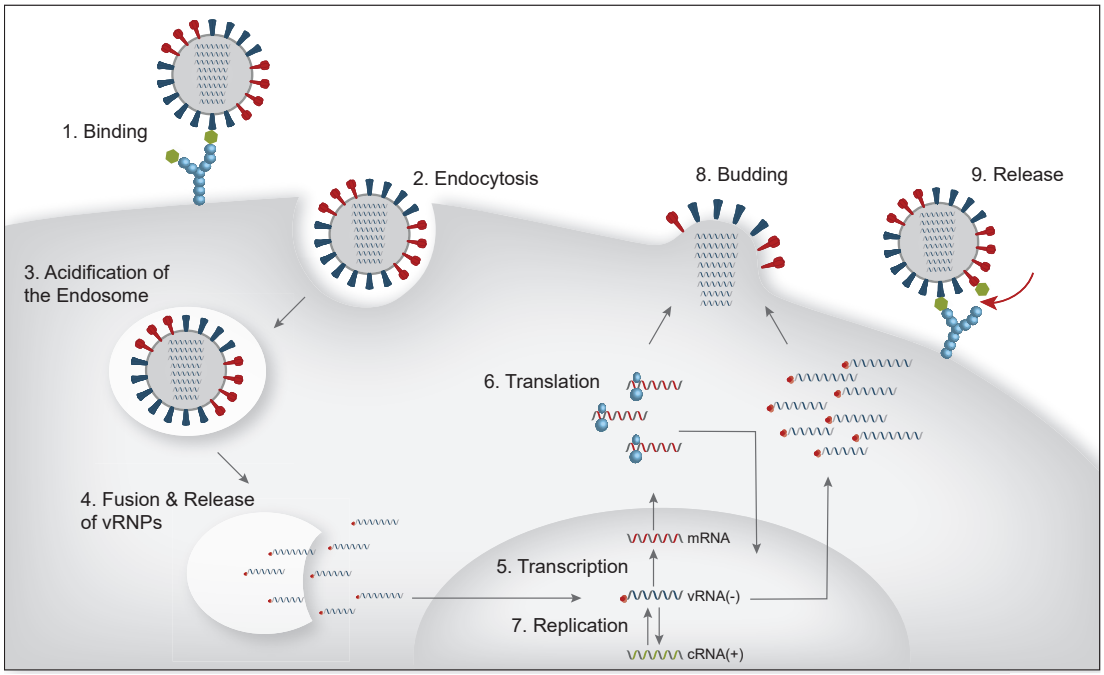


**Fig. 4 | Influenza A virus replication cycle.** Virus infection is inititated by binding of its surface glycoprotein hemagglutinin to sialic acid residues on the host cell. The virus particle is then endocytosed and upon acidification of the endosome, fusion of viral and endosomal membranes occurs, which enables the release of viral ribonucleoproteins (vRNPs) into the cytoplasm.The viral genome is subsequently translocated to the nucleus, where it is transcribed and replicated. Viral protein synthesis and particle assembly in the host cell prepares the virion progeny for the budding process to exit the host cell. The neuraminidase cleaves the terminal sialic acid residues from both the newly synthesized virion glycoprotein as well as from the host cell surface. Modified from (Shi *et al.*, 2014).

Initially, the viral polymerase transcribes viral mRNAs, which are then exported from the nucleus to the cytoplasm and translated. The surface proteins HA, NA, and M2 are being transported to the cellular membrane, whereas the remaining proteins are being imported into the nucleus, where they trigger the switch from transcription to replication. In order for the genome to be transcribed, it first has to be converted in a positive sense antigenomic cRNA to serve as a template for the replication of genomic RNA. The resulting genomic RNA is encapsidated by NP and assembles together with the proteins that form the polymerase complex to vRNPs. The vRNPs associate with M1 proteins, and are exported from the nucleus, which is mediated by the NS2 protein (Krug *et al.*, 1989). Egress of new virions occurs at the cell surface, where they remain initially bound to SAs. NA acts as a receptor-destroying enzyme by cleaving these SAs thereby releasing the newly formed virions to infect naïve cells (Palese and Shaw, 2007).

## 1.4. Antigenic Shift and Drift

The epidemiology of IAV is shaped by the ability to undergo antigenic change, which occurs in two ways: antigenic drift and antigenic shift (Fig. 5) (Sandbulte *et al.*, 2015).

Antigenic drift is a process of gradual and relatively continuous change in the viral HA and NA proteins. The IAV RNA-dependent RNA-polymerase has no proof-reading mechanism and is therefore extremely error-prone. This results in the accumulation of point mutations in the HA and NA genes (Hilleman, Mason and Buescher, 1950; Both *et al.*, 1983). The antigenic changes resulting from antigenic drift account for the annual cycle of flu epidemics and necessity of updating the influenza vaccines.

In addition to antigenic drift, IAV can also undergo a more dramatic type of change called antigenic shift. Antigenic shift occurs infrequently and unpredictably and is defined as the emergence of a virus carrying HA and/or NA proteins that have not been circulating among humans in recent years. The fact that avian upper respiratory tract epithelial cells preferentially express α(2,3)-linked SAs, whereas α(2,6)-linked SAs are predominantly present in the human upper respiratory tract, and swine express both types has led to the hypothesis of the pig as a "mixing vessel": The permissiveness of the pig respiratory epithelium for both avian and human lineage IAV strains is proposed to facilitate reassortment and the generation of new human pandemic strains with efficient human-to-human transmission (Cox and Subbarao, 2000; Carrat and Flahault, 2007). The eight RNA segments in IAV enable genomic mixing when two or more influenza viruses infect a cell. Since antigenic shift results in the emergence of an antigenically new influenza virus, a large proportion of the world's population will not have protective antibodies. If the new strain is capable of causing disease in humans and of establishing sustained human-to-human transmission, such a virus has the potential to cause a worldwide pandemic (Sandbulte *et al.*, 2015).

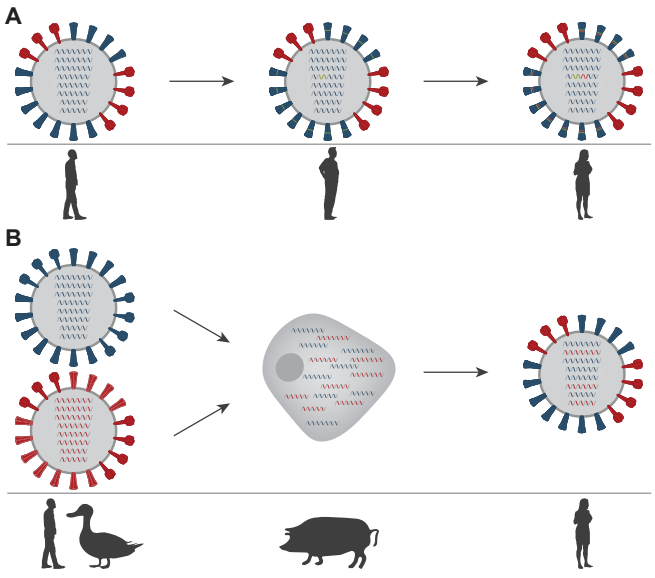


**Fig. 5 | Antigenic Drift and Shift of Influenza A Viruses. A** | The surface hemagglutinin (blue) and neuraminidase (red) proteins undergo frequent mutation (antigenic drift) in their human hosts, giving rise to new virus variants (green and red regions in HA protein). **B** | Less frequently, entire segments of the genome of different viruses reassort during co-infection of the same cell, resulting in a virus that expresses hemagglutinin or neuraminidase proteins, to which there is no prior immunity in human populations (antigenic shift). These reassortement events can give rise to pandemics. Adapted from (Sandbulte *et al.*, 2015).

Although influenza outbreaks occur almost every year, the incidence and severity of disease can vary substantially. They are affected by several factors including the types, subtypes and strains of circulating viruses, and the level of protective antibodies in the population. In general, seasonal epidemics cause an estimated 250,000 to 500,000 deaths annually worldwide (WHO). In contrast, the morbidity and mortality of the more infrequent pandemics will affect all age groups and are more difficult to predict, as they can range from 200,000 deaths for the 2009 H1N1 pandemic to 50 million for the 1918 H1N1 pandemic (Johnson and Mueller, 2002; Simonsen *et al.*, 2013).

## 1.5. Influenza Animal Models

Different animal models are used to characterize the host and its immune response to infection, course of disease, pathogenesis, and transmission of IAVs. These studies then constitute the basis for the development of diagnostics, therapeutics, and vaccines. The first influenza animal transmission study was conducted in 1933, with Smith *et al.* infecting ferrets with a human H1N1 isolate from Puerto Rico in 1934 (PR5) and passaging the isolate in these animals, which accidently transmitted back to humans during the course of the study (Smith, Andrewes and Laidlaw, 1933; Francis, 1934). One of the ferret isolates was later used to inoculate mice, resulting in a highly variable disease outcome. However, further passaging in mice resulted in the mouse-adapted H1N1 A/Puerto Rico/8/1934 (PR8) strain, which is widely used in IAV research (Francis, 1937). For the next 30 years, IAV was the most extensively studied viral pathogen of humans with the goal to develop a safe and efficacious vaccine, resulting in the first licensed vaccine in 1945 (Barberis *et al.*, 2016). The use of animals as surrogates for humans in efficacy trials came under FDA inspection in the late 1950s because many therapeutics that were being introduced were not effective or had serious side effects (Luke and Subbarao, 2006; Anderson and Swearengen, 2012). Today the animal models used for vaccine efficacy studies are better understood, more tightly standardized, and constitute an important step in the development of safe and efficacious vaccines.

### 1.5.1. The Ferret Model

The ferret, as the first animal model used for influenza research, continues to have a major role in studying various aspects of virus-host interactions. One of the reasons is that influenza infection in ferrets closely resembles that in humans with respect to clinical signs, pathogenesis, and immunity, and that human influenza A and B viruses infect ferrets without adaptation. Physical characteristics of ferrets, including their airway morphology and sneeze response make them amenable for characterizing clinical and immunological aspects of disease (Maher and DeStefano, 2004; Luke and Subbarao, 2006). Ferrets and humans experience a similar clinical course of disease

(Leigh *et al.*, 1995) that varies in severity and duration, depending on virus strain, and age and health of the individual. Infection with seasonal human influenza viruses is generally restricted to the upper respiratory tract, and include a rapid onset of sneezing, nasal discharge, malaise, and pyrexia. Illness is usually acute and mild, lasting for up to a week (Haff, Schriver and Stewart, 1966; Renegar, 1992; Connole *et al.*, 2000; Herlocher *et al.*, 2001; Maher and DeStefano, 2004). The nasal turbinates (NT) are the primary site of viral replication, while particularly virulent IAV strains are also capable of spreading to the lower respiratory tract. This can be explained by the predominant distribution of α(2,6)-linked SAs in the ciliated respiratory epithelium of ferrets and humans, while the lower respiratory tract contains mostly α(2,3)-linked SA bronchiolar cells and type II alveolar cells and less that carry α(2,6)-linked SAs (Shinya *et al.*, 2006). Finally, the comparable density of these SA receptors may further contribute to the similarities in susceptibility and disease severity between ferrets and humans (Leigh, Cheng and Boat, 1989).

### 1.5.2. The Murine Model

The first inoculation of mice with a ferret isolate in 1934 (Francis, 1934) initiated the extensive use of mice in various aspects of influenza virus research. Even though wild mice are not a natural host for influenza viruses, laboratory strains can be infected with certain strains. As in the initial experiment, most viruses have first to be adapted via multiple passaging in mouse lungs, which results in mutations that improve receptor binding and replication and thereby increase virulence. However, the level of susceptibility also depends on the mouse strain (Matrosovich *et al.*, 2004a; Narasaraju *et al.*, 2009; Sakabe *et al.*, 2011; Margine and Krammer, 2014). This process highlights one of the major drawbacks of the murine influenza model: adaptation may lead to considerable antigenical and phenotypical difference between the initial and the mouse-adapted strain. Physiologically, mice were found to predominantly express α(2,3)-linked SA throughout their respiratory tract, which might explain their increased natural susceptibility to HPAI (Ibricevic *et al.*, 2006; Xu *et al.*, 2013). Clinical signs of influenza infection in mice develop 2-3 days after infection and differ from that observed in humans. They include lethargy, anorexia, and weight loss, depending on the virus and mouse strain used, but signs such as coughing, nasal discharge and fever do not occur (Luke and Subbarao, 2006; Margine and Krammer, 2014). Overall, weight loss and associated mortality remains the most reliable and quantitative readout in vaccine effectiveness experiments. Taken together, mice remain the most widely used animal model for influenza research, due to their advantages such as small size, availability of numerous inbred and transgenic strains immunological reagents and assays (Novak *et al.*, 1993; Luke and Subbarao, 2006; Matsuoka, Lamirande and Subbarao, 2009;

Margine and Krammer, 2014).

## 1.6. Influenza Vaccines

Currently licensed influenza vaccines are trivalent or quadrivalent, containing a mixture of the H1N1 and H3N2 IAV strains and influenza B strains of the Victoria and Yamagata lineage predicted to circulate during the next season. Strains for the upcoming season are usually selected in February for the Northern Hemisphere, recommendations are made by the World Health Organization (WHO) and the U.S. Public Health Service (Houser and Subbarao, 2015). Currently there are licensed inactivated or live-attenuated vaccines. The composition for the 2017/18 season in the Northern Hemisphere includes an A/Michigan/45/2015 pdmH1N1-like virus, A/Singapore/INFIMH-16-0019/2016 (H3N2)-like virus, a B/Colorado/06/2017-like virus (B/Victoria/2/87 lineage), and an optional B/Phuket/3073/2013-like virus (B/Yamagata/16/88 lineage) in the quadrivalent vaccine (Organisation, 2015).

Vaccine efficacy can vary widely between seasons, depending on how well vaccine and circulating strains match. The estimated overall vaccine effectiveness for influenza seasons from 2005-2016 was between 10 and 60%, with recent studies showing that vaccination reduced the risk of influenza illness by 40–60% when circulating viruses match the vaccine strains (Zimmerman *et al.*, 2016). However, during the 2014–2015 season for instance, the overall vaccine effectiveness was 19%, and only 6% against the H3N2 component because two thirds of the circulating strains had drifted from the previous year (Zimmerman *et al.*, 2016).

### 1.6.1. Inactivated Influenza Vaccines (IIV)

Most licensed influenza vaccines are inactivated. Their production starts with the generation of reassortant viruses as seed strains for further vaccine production. While seed strains for the production of influenza B vaccines are field isolates, IAV vaccine strains are hybrid viruses containing the internal genes of the high growth-adapted H1N1 PR8 or PR8-like master strains that support efficient growths in embryonated chicken eggs in combination with genes coding for the surface proteins of the annual target strains (Kilbourne *et al.*, 1971; Gerdil, 2003; Wright, Neumann and Kawaoka, 2007). This process might take several weeks, including possible additional adaption steps for improved growth efficiency in eggs through serial passages and subsequent standardization tests and sequence analyses (Gerdil, 2003; Lambert and Fauci, 2010). Manufacturers then amplify these seed viruses in the allantoic cavity of millions of embryonated chicken eggs from February to late summer. The virus is subsequently harvested, inactivated with formalin or beta-propiolactone, followed by purification by zonal centrifugation or column chromatography. Virus particles are then split or

solubilized using ether and a detergent or a detergent alone, respectively (Gerdil, 2003; Wright, Neumann and Kawaoka, 2007).

One egg yields between one and three vaccine doses. The quantity of HA antigen in each vaccination dose is standardized by single radial immuno-diffusion assay to 15 μg per component for adult application and 7.5 μg for children under 3 years, as recommended by the Advisory Committee on Immunization Practices (Schild, Wood and Newman, 1975). In Western Europe, the European Medicines Agency (EMA) requires that the safety and immunogenicity of each new influenza vaccine formulation be evaluated in a clinical study (Wood and Levandowski, 2003). Because of the instability of this protein during purification and storage, and due to the variable HA:NA ratio between strains, NA content is usually not determined. To date, only vaccines containing both surface antigens, HA and NA, are licensed. Inactivated influenza vaccines (IIVs) have been used in humans for over 50 years to protect from seasonal influenza viruses, and have also been developed as pre-pandemic vaccines (Barberis *et al.*, 2016). However, IIVs usually require multiple administrations and occasionally the addition of adjuvants to elicit sufficient serum antibody responses for effective protection against the infection in naïve individuals.

### 1.6.2. Live-Attenuated Influenza Vaccines (LAIV)

Live-attenuated influenza vaccines (LAIV) have recently been licensed for use in healthy individuals between the ages of 2 and 49 years (*FDA Information Regarding FluMist Quadrivalent Vaccine*, 2018). Similar to IIVs, 6:2 LAIV reassortant variants are being produced by transfer of genes from an attenuated donor virus to the new target strain (Kendal, Bozeman and Ennis, 1980; Subbarao and Joseph, 2007). This results in an attenuated reassortant live vaccine virus containing the HA and NA genes from the virulent wild-type virus and the genes that confer attenuation from the donor virus (Wright, Neumann and Kawaoka, 2007). The critical step in developing LAIV is to provide a candidate virus strain that is as avirulent as possible to address the safety issues associated with using a live virus, while maintaining a high level of replication to induce sufficient immune responses to protect from infection. The cold-adaptation of influenza viruses has proven a powerful tool for stable attenuation, and thus has long served as a reliable and practical platform for the generation of LAIVs against seasonal and pandemic influenza viruses (Fiore, Bridges and Cox, 2009; Jin and Chen, 2014). Each LAIV is tested to ensure that it retains the cold-adapted, temperature-sensitive and attenuated phenotypes before the vaccine virus seed can be released for further manufacturing (Jin *et al.*, 2003). Particularly the viral titer reduction at 25.8°C has to be <100-fold compared to its replication at 33.8°C and at 39.8°C for A strains or 37.8°C for B strains >100-fold compared to its replication at 33.8°C. The attenuated phenotype is

assessed in a ferret model, in which decreased levels of replication in the lower but not the upper respiratory tract reflect viral attenuation (*FDA Information Regarding FluMist Quadrivalent Vaccine*, 2018).

In contrast to the intramuscularly injected IIVs, LAIVs are administered intranasally. Therefore, IIVs induce relatively low levels of mucosal immunity, which is considered the first line of defense against influenza virus infection. They are also unable to induce an effective cell-mediated immunity, which is believed to contribute to cross-protection against antigenically distant strains and rapid recovery from illness (Jang and Seong, 2014). LAIVs, in contrast, elicit innate and local mucosal IgA antibodies and cell-mediated immune responses and thereby offer broader and longer lasting protection against not only homologous strains but also heterologous infections, especially in children (Basha *et al.*, 2011; Cheng *et al.*, 2013). Furthermore, its high production yield in eggs and 'needle-free' nasal administration make LAIV a desirable vaccine for use in a pandemic setting (Jin and Chen, 2014).

## 1.7. New Approaches to Influenza Vaccine Development

The described currently available vaccines still leave a need for more effective vaccines and less complex, more rapid, and reliable vaccine-production technologies (Lambert and Fauci, 2010). New "universal" influenza vaccine approaches attempt to overcome the highly variable nature of influenza viruses by stimulating both humoral and cell-mediated arms of the immune system and thereby inducing cross-protective broadly neutralizing immunity (Rajão and Pérez, 2018). The most promising approaches currently under investigation target highly conserved epitopes of the surface glycoproteins HA or NA, or the extracellular domain of the M2 protein (M2e) for cross-reactive humoral immune responses. Furthermore, internal proteins like NP or M1 are targeted to induce cross-reactive T cell responses (Fig. 6, Table 1). Antibodies generated against the HA protein correlate with the greatest extent of protection. However, antibodies directed against the NA protein also correlate with a reduction in disease severity, and antibodies generated against the highly conserved M2e domain interfere with virus assembly or constrain proton transport and are highly cross-reactive across virus subtypes (Rajão and Pérez, 2018).

### 1.7.1. Hemagglutinin-Based Approaches

Antibodies against the HA protein are predominantly directed against the globular head domain. Their functional activity can be measured in surrogate *in vitro* assays such as the hemagglutination inhibition (HI) or virus neutralizing (VN) assays and correlates with protection. HI titers >1:40 are considered protective and the accepted standards used by regulatory agencies (Rimmelzwaan and McElhaney, 2008). A major drawback

of these antibodies is that the globular head is highly variable and rapidly acquires mutations that result in antigenic variation, so most HA head-specific antibodies are only protective against closely related strains.

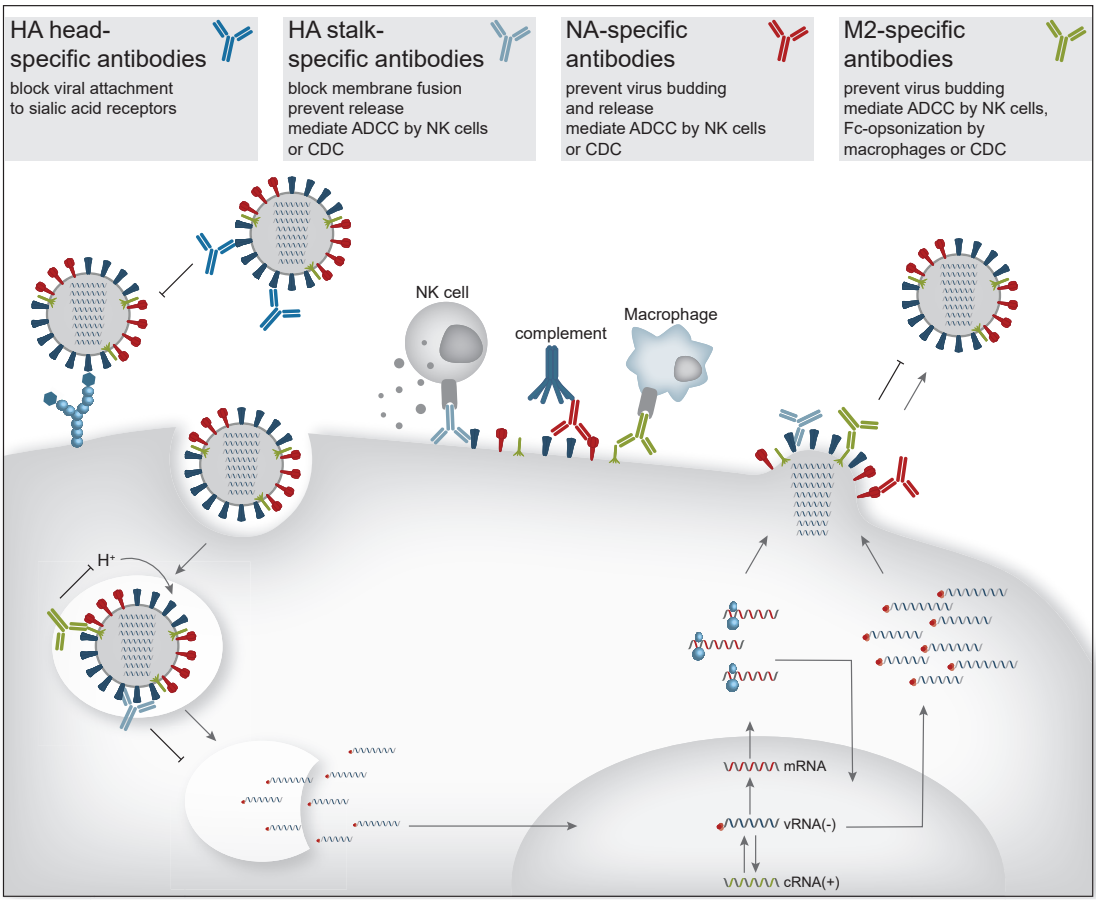


**Fig. 6 | Antibody-mediated immune responses elicited by different influenza vaccines.** The HA, NA and M2 proteins account for most of the known functional epitopes. Antibody-mediated immune responses are described in the panels above and are illustrated by the respective antibodies. HA head-specific antibodies block attachment of the virus to the host cell receptor and prevent virus entry into the host cell. HA stalk-specific antibodies prevent fusion of viral and endosomal membranes, inhibit budding and release of new virions, and mediate antibody dependent cell-mediated cytotoxicity (ADCC) by natural killer (NK) cells or complement-dependent cytotoxicity (CDC). NA-specific antibodies inhibit budding and release of new virions and mediate ADCC and CDC. M2e-specific antibodies inhibit budding and release of new virions, and mediate ADCC by NK cells, Fc-opsonization by macrophages or CDC. Modified from (Rajao and Perez, 2018).

Nonetheless, cross-reactive neutralizing HA head-specific antibodies have been detected in mice and humans, suggesting that the head domain does contain potential epitope targets for broadly protective vaccines (Yoshida *et al.*, 2009; Whittle *et al.*, 2011; Ekiert *et al.*, 2012; Lee *et al.*, 2012, 2014). Another HA-based approach towards a "universal" vaccine is the Computationally Optimized Broadly Reactive Antigen (COBRA) technology (Table 1). Consensus sequences are used to design vaccines representing multiple circulating strains simultaneously. Towards this, a H1 virus-like particle (VLP) vaccine has been developed and was successful at inducing highly cross-

reactive and protective antibodies (Carter *et al.*, 2016). Finally, the stalk domain is much more conserved across HA subtypes and phylogenetically only clusters into group 1 and group 2 HAs (Fig. 2B). It is thus a promising antigen for the induction of broadly reactive antibodies.

Influenza infection, in contrast to vaccination, can naturally induce low levels of stalk-reactive antibodies and those antibodies can have broadly neutralizing activity (Ekiert *et al.*, 2009; Corti *et al.*, 2011). While HA head-specific antibodies neutralize infection by preventing binding to cellular receptors or membrane fusion (Fig. 6), HA stalk-specific antibodies have no neutralizing activity and instead act by inhibiting either entry or release, or by mediating antibody-dependent cell-mediated cytotoxicity (ADCC) or complement-dependent cytotoxicity (CDC) (Fig. 6) (Rajão and Pérez, 2018). "Headless" HA are now being explored as vaccine antigen. In mice, broadly neutralizing stalk-reactive antibodies resulted in protection from lethal homologous (Corti *et al.*, 2011) and heterosubtypic challenge (Steel *et al.*, 2010). A similar approach confirmed these findings in cynomolgus monkeys (Impagliazzo *et al.*, 2015). Furthermore, vaccination with a conformational peptide mimicking the H5 stem resulted in protective responses against lethal challenge with group 1 as well as group 2 influenza viruses (Valkenburg *et al.*, 2016). Sequential immunization with chimeric HA constructs, expressing identical stalk, but irrelevant divergent head domains, also induced broadly reactive, stalk-specific antibodies that protected mice against heterologous challenge (Krammer *et al.*, 2013; Ermler *et al.*, 2017), and may be easier to produce and standardize in the established vaccine production pipeline.

### 1.7.2. Neuraminidase-Based Approaches

The currently licensed influenza vaccines are not standardized for their NA protein content or quality, or NA-specific immune responses they induce. Antibodies that inhibit NA activity prevent virus budding and release from the cell surface. Consequently, they reduce the amount of infectious particles available to induce the subsequent rounds of infection. Moreover, NA-specific antibodies may result in ADCC and might also enhance trapping of the virus particles by mucins, which no longer get cleaved in the presence of NA-specific antibodies (Fig. 6) (Rajão and Pérez, 2018). Since NA proteins are antigenically more conserved than HA proteins, and there is increasing evidence that NA-specific antibodies can provide protection from influenza viruses, including reports about broad binding and inhibition of NA activity, there is increasing interest in exploring the potential of this protein as vaccine antigen (Johansson *et al.*, 1987; Wohlbold and Krammer, 2014; Halbherr *et al.*, 2015; Wan *et al.*, 2015; Wilson *et al.*, 2016; Wohlbold *et al.*, 2016, 2017). When administered separately, HA and NA proteins induced comparable total antibody titers (Johansson, Bucher and Kilbourne,

1989). Immunization with NA alone decreased lung virus titers in mice and reduced severe clinical signs and viral shedding in patients (Schulman, 1969; Couch *et al.*, 1974; Rott, Becht and Orlich, 1974; Johansson, Bucher and Kilbourne, 1989; Wohlbold *et al.*, 2015). The resulting antibody responses cross-react with other NA proteins of the same subtype, and NA-specific immunity protected mice from infection with antigenic drift variants but not from strains carrying a heterosubtypic NA protein (Chen *et al.*, 2000; Wohlbold *et al.*, 2015). The level of cross-reacting neuraminidase-inhibiting (NI) antibodies has thus been proposed as indicator for protection (Rockman *et al.*, 2013).

## 1.8. Novel Vaccine Platforms

In the context of ongoing efforts to develop a universal influenza vaccine, a variety of vaccine platforms and technologies have been investigated. The ideal approach would have to be easy to standardize, rapidly produced, and have an excellent safety profile (Rajão and Pérez, 2018). Ultimately, this vaccine would serve as endemic and epidemic vaccine, but also allow rapid adaptation to pandemic scenarios. Currently studied strategies focus mostly on protein-based or VLP vaccines, but nucleic acid on viral vectors-based platforms are also being explored (summarized in Table 1).

**Table 1** | Overview of novel influenza virus vaccine technologies. Adapted from (Rajão and Pérez, 2018).

| Vaccine platform | Vaccine type | Efficacy | Development stage | Ref. |
|---|---|---|---|---|
| **Recombinant, protein-based and virus-like particle vaccines** | Baculovirus expression vector systems (BEVS) | safe and immunogenic, heterologous protection | experimental | (Crawford *et al.*, 1999; King *et al.*, 2009; Baxter *et al.*, 2011) |
| | virus-like particles (VLPs) | safe and immunogenic, homologous and heterologous protection | clinical phase 1-2 | (López-Macías *et al.*, 2011; Low *et al.*, 2014; Pillet *et al.*, 2016; Valero-Pacheco *et al.*, 2016) |
| | VLP-COBRA | cross-reactive response, homologous protection | pre-clinical | (Giles and Ross, 2011; Crevar *et al.*, 2015) |
| | headless HA | broadly neutralizing antibody response, homologous and partial heterologous protection | pre-clinical | (Steel *et al.*, 2010; Krammer and Palese, 2013; Impagliazzo *et al.*, 2015; Valkenburg *et al.*, 2016) |

| | | | | |
|---|---|---|---|---|
| | chimeric HA | induces broadly neutralizing antibodies to the HA stalk domain, broad, universal protection | pre-clinical | (Krammer *et al.*, 2013; Ryder *et al.*, 2016; Ermler *et al.*, 2017) |
| | sequential immunization | broadly neutralizing antibody response, heterologous protection | pre-clinical | (Krammer and Palese, 2013; Krammer *et al.*, 2013; Nachbagauer *et al.*, 2014; Kirchenbaum, Carter and Ross, 2016; Ermler *et al.*, 2017) |
| | NA-based | cross-reactive response, homologous and partial heterologous protection | experimental | (Sylte, Hubby and Suarez, 2007; Van Reeth *et al.*, 2009; Wohlbold *et al.*, 2015) |
| | M2e-based | broad cross-reactive response, heterologous cross-protection | pre-clinical, phase 1, experimental | (Turley *et al.*, 2011; Lee *et al.*, 2015; Kolpe *et al.*, 2017; Tang *et al.*, 2017; Tao *et al.*, 2017) |
| **Nucleic acid-based** | DNA | safe and immunogenic with prime-boost regimen, strain-specific, highly cost-effective | clinical phase 1, licensed, experimental | (Ledgerwood *et al.*, 2012; Crank *et al.*, 2015; Borggren *et al.*, 2016; Stachyra *et al.*, 2017) |
| | messenger RNA (mRNA) | safe and immunogenic, homologous and heterologous protection | clinical phase 1, experimental | (Petsch *et al.*, 2012; Bahl *et al.*, 2017) |
| **Viral vector vaccine** | modified vaccinia virus Ankara (MVA) –conserved proteins | broad cross-reactive response, partial/total homologous protection and partial cross-protection | clinical phase 1 | (Lillie *et al.*, 2012; Boyd *et al.*, 2013; Florek *et al.*, 2014; Hessel *et al.*, 2014; Ducatez *et al.*, 2016) |
| | Adenovirus | partial homologous/ heterologous protection | clinical phase 1, experimental | (Wesley, Tang and Lager, 2004; Boyd *et al.*, 2013; Crosby *et al.*, 2017) |
| | Alphavirus | partial/total homologous and partial heterologous protection | experimental | (Vander Veen *et al.*, 2012, 2013; Santos *et al.*, 2017) |

### 1.8.1. Viral Vectors as Vaccine Platforms

Viral vectors are increasingly recognized as promising vaccine platforms, since they can efficiently mimic the natural infection and the antigens of interest are expressed in their native conformation, which often results in higher antibody specificity. Vector vaccines are a safe approach that excludes the risk of recombination or reversion to virulence, and they can be rapidly produced to large scale without the use of fertilized chicken eggs (Rajão and Pérez, 2018). Viral vectors are derived from wild type viruses by deleting a part of or all viral genes or introducing attenuating mutations.

Among the non-replicating vector vaccines, modified vaccinia virus Ankara (MVA) has been most extensively characterized. Expression of different T cell epitopes or conserved proteins of influenza viruses results in high $CD4^+$ and $CD8^+$ T cell responses in mice, macaques and chickens, and confers partial protection from challenge infection (Goodman *et al.*, 2011; Florek *et al.*, 2014; Hessel *et al.*, 2014). Other systems based on alphavirus, parainfluenza virus or adenovirus vectors have also been used and pre-clinical studies have shown strong induction of anti-HA antibodies and T cell responses, leading to protection from homologous infection (Yang *et al.*, 2009; Li *et al.*, 2015; Rajão and Pérez, 2018). Those technologies allow for rapid updates and possess the opportunity of various automated administration methods that can be adapted to the respective host (Rajão and Pérez, 2018).

#### *1.8.1.1. Vesicular Stomatitis Virus*

Vesicular stomatitis virus (VSV) is a non-segmented negative-sense RNA virus, of the *Rhabdoviridae* family. The virus infects a broad range of animals including cattle, horses, and swine, with insects serving as vectors. Even though, VSV rarely causes fatal disease, clinical signs resemble those associated with foot-and-mouth disease, which leads the virus to be considered a reportable animal disease in many countries. However, laboratory adapted VSV strains are generally attenuated in the original host species (Fields, Knipe and Howley, 1996).

VSV forms bullet shaped particles of 180 nm length and 80 nm width (Fields, Knipe and Howley, 1996). Like influenza, VSV also possess a lipid envelope derived from the host cell (Fig. 7) (Li and Zhang, 2012). The only surface glycoprotein (G) is responsible for viral attachment, entry, and fusion activities. Attachment of the virus to host cells is mediated by binding to a highly ubiquitous low density lipoprotein (LDL) receptor, whereas other LDLR family members serve as alternative receptors, explaining the wide tropism of VSV (Finkelshtein *et al.*, 2013). Replication takes place in the cytoplasm and interrupts the host protein translation by blocking the nuclear export of cellular mRNAs via its matrix protein (M) (Lichty *et al.*, 2004). The M protein is also thought to

be involved in inducing the characteristic rounding of cells and apoptosis.

VSV has a simple genome consisting of 11.161 nucleotides organized into five genes, encoding nucleocapsid (N), phospho- (P), M, G, and large polymerase (L) proteins. The genome is encapsidated by the N protein, forming a helical N-RNA nucleocapsid resistant to nuclease activity, which together with the L and P proteins forms the RNP complex. The P protein mediates binding of L with the N protein-RNA template, whereas the L protein is responsible for all RNA synthesis activities (Fields, Knipe and Howley, 1996).

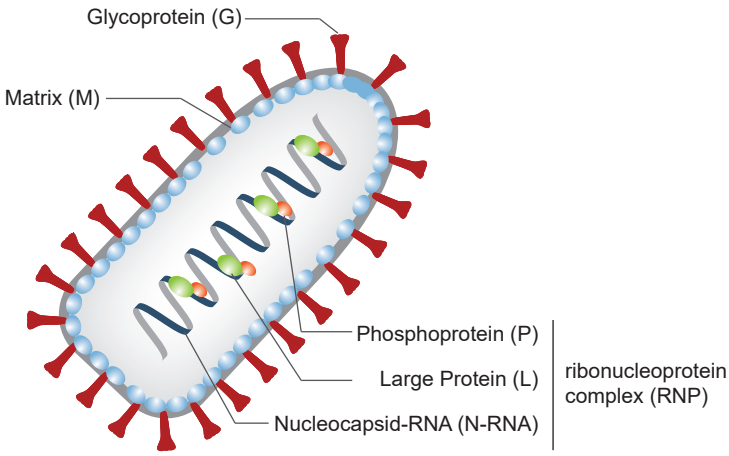


**Fig. 7 | Schematic structure of the vesicular stomatitis virus particle.** The viral envelope is derived from the host cell membrane. The glycoprotein (G) is embedded in the lipid bilayer and the matrix protein (M) lines the viral envelope from the inside. The non-segmented single-stranded RNA genome is encapsidated by the nucleocapsid protein (N) and associated with the phosphoprotein (P) and the large protein (L) that together form the ribonucleoprotein (RNP) complex. Adapted from (Li and Thang, 2012).

Negative-sense RNA virus vectors have been primarily generated with non-segmented NSV such as Sendai virus, Newcastle disease virus (NDV) or VSV. For the generation of VSV replicons, the G protein is deleted from the genome and replaced by the target antigens of interest (e.g. influenza) (Zimmer, 2010). Recent studies have shown that such a propagation-incompetent VSV replicon encoding the HA protein from H7N1 influenza virus protects chicken from challenge infection with the homologues HPAIV strain (Kalhoro *et al.*, 2009). Similar results have been achieved for the HPAIV H5N1 influenza virus (Halbherr *et al.*, 2013). While a single injection of about $10^8$ infectious replicon particles conferred sufficient protection against challenge infection, a second immunization strongly boosted the humoral immune response and completely prevented shedding of challenge virus and transmission to sentinel birds (Halbherr *et al.*, 2013).

#### *1.8.1.2. Adeno-Associated Virus*

Adeono-associated virus (AAV) is a small (25 nm) nonenveloped virus that is inherently non-pathogenic and replication-defective (Nieto and Salvetti, 2014). AAV belongs to the family *Parvoviridae* and is placed in the genus *Dependovirus*, because productive infection by AAV occurs only in the presence of a helper virus, either adenovirus or

herpesvirus.

AAV vectors are gutless, which means that they no longer encode any viral gene. AAV vectors usually carry a single-stranded (ss) DNA molecule containing the transgene expression cassette flanked by the viral inverted terminal repeats (Daya and Berns, 2008), but AAV particles containing a double-stranded genome can be also generated, which improves the kinetics and the level of transgene expression (McCarty, 2008). The AAV life cycle is divided into two stages: the lytic and lysogenic stage. After infection in the presence of a helper virus, the virus enters the lytic stage characterized by genome replication, viral gene expression, and virion production. Hereby the helper virus regulates gene expression, and provides polymerase function and a permissive intracellular milieu for AAV infection (Daya and Berns, 2008). In the absence of helper viruses, there is limited AAV replication, viral gene expression is repressed, and the AAV genome can establish latency by integrating into a 4-kb region on chromosome 19, termed AAVS1 (Linden *et al.*, 1996; Kay *et al.*, 2000).

AAV vectors possess the capacity to efficiently transduce various tissues *in vivo* and the isolation of several AAV serotypes and capsid variants provides the opportunity to develop prime/boost strategies by switching the AAV capsid and thereby avoiding anti-capsid neutralizing antibodies induced after the first immunization. A remarkable feature of AAV vector vaccines is their capacity to induce strong and long-lasting Ab responses after a single administration. Several studies documented the induction of humoral responses lasting for many months up to more than one year, which may be linked to the sustained high level expression of the transgene (Manning *et al.*, 1997; Kuck *et al.*, 2006; Nieto *et al.*, 2009; Li *et al.*, 2012; Ploquin *et al.*, 2013). Recent studies have shown that immunization of mice with an AAV9 vector expressing HA, NP or M1 of pdmH1N1 conferred complete homologous and partial heterologous protection against challenge infection (Sipo *et al.*, 2011). A more recent study attempted to develop an AAV-based passive universal vaccine, by expressing broadly neutralizing HA antibodies. Transduced mice expressed cross-reactive neutralizing antibodies against various HA subtypes and were protected against intrasubtypic H1N1 infection, illustrating the potential of this approach (Balazs *et al.*, 2013).

## 1.9. Aim of the Study

Annual vaccination is the primary prophylactic countermeasure against seasonal influenza outbreaks. However, the effectiveness of current influenza vaccines is limited, because they require high antigenic similarity between the selected vaccine strains and circulating influenza isolates to confer protective immunity. This study aimed at providing proof-of-concept that a more broadly protective influenza vaccine

can be developed that is capable of conferring at least partial protection against both seasonal and newly emerging pre-pandemic strains. Towards this, two complementary approaches were chosen: on the one hand exploring the protective potential of the more conserved NA protein, and on the other hand targeting the HA stalk domain.

### 1.9.1. Evaluating the extent of cross-protection conferred by the influenza neuraminidase

The primary goal of this study was to investigate the potential of the NA protein to confer protection in mammals against heterologous influenza strains carrying the same NA subtype. Towards this, single cycle VSV replicon particles expressing different NA and HA proteins were generated. Antigen expression was characterized *in vitro* and C57BL/6 mice and ferrets were immunized with the respective replicons. After analyzing the immune response kinetics and the levels of cross-reactive antibodies in mice and ferrets, the protective efficacy against a challenge with H1N1 PR8 or pdmH1N1 A/Mexico/InDRE4487/2009, respectively, was assessed. The contribution of antibodies to the observed protection was subsequently investigated with a passive transfer experiment in mice.

This experimental setup allowed us to not only compare the efficacy of NA- and HA-expressing VSV replicon vaccines, but also examine the extent of cross-protection conferred by the NA against heterologous H1N1 virus and NI antibodies as possible correlates of protection.

### 1.9.2. Comparing the efficacy of hemagglutinin stalk-induced immune responses in ferrets

In the context of an earlier study performed by Daniel Demminger and Thorsten Wolff at the Robert Koch Institute in Berlin, AAV vectors expressing wild type or chimeric HA proteins were generated to evaluate their potential to broaden the specificity and the functionality of the antibody response. This group vaccinated C57BL/6 mice with the different vectors and found that the AAV vector vaccines as well as the currently licensed IIV resulted in intra-subtypic cross-reaction of HA-specific antibodies. However, only AAV vector vaccines protected mice against heterologous influenza virus challenge. Here, we followed up on this finding by assessing the immunogenicity and efficacy of these AAV vector vaccines in the more clinically relevant ferret model. Towards this, ferrets were vaccinated with the different vaccine candidates or the licensed IIV and immune responses and levels of protection against the pandemic H1N1 A/Mexico/InDRE4487/2009 were investigated.

This study confirmed the results obtained in mice and supports further pre-clinical exploration of AAV-based vaccine platforms for influenza.

# 2. MATERIALS

## 2.1. Chemicals and Reagents

| PRODUCT | CONCENTRATION | SOURCE |
|---|---|---|
| 1.5 % Sodium citrate Solution | | Paul-Ehrlich-Institut, Langen |
| Acrylamid/Bisacrylamid Rotiphorese | 30 % (w/v) Acrylamid, 0,8 % Bisacrylamid Gel 30 | Bio-Rad Laboratories, München |
| Agarose | | Carl Roth, Karlsruhe |
| Ammonium persulfate (APS) | | Carl Roth, Karlsruhe |
| Ampicillin | | Carl Roth, Karlsruhe |
| Antisedan, Alzane | | Laboratorios SYVA, León |
| Beta-propiolactone (BPL)-inactivated PR8, NR-19325 | | BEI Resources, NIAID, NIH |
| BSA for ELLA | | Sigma-Aldrich, München |
| Chicken erythrocytes | | Paul-Ehrlich-Institut, Langen |
| Complete, Mini, EDTA-free protease inhibitor cocktail | | greiner bio-one, Kremsmünster |
| DAPI Fluoromount-G | | Southern Biotech, Birmingham, AL |
| Dimethyl sulfoxide (DMSO) | | Sigma-Aldrich, München |
| DNA loading dye 6x | | Thermo Scientific, Karlsruhe |
| dNTPs | | Agilent Technologies, Waldbronn |
| Domitor, Sedin | | Vetpharma animal health S.L., Barcelona |
| DTT | 0.1 M | Thermo Scientific, Karlsruhe |
| Dulbecco's modified Eagle medium (DMEM) | 4.5 g/l Glucose | Lonza, Zurich |
| Dulbecco's PBS | | Paul-Ehrlich-Institut, Langen |
| Ethanol, 96 % | | Paul-Ehrlich-Institut, Langen |
| EZ-Link NHS-LC-LC-Biotin | stock solution 0.25 M in DMSO | Thermo Scientific, Karlsruhe |
| Fetal bovine serum (FBS) | | Thermo Scientific, Karlsruhe |
| Fetuin in coating buffer | 25 mg/ml | Sigma-Aldrich, München |
| GelRed | 10,000x | Biotium, Fremont, CA |
| GeneRuler 100 bp Plus DNA Ladder | | Thermo Scientific, Karlsruhe |
| Glycine | | GE Healthcare, Buckinhamshire |
| Histopaque-1077 | | Sigma-Aldrich, München |
| Hydrogen peroxide solution ($H_2O_2$) | 30 % (w/w) in $H_2O$ | Sigma-Aldrich, München |
| Hygromycin B from *Streptomyces hygroscopicus* | | Sigma-Aldrich, München |
| Influenza A H1N1 A/Puerto Rico/8/34 Hemagglutinin protein (His Tag) | | Thermo Scientific, Karlsruhe |

| | | |
|---|---|---|
| Isopropanol | | Paul-Ehrlich-Institut, Langen |
| Ketamin | | Bela-Pharm, Vechta |
| Ketamin, | 10 % | bela-pharm, Vechta |
| KPL coating buffer | 10x | seracare, Milford, Massachusetts |
| LB Agar plates | 100 µg/ml Ampicillin | IVI, Mittelhäusern |
| LB-Medium | | IVI, Mittelhäusern |
| Lectin from Arachis hypnogaea (peanut)-Peroxidase | | Sigma-Aldrich, München |
| L-glutamine | 200 mM | Biochrom AG, Berlin |
| MEM Earles's medium | 0.85 g/L $NaHCO_3$ | Biochrom AG, Berlin |
| Methanol | | Paul-Ehrlich-Institut, Langen |
| Mifepristone (stock solution: 1 mM in ethanol) | Stock solution was diluted to $10^{-6}$ M in 96 % ethanol. Cells were induced at $10^{-9}$ M by further diluting the working solution in media by 1:1000 | Sigma-Aldrich, München |
| N,N-dimethylformamide (DMF) | | Sigma-Aldrich, München |
| O-phenylenediamine dihydrochloride (OPD) | | Sigma-Aldrich, München |
| Opti-MEM reduced serum medium | | Invitrogen, Karlsruhe |
| Paraformaldehyde | | Roth, Karlsruhe |
| PBS without magnesium and calcium | pH 7.1 | Paul-Ehrlich-Institut, Langen |
| Penicillin-streptomycin | 10,000 units penicillin / 10 mg streptomycin per ml | Sigma-Aldrich, München |
| Phosphate-citrate buffer with sodium perborate | | Sigma-Aldrich, München |
| Protein G Plus Agarose Beads | | Santa Cruz |
| Protein ladder PageRuler Plus Prestained | | Thermo Scientific, Karlsruhe |
| RPMI 1640 | | TH Geyer, Renningen |
| SDS | 10x | Paul-Ehrlich-Institut, Langen |
| Skim milk powder | | Carl Roth, Karlsruhe |
| SOC Medium | | IVI, Mittelhäusern |
| Sucrose | | Sigma-Aldrich, München |
| Sulfuric acid | 5N | Sigma-Aldrich, München |
| T61 | | Intervet, Unterschleißheim |
| TBS | 10x | Paul-Ehrlich-Institut, Langen |
| Tolyl- sulfonyl phenylalanyl chloromethyl keton (TPCK)-trypsin | 5 mg/ml | Sigma-Aldrich, München |
| Trypanblue solution | | Sigma-Aldrich, München |
| Trypsin-EDTA | 0.05 % (w/v) Trypsin, 0.002 % (w/v) EDTA | Paul-Ehrlich-Institut, Langen |

| | | |
|---|---|---|
| Tween20 for ELLA | | Sigma-Aldrich, München |
| Tween20 for SDS-PAGE | | |
| Xylavet | 100 mg/ml | cp-pharma, Burgdorf |
| Zeocin | | Sigma-Aldrich, München |
| β-Mercaptoethanol | | Sigma-Aldrich, München |

## 2.2. Buffers

| BUFFER | COMPOSITION |
|---|---|
| 0.85 % Sodium chloride | 0.145 M NaCl in $H_2O$ |
| AEC substrate | 5 ml 0.05 M $C_2H_3NaO_2$<br>300 µl 3-amino-9-ethylcarbazole in DMF<br>2.5 µl $H_2O_2$ (30 %) |
| Alsever solution | 71.9 mM NaCl<br>27.2 mM $C_6H_5Na_3O_7$ x 2 $H_2O$<br>2.6 mM $C_6H_{10}O_8$<br>1 M $C_6H_{12}O_6$<br>in $H_2O$, pH 6.1 |
| Calcium saline solution, pH 7.2 | 6.8 mM $CaCl_2$ x 2 $H_2O$<br>154 mM NaCl<br>19.4 mM $H_3BO_3$<br>0.1 mM $Na_2[B_4O_5(OH)_4]$ x 8 $H_2O$<br>in $H_2O$ |
| Dulbecco's PBS | 136.9 mM NaCl<br>2.68 mM KCl<br>0.5 mM $MgCl_2$<br>1.47 mM $KH_2PO_4$<br>8.1 mM $Na_2HPO_4$<br>0.9 mM $CaCl_2$<br>in $H_2O$, pH 7.1 |
| ELLA and ELISpot wash buffer | PBS, pH 7.1<br>0.05% Tween20 |
| ELLA coating buffer | 10ml 10x KPL coating buffer<br>90 ml $H_2O$ |
| ELLA Conjugate Diluent | Dulbecco's PBS<br>1% BSA |
| ELLA sample diluent | Dulbecco's PBS<br>1% BSA<br>0.5% Tween20 |
| ELLA stop solution | 1 N sulfuric acid |
| EZ-Link NHS-LC-LC-Biotin | 2 mM Biotin of a 0.25 M stock in DMSO in PBS |
| LB-Medium | 1 % (w/v) Trypton from Casein<br>0,5 % (w/v) Hefeextrakt<br>1 % (w/v) NaCl<br>in $H_2O$, pH 7,0 |
| NA assay buffer | 4 mM $CaCl_2$<br>in TBS, pH 7.0 |

| | |
|---|---|
| NA assay stop buffer | 25% Ethanol<br>0.2 M Glycin<br>0.3% Tween20<br>in $H_2O$, pH 10.7 |
| OPD substrate | 20ml $H_2O$ with phosphate-citrate buffer<br>with sodium perborate<br>10 mg OPD |
| PBS buffer | 137 mM NaCl<br>2.7 mM KCl<br>1.5 mM $KH_2PO_4$<br>8.1 mM $Na_2HPO_4$<br>in UPW, pH 7.1 |
| PBS buffer (0.01 M), pH 7.2 for HI | 4.9 mM $Na_2HPO_4$<br>2.2 mM $NaH_2PO_4$ x $H_2O$<br>145 mM NaCl<br>in $H_2O$, pH 7.2 |
| PBS-Glycine | 100 mM glycine<br>in PBS |
| RIPA buffer | 50 mM Tris, pH 8<br>150 mM NaCl<br>0.5% sodium deoxycholate<br>1% Triton X-100 |
| $RPMI_{Elispot}$ | RPMI 1640<br>10% FBS<br>1% L-glutamine<br>1% Pen/Strep |
| SDS, 10x | 250 m M Tris<br>1921 mM glycine<br>1% (w/v) SDS |
| SOC Medium | 2 % (w/v) Trypton from Casein<br>0,5 % (w/v) Hefeextrakt<br>10 mM MgCl2<br>10 mM MgSO4<br>10 mM NaCl<br>2,5 mM KCl<br>20 mM D(+)-Glucose<br>in $H_2O$, pH 7,0 |
| TBS-T for Western Blot | 0.1% Tween20<br>in TBS 1x |
| Tris buffered saline (TBS), 10x | 50 mM Tris<br>150 mM NaCl, pH7,4 |

## 2.3. Kits, Substrates and Enzymes

| **PRODUCT** | **SOURCE** |
|---|---|
| 3-amino-9-ethylcarbazole substrate | Sigma-Aldrich, München |
| Mouse IFNγ ELISPOT Ready-SET-Go! | eBioscience, Frankfurt am Main |
| BCA Protein Assay | Sigma-Aldrich, München |
| Kit | Thermo Scientific, Karlsruhe |
| Phusion Hot Start II High-Fidelity DNA Polymerase Kit, F-549S | Thermo Scientific, Karlsruhe |

| | |
|---|---|
| NucleoSpin Gel and PCR clean-up | Macherey-Nagel, Düren |
| T4 DNA Ligase | Thermo Scientific, Karlsruhe |
| NucleoBond Xtra Midi EF | Macherey-Nagel, Düren |
| FastDigest MluI | Thermo Scientific, Karlsruhe |
| 10x FastDigest Buffer | Thermo Scientific, Karlsruhe |
| FastDigest Eco91I (37°C Isoschizomer of BstEII (60°C)) | Thermo Scientific, Karlsruhe |
| 2'-(4-Methylumbelliferyl)-α-D-N-acetylneuraminate (MUNANA) | Sigma-Aldrich, München |
| ECL Western Blot substrate | GE Healthcare, Backinghamshire |
| BigDye Terminator V3.1 Cycle Sequencing Kit | Applied Biosystems, Foster City, CA |
| NucleoSEQ Columns | Macherey-Nagel, Düren |

## 2.4. Consumables

| **PRODUCT** | **SOURCE** |
|---|---|
| BD Eclipse Needle 27 G x ¾ (0.4 mm x 19 mm) for mouse cardiac puncture | BD Becton Dickinson, Franklin Lakes |
| Blood collection needle with integrated holder BD Vacutainer® Eclipse™ Signal™ (21 G, 1.25 in., 32 mm) for ferret blood sampling | BD Becton Dickinson, Franklin Lakes |
| cell culture flasks, tissue culture treated (T25, T75, T175) | Greiner bio-one, Frickenhausen |
| Corning Costar black 96-well plates with clear bottom for NA activity assay | Thermo Scientific, Karlsruhe |
| Cryo tubes (Cryo STM) | Greiner bio-one, Frickenhausen |
| Falcons (15 and 50 ml) | Greiner bio-one, Frickenhausen |
| Injection needles, 21 G x 1 1/2' (0,8 mm x 40 mm) for ferret blood sampling | BD Becton Dickinson, Franklin Lakes |
| Lysing Matrix D Tubes | MP Biomedicals, Eschwege |
| MultiScreen-IP, 0.45 µm, 96-well plates for ELISpot | Millipore/Merck, Darmstadt |
| Multiwell-plates (6-, 12-, 24- and 96-well plates) | Nunc, |
| Nunc MaxiSorp 96-well plates for ELLA | VWR |
| Omniccan F, 1ml syringes | B. Braun, Melsungen |
| PCR reaction tubes, 0.2 ml | Thermo Scientific, Karlsruhe |
| Pipette filter tips (10, 100, 300 and 1000 µl) | 4titude Ltd., Berlin |
| Pipette tips (20, 200 and 1000 µl) | Eppendorf, Hamburg |
| Plate sealers, 96-well plates | Sarstedt, Nümbrecht |
| Polyvinylidendifluorid (PVDF) membrane | Millipore/Merck, Darmstadt |
| Serological pipettes (5, 10 and 25 ml) | Greiner bio-one, Frickenhausen |
| Serum tubes, 1.1 ml with Gel Separator | Sarstedt, Nümbrecht |
| Serum tubes, Z serum clot activator tube with gel separator (2 ml, 5 ml) Vacuette | Greiner bio-one, Frickenhausen |
| Single-use reagent reservoir, 50 ml | Roth, Karlsruhe |

| | |
|---|---|
| Single-use syringes B. Braun Omnifix F (1 ml) | B. Braun, Melsungen |
| U-bottom multiplate, PS-Microplate (96-well) | Greiner bio-one, Frickenhausen |
| Whatman filter paper | GE Healthcare, Backinhamshire |

## 2.5. Equipment and Instruments

| PRODUCT | SOURCE |
|---|---|
| ABI Prism 3100 Genetic Analyzer | Thermo Scientific, Karlsruhe |
| Cell culture incubator Heracell 150i | Thermo Scientific, Karlsruhe |
| Centrifuge Eppendorf 5417 R equipped with rotor FA-45-24-11 | Eppendorf, Hamburg |
| Centrifuge Eppendorf 5418 equipped with rotor FA-45-18-11 | Eppendorf, Hamburg |
| Centrifuge Eppendorf 5810 R equipped with swinging bucket rotor A-4-81 | Eppendorf, Hamburg |
| chemiluminescent imaging system: MicroChemi 4.2, Kamera MicroLine ML 4022 | DNR Bio Imaging Systems, Jerusalem |
| Class II biological safety cabinet | Thermo Scientific, Karlsruhe<br>Labotec, Ormond Beach, Florida |
| Drying cabinet: WTC | Binder, Tuttlingen |
| ELISA reader TECAN sunrise | Tecan Group Ltd., Männedorf |
| Flourescence/Absorbance plate reader: Genios plus | Tecan Group Ltd., Männedorf |
| Freezer (-20°C) GG4010-20 | Liebherr, Biberach an der Riss |
| Freezer (-80°C) HERAfreeze Top | Thermo Scientific, Karlsruhe |
| Fridge FKS 1800-20 | Liebherr, Biberach an der Riss |
| Gel electrophoresis chamber: Mini-Protean | Bio-Rad Laboratories, München |
| Gel electrophoresis chamber: RunOne Electrophoresis Cell | EmbiTec, San Diego, CA |
| Heating block MR Hei-Standard | Heidolph Instruments GmbH & Co. KG, Schwabach |
| Highspeed-centrifuge: Avanti® J-26S XPI | Beckmann Coulter, Krefeld |
| Homogenisator | PEQLAB Biotechnologie GMBH, Erlangen |
| Incubator Heraeus Instruments | Thermo Scientific, Karlsruhe |
| Incubator shaker Innova® 42 | New Brunswick Scientific, Edison (NJ) |
| Microscope Nikon ECLIPSE Ti-S equipped with camera Nikon DIGITAL SIGHT DS-QiIMc-U3 and software Nis-Elements 4.20.00 LO | Nikon GmbH , Düsseldorf |
| Microscope Nikon Eclipse TS100-F | Nikon GmbH, Düsseldorf |
| Microwave: 7809 | Severin, Sundern |
| Mr. Frosty Freezing container | Thermo Scientific, Karlsruhe |
| Multichannel pipette: Finnpipette F2 | Thermo Scientific, Karlsruhe |
| Neubauer chamber: Neubauer Brightlight | LO-Laboroptik, Friedrichsdorf |
| PCR-Cycler: TProfessional TRIO 48 | Biometra, Göttingen |
| Pipetter: accu-jet pro | Brand, Wertheim |

| | |
|---|---|
| Pipettes: Reference 2 (0.1–0.5 µl, 0.5–10 µl, 10–100 µl, 20–200 µl, 100–1000 µl) | Eppendorf, Hamburg |
| Shaker SSL4 | Stuart, Villepinte |
| Spectrometer: NanoDrop 2000c | Thermo Scientific, Karlsruhe |
| Tissue culture hood MSC-Advantage 1.2 | Thermo Scientific, Karlsruhe |
| Transfer system: Trans-Blot SD Semy-Dry | Bio-Rad Laboratories, München |
| Ultra-centrifuge: Optima L-80 XP, Swinging bucket rotors: SW 32 Ti, SW 41 Ti | Beckmann Coulter, Krefeld |
| Vacuum pump TopStream 3000 | Fastbiotech, Frankfurt |
| Vortex mixer | Heidolph Instruments, Schwabach |
| Water bath | GFL, Burgwedel |

## 2.6. Software

| SOFTWARE | SOURCE |
|---|---|
| Chimera 1.11.2. | UCSF |
| Clone Manager Professional 9 | Sci-Ed Software |
| GenBank | NCBI |
| ImageJ | National Institutes of Health, USA |
| Magellan 7.1 Sp1 | Tecan Group Ltd., Männedorf |
| MEGA, Version 7.0.26 | Molecular Evolutionary Genetics Anaylsis version 7.0 for bigger datasets |
| Prism 7 for Windows, Version 7.04, 2017 | GraphPad Software, Inc., La Jolla (CA) |
| Sequencher 5.3 | Gene Code Corporation |

## 2.7. Eukaryotic cell lines

| CELLS | ATCC | DESCRIPTION |
|---|---|---|
| BHK-21 | CCL-10 | Baby hamster kidney cells, German Collection of Microorganisms and Cell Culture, Braunschweig |
| BHK-G43 | | BHK-21 cells expressing the VSV-G gene in an inducible manner (Hanika et al. 2005) |
| MDCK | CCL-34 | Madin-Darby canine kidney cells, Paul-Ehrlich-Institut, Langen |
| VeroE6 | CRL-1586 | Cercopithecus aethiops kidney cells, Paul-Ehrlich-Institut, Langen |

## 2.8. Plasmids

| PLASMID | DESCRIPTION | GENBANK | SOURCE |
|---|---|---|---|
| VSV*ΔG | Genomic plasmid VSV*ΔG containing 5 distinct transcription units (N-P-M-eGFP_L) | - | Gert Zimmer, IVI, Mittelhäusern |

| | | | |
|---|---|---|---|
| VSV*ΔG($NA_{H5N1}$) | Genomic plasmid pVSV*ΔG(NA) containing 5 distinct VSV transcription units and Influenza A virus (A/chicken/Yamaguchi/7/2004(H5N1)) NA gene for neuraminidase (N-P-M-NA-eGFP-L) | AB166864.1 | (Halbherr *et al.*, 2015) |
| VSV*ΔG($HA_{PR8}$) | Genomic plasmid pVSV*ΔG(HA) containing 5 distinct VSV transcription units and Influenza A virus (A/Puerto Rico/8/1934(H1N1)) HA gene for hemagglutinin (N-P-M-HA-eGFP-L | CY009444.1 | Gert Zimmer, IVI, Mittelhäusern |
| VSV*ΔG($NA_{PR8}$) | Genomic plasmid pVSV*ΔG(NA) containing 5 distinct VSV transcription units and Influenza A virus (A/Puerto Rico/8/1934(H1N1)) NA gene for neuraminidase (N-P-M-NA-eGFP-L) | CY009446.1 | this thesis |
| VSV*ΔG($NA_{USSR}$) | Genomic plasmid pVSV*ΔG(NA) containing 5 distinct VSV transcription units and Influenza A virus (A/USSR/90/1977(H1N1)) NA gene for neuraminidase (N-P-M-NA-eGFP-L) | CY121880.1 | this thesis |
| VSV*ΔG($NA_{H7N9}$) | Genomic plasmid pVSV*ΔG(NA) containing 5 distinct VSV transcription units and Influenza A virus (A/Hangzhou/1/2013(H7N9)) NA gene for neuraminidase, synthetically generated plasmid with MluI and BstEII restriction sites flanking the NA ORF (N-P-M-NA-eGFP-L) | KC853765.1 | Gert Zimmer, IVI, Mittelhäusern |
| VSV*ΔG($HA_{pdmH1N1}$) | Genomic plasmid pVSV*ΔG(HA) containing 5 distinct VSV transcription units and Influenza A virus (A/California/04/2009(H1N1)) HA gene for hemagglutinin (N-P-M-HA-eGFP-L) | CY185302.1 | Dr. Gert Zimmer, IVI, Mittelhäusern |
| VSV*ΔG($NA_{pdmH1N1}$) | Genomic plasmid pVSV*ΔG(NA) containing 5 distinct VSV transcription units and Influenza A virus (A/Mexico/InDRE4487/2009 (H1N1)) NA gene for neuraminidase (N-P-M-NA-eGFP-L) | FJ969517.1 | this thesis |

## 2.9. Replicon Vaccine Vectors (VSV Plasmids)

| VECTOR | DESCRIPTION |
|---|---|
| VSV*ΔG | G- deleted VSV, expression of eGFP from an additional open reading frame |
| VSV*ΔG($HA_{PR8}$) | G- deleted VSV, expression of eGFP and HA(PR8) from an additional open reading frame |
| VSV*ΔG($NA_{PR8}$) | G- deleted VSV, expression of eGFP and NA(PR8) from an additional open reading frame |
| VSV*ΔG($NA_{USSR}$) | G- deleted VSV, expression of eGFP and NA(USSR) from an additional open reading frame |
| VSV*ΔG($NA_{H5N1}$) | G- deleted VSV, expression of eGFP and NA(H5N1) from an additional open reading frame |
| VSV*ΔG($NA_{H7N9}$) | G- deleted VSV, expression of eGFP and NA(H7N9) from an additional open reading frame |
| VSV*ΔG($HA_{pdmH1N1}$) | G- deleted VSV, expression of eGFP and HA(California) from an additional open reading frame |
| VSV*ΔG($NA_{pdmH1N1}$) | G- deleted VSV, expression of eGFP and NA(Mexico) from an additional open reading frame |

## 2.10. Oligonucleotides

| Oligonucleotide | Sequence |
|---|---|
| HA(PR8)-S (MluI) | TTCCTTACGCGTATGAAGGCAAACCTACTGGTCCTGTTA |
| HA(PR8)-AS (BstEII) | TTCCTTGGTAACCCTCAGATGCATATTCTGCACTGCAAA |
| NA(PR8)-S (MluI) | TTCCTTACGCGTAAAATGAATCCAAATCAGAAAATAAT |
| NA(PR8)-AS (BstEII) | TTCCTTGGTAACCCTACTTGTCAATGGTGAATGGCAACT |
| NA(USSR)-S (MluI) | TTCCTTACGCGTAAAATGAATCCAAATCAGAAAATAAT |
| NA(USSR)-AS (BstEII) | TTCCTTGGTAACCCTACTTGTCAATGGTGAATGGCAAC |
| NA(H5N1)-S (MluI) | TTCCTTACGCGTCACTATGAATCCAAATCAGAAGATAATAAC |
| NA(H5N1)-AS (BstEII) | TTCCTTGGTAACCCTACTTGTCAATGGTGAATGGCAACTC |
| HA(pdmH1N1)-S (MluI) | CGATCTGTTTACGCGTCACCATGAAGGCAATACTAGTAG |
| HA(pdmH1N1)-AS (BstEII) | TTCCTTGGTAACCTTAAATACATATTCTACACTGTAGA |
| NA(pdmH1N1)-S (MluI) | TCCTTACGCGTAAAATGAATCCAAACCAAAAGATAAT |
| NA(pdmH1N1)-AS (BstEII) | TTCCTTGGTAACCTTACTTGTCAATGGTAAATGGCAACT |
| VSV-IS | AGCCTCTCGAACAACTAATATCC |
| pEGFPN1_rev | GTCCAGCTCGACCAGGATG |

## 2.11. Viruses

| VIRUS | SOURCE |
|---|---|
| Influenza A virus (A/California/04/2009 (H1N1)) | Prof. Dr. Veronika von Messling, Paul-Ehrlich-Institut, Langen |
| Influenza A virus (A/Mexico/InDRE4487/2009 (H1N1)) | Prof. Dr. Veronika von Messling, Paul-Ehrlich-Institut, Langen |
| Influenza A virus (A/Puerto Rico/8/34 (H1N1)) | Prof. Dr. Veronika von Messling, Paul-Ehrlich-Institut, Langen |

| | |
|---|---|
| Influenza A virus (A/USSR/90/1977 (H1N1)) | Prof. Dr. Veronika von Messling, Paul-Ehrlich-Institut, Langen |
| Influenza A virus PR8 HANA H5N1 - derived by reverse genetics: comprises HA and NA genes derived from the clade 1 virus A/Viet Nam/1194/2004 on a PR8 backbone | Prof. Dr. Veronika von Messling, Paul-Ehrlich-Institut, Langen |
| Newcastle disease virus | Dr. Andreas Motitschke, Paul-Ehrlich-Institut, Langen |
| Modified vaccinia Ankara (MVA)-T7 | Prof. Dr. Gerd Sutter, Ludwig-Maximilians-University, München |
| Beta-propiolactone (BPL)-inactivated PR8 | BEI Resources, NIAID, NIH |

## 2.12. Antibodies

| ANTIBODY | DILUTION | SOURCE |
|---|---|---|
| chicken serum anti-$NA_{H5N1}$ | 1:500 | Dr. Gert Zimmer, IVI, Mittelhäusern |
| goat anti-chicken IgG Alexa 546 | 1:500 | Invitrogen, Karlsruhe |
| Ferret serum anti-pdmH1N1 | 1:500 | Prof. Dr. Veronika von Messling, Paul-Ehrlich-Institut, Langen |
| Ferret serum anti-H1N1 PR8 | 1:500 | Prof. Dr. Veronika von Messling, Paul-Ehrlich-Institut, Langen |
| Goat anti-Ferret IgG-h+I HRP conjugated | 1:750 | Biomol, Hamburg / Germany |
| Sheep serum anti-H1N1 PR8 HA sheep serum | 1:1,000 | NIBSC, London |
| Peroxidase AffiniPure Donkey anti-sheep IgG (H+L) antibody | 1:20,000 | Dianova, Hamburg |
| Pierce High Sensitivity Streptavidin-HRP | 1:4,000 | Thermo Scientific, Karlsruhe |
| mouse anti-bovine IFNgamma MCA 1783, ferret ELISpot capture antibody | 1:100 | Bio-Rad, Puchheim |
| rabbit anti-IFNgamma antibody, biotinylated | 1:250 | Dr. Veronika von Messling, Yvonne Krebs, Paul-Ehrlich-Insitut, Langen |

# 3. METHODS

## 3.1. Molecular Biology Methods

### 3.1.1. Polymerase chain reaction (PCR)

PCR was used for the specific amplification of gene segments. Towards this, double stranded DNA was denatured and sense (S) and anti-sense (AS) primers specific for the selected gene segment annealed to the matching DNA strand. Nucleotides were added to the templates using a polymerase, resulting in an identical replicate of the template in each cycle.

For amplification of gene segments from plasmid DNA the Phusion Hot Start II High-Fidelity Kit and 0.4 µM specific primers were used. 50 ng of plasmid DNA, 10 µM dNTP mix, 10x the Phusion Hot Start II High-Fidelity Buffer and 1 unit (U) polymerase were added to a total volume of 50 µl.

The temperature-cycle program was as follows:

**Table 2** | Polymerase chain reaction standard temperature-cycle program.

| **Step** | **Temperature** | **Duration** | |
|---|---|---|---|
| Initial denaturation | 98°C | 1 min | |
| Denaturation | 98°C | 10 sec | 20x |
| Annealing | 55°C | 20 sec | |
| Elongation | 72°C | 4 min | |
| Prolonged elongation | 72°C | 10 min | |
| Cooldown | 4°C | ∞ | |

PCR products were stored at -20°C until further use or directly loaded onto an agarose gel.

### 3.1.2. Agarose gel electrophoresis

Gel electrophoresis was used to separate DNA fragments of different lengths for the detection of PCR products or to purify DNA fragments. PCR products were analyzed using gels made of 1% agarose in 1x TBE-buffer with 2 µl 10 mg/ml ethidium bromide per 40 ml gel. 6x loading dye was added to the PCR products and the 1kb DNA ladder before loading them on the gel. The electrophoresis was performed at 100 V for 40 min and the results were then visualized with a UV-illuminator and photographs were taken. The NucleoSpin Gel and PCR clean-up was used to purify DNA from PCR reagents and enzymes. DNA was bound to a silica-gel membrane in the presence of high salt concentrations, while impurities are removed. After a washing step, pure DNA was eluted under low ionic strength conditions with 5 mM Tris/HCl (pH 8.5).

For purification of DNA fragments and gel extraction, 0.8% agarose was dissolved in 1x TAE-buffer, mixed with 4 µl ethidium bromide at 10 mg/ml per 100 ml solution, and cast. 6x loading dye was added to the PCR products and the 1 kb DNA ladder before loading them on the gel. The electrophoresis was performed at 70 V for 45 min and the results were then visualized and cut under UV light for subsequent extraction of DNA. DNA samples used for further experiments were not directly exposed to UV light. For DNA extraction from the agarose gel, the gel containing DNA was dissolved in the buffer supplied with the kit at 50 °C before loading it on the column. DNA concentration was measured using the NanoDrop spectrophotometer.

### 3.1.3. Cleavage of DNA fragments by restriction digest

To cleave double stranded DNA at specific restriction sites inserted into PCR amplicons and the vector plasmid VSV*ΔG(X), cDNAs were incubated with 0.5 U of the Fast Digest restriction endonucleases Mlu*I* and Eco*91I* (isoenzyme of BstE*II* with a enzymatic activity at 37 °C) in the buffer system as recommended by the manufacturer at 37 °C overnight. Resulting DNA fragments were separated on agarose gels and DNA was extracted as described above.

### 3.1.4. Ligation of DNA fragments

For the subsequent ligation of plasmid DNA and PCR fragments digested with the same restriction endonucleases, ligation reactions were performed with 5 U of bacteriophage T4 DNA ligase in the recommended reaction buffer. A molar ratio of plasmid DNA to PCR fragment of 1:5 was used. The ligation reaction was performed at 14 °C overnight in a final volume of 20µl.

### 3.1.5. Plasmid Transformation

For the amplification of plasmids, 0.1 - 100 ng of plasmid DNA resulting from ligation were added to chemically competent E. coli XL-1. A frozen aliquot of 50 µl chemocompetent *E. coli* was thawed on ice, 4 µl of plasmid DNA resulting from ligation was added to the cell suspension and incubated on ice for 30 min. For uptake of plasmid DNA triggered by heat-shock, the bacteria were incubated for 30 sec at 42 °C. The tubes were immediately transferred onto ice to stop the reaction. After addition of 1 ml of SOC-medium, the cultures were incubated for 60 min at 37 °C on a shaker. 100µl of the bacteria were plated on agar plates containing Ampicillin and incubated over night at 37 °C.

### 3.1.6. Colony PCR

A colony PCR was performed with appropriate primers at a final volume of 25 µl to select the bacterial clones containing the recombinant plasmid DNA of interest. Individual clones of *E. coli* were picked and dispersed first into PCR reaction mix and then transferred into a 1.5ml reaction tube containing 250 µl LB-Medium with Ampicillin. Inoculated tubes with LB-Medium were incubated at 37 °C for 2 h. Standard reaction conditions for PCR amplification were as follows:

**Table 3** | Colony PCR standard temperature cycle program.

| Step | Temperature | Duration | |
|---|---|---|---|
| Initial denaturation | 95°C | 1 min | |
| Denaturation | 95°C | 15 sec | 20x |
| Annealing | 55°C | 30 sec | |
| Elongation | 72°C | 1 min | |
| Prolonged elongation | 72°C | 5 min | |
| Cooldown | 4°C | ∞ | |

The PCR products were analyzed by gel electrophoresis. The corresponding cultures of positive clones were used to inoculate 100 ml of LB medium for midi plasmid DNA preparations, respectively. The resulting plasmids are referred to as VSV*ΔG(X), respectively.

### 3.1.7. Plasmid DNA preparation

For plasmid purification of overnight bacterial cultures, bacteria were pelleted by was performed by centrifugation at 6000× g, 4 °C for 15 min. The plasmid DNA isolation was performed with a NucleoBond Xtra Midi EF Kit according to the manufacturer's protocol and purified plasmid DNA was eluted in 100 µl of the provided TE-EF buffer. DNA concentration was then determined using the NanoDrop ND-100 Spectrophotometer. An additional restriction digest was performed to confirm the resulting product.

### 3.1.8. Sequencing and data analysis

Cycle sequencing of the resulting constructs was performed using the BigDye Terminator V3.1 Cycle Sequencing Kit. Briefly, 2 µg DNA and 2 µM of one of the matching primers VSV-1S or pEGFP1_rev was prepared according to the manufacturer's instructions. Standard reaction conditions for PCR amplification were as follows:

**Table 4** | Temperature-cycle program for PCR amplification for sequencing analysis.

| Step | Temperature | Duration | |
|---|---|---|---|
| Initial denaturation | 96°C | 1 min | |
| Denaturation | 96°C | 10 sec | 25x |
| Annealing | 50°C | 5 sec | |
| Elongation | 60°C | 4 min | |
| Cooldown | 4°C | ∞ | |

The constructs were purified subsequently using the NucleoSEQ Columns and 10 µl of a 1:2 dilution of product in HIDI Formamid were analyzed by the capillary method via the ABI Prism 3100 Genetic Analyzer.

## 3.2. Cell Culture Methods

### 3.2.1. Cultivation of cell lines

All cell lines were maintained at 37 °C in a humidified incubator ventilated with 5% $CO_2$. BHK-21 cells were obtained from the German Cell Culture Collection (DSZM, Braunschweig; Germany) and grown in Earle's minimal essential medium supplemented with 10% fetal bovine serum (FBS) and 200 mM L-glutamine. BHK-G43 cells, which are BHK-21 cells that inducibly express the VSV G protein, were maintained as described previously (Hanika *et al.*, 2005). Madin-Darby canine kidney (MDCK) cells and Vero E6 were provided by Veronika von Messling (Paul-Ehrlich-Institut, Langen, Germany), maintained in Dulbecco's modified Eagle medium (DMEM) supplemented with 5% FBS and 200 mM L-glutamine and passaged twice weekly. Towards this, they were washed with sterile Phosphate-buffered saline (PBS) and detached from the surface using trypsin-EDTA. The detached cells were then resuspended in pre-warmed medium and split at a ratio of 1:10. BHK-G43 cells were treated with 0.5 mg/ml Zeocin and 125 µg/ml Hygromycin B every fourth passage.

### 3.2.2. Cryo-preservation and thawing of cell lines

For cryo-preservation of eukaryotic cell lines, trypsin-EDTA-detached cells were centrifuged at 4 °C and 5000x g for 3 min and washed once with PBS. Cell pellets were resuspended in 90% FBS and 10% DMSO and aliquoted into cryo tubes and frozen at -80 °C using a Mr. Frosty Freezing container filled with Isopropanol. 24 h later, cells were stored at -80 °C. For thawing, cells were incubated for 1 to 2 min in a 37 °C water bath and transferred into a cell culture flask with pre-warmed medium supplemented with 10% FBS and 1% L-glutamine. Cell culture medium was exchanged the next day and cells were cultured as previously described.

### 3.2.3. Propagation of recombinant VSV replicons

To obtain VSV replicon particles, BHK-G43 cells were infected with recombinant MVA-T7 virus expressing the T7 RNA polymerase (Sutter, Ohlmann and Erfle, 1995). Prior to infection, expression of the VSV G protein was induced by adding mifepristone at a concentration of $10^{-9}$ M to the cell culture medium. Cells were co-transfected with the respective genomic plasmid along with three helper plasmids encoding the VSV N, P, and L proteins under control of the T7 promoter, as described previously (Halbherr *et al.*, 2013). After 24 h incubation, the cells were trypsinized and seeded along with an equal number of fresh BHK-G43 cells and incubated for an additional 24 h at 37 °C in the presence of mifepristone (Rentsch and Zimmer, 2011). The supernatant was clarified by low-speed centrifugation at 1000x g for 15 min at 4 °C, and stored at -80 °C. An additional control plasmid, VSV*-ΔG, containing 5 genes in the order (N-P-M-eGFP-L) but lacking the glycoprotein gene was kindly provided by Dr. Gert Zimmer (IVI Mittelhäusern, Switzerland).

For amplification of the replicons, BHK-G43 cells were induced to express VSV G protein by adding mifepristone before infection with the respective replicons. When the cytopathic effect was widespread, the supernatant was harvested, clarified by centrifugation at 1000x g for 15 min at 4 °C, followed by purification through a 20% (w/v) sucrose cushion at 100,000 x g for 1 h at 4ºC, and resuspended in PBS. Replicon stocks were stored at -80 °C.

### 3.2.4. VSV replicon titration

All VSV replicons were titrated on BHK-21 cells. Towards this, the cells were seeded in 96-well plates to 90% confluence and duplicate wells were inoculated with 10-fold serial virus dilutions. After 8 to 12 h at 37 °C and 5% $CO_2$, cells expressing GFP were detected with a fluorescence microscope. Virus titers were calculated as number of GFP-expressing cells × dilution factor × volume of inoculums/ml and expressed as fluorescence forming unit per milliliter (ffu/ml).

### 3.2.5. Virus production

The H1N1 influenza strains A/Puerto Rico/08/34 (PR8) and A/USSR/90/1977 (USSR), H5N1 A/chicken/Yamaguchi/7/2004 (H5N1), H7N9 A/Hangzhou/1/2013 (H7N9), and pdmH1N1 A/Mexico/InDRE4487/2009 were grown on MDCK cells in serum-free DMEM supplemented with 0.75 µg/ml tosylsulfonyl phenylalanyl chloromethyl ketone-treated trypsin (TPCK-trypsin). When cytopathic effect was widespread, the supernatant was harvested, clarified by centrifugation at 3000x g for 15 min at 4 °C, aliquoted and stored at -80 °C.

For egg-grown PR8 or Newcastle Disease Virus (NDV) eleven-day-old embryonated eggs were inoculated by the allantoic route and incubated at 37 °C and 60% humidity in an egg incubator. Infected allantoic fluid was harvested under sterile conditions 48 h after inoculation and purified through a 20% (w/v) sucrose cushion at 135,000x g for 2 h at 4 °C. Pellets were resuspended in PBS with 10% FBS and the hemagglutination titer of each virus was determined (see 3.2.7).

### 3.2.6. Virus and nasal wash quantification

To quantify influenza virus titers after one freezing cycle, MDCK cells were seeded in 96-well plates at 90% confluence, and quadruplicate wells were inoculated with 10-fold serial dilutions of the supernatant. After two days of incubation at 37 °C and 5% $CO_2$, the plates were washed once with PBS diluted 1:3 in double-distilled H2O, air dried for 15 min, and fixed at 65 °C for 8 h. Infected cells were stained by adding a matched ferret anti-influenza serum at a dilution of 1:500, followed by an incubation for 2 h at room temperature. The plates were then washed with PBS and incubated with a 1:750 dilution of a horseradish peroxidase-coupled anti-ferret secondary antibody for 1 h at room temperature. Following a final washing step, positive cells were visualized with 3-amino-9-ethyl-carbazole staining. Virus titers were expressed as the 50% tissue culture infectious dose per ml ($TCID_{50}$/ml), and were calculated according to Spearman and Kaerber (Spearman, 1908; Kärber, 1931) as follows:

$$logTCID_{50} = x_k + \frac{d}{2} - d\sum p$$

$x_k$ = decadic logarithm of the highest dilution in which all wells show a cytopathic effect

d = decadic logarithm of the dilution factor

p = amount of wells showing a cytopathic effect in higher dilutions than $x_k$.

Nasal washes in 50 ml centrifugation tubes were centrifuged at 1600x g and 4 °C for 3 min and the supernatant transferred into 1.5 ml Eppendorf tubes on ice. Dilution of nasal wash fluid was performed as described above using DMEM + 3% Pen/Strep to prevent bacterial overgrowth.

### 3.2.7. Hemagglutination assay (HA)

The hemagglutination assay (HA) is a common method used for influenza virus titration. The principle of this assay is based on the ability of the influenza HA protein to bind to N-acetylneuraminic acid of red blood cells, thereby forming a lattice-like structure. In the absence of viral particles, the erythrocytes do not agglutinate and instead form a round spot at the bottom of the plate. Towards this, chicken blood samples diluted 1:1 in Alsever's solution were centrifuged for 10 min at 1500x g and

4 °C. Subsequently two washing steps with 2 times the volume of erythrocytes in 0.85% NaCl, and centrifugation at 1500x g and 4 °C for 5 min were performed. After a third washing step, the red blood cell (RBC)-solution was centrifuged for another 10 min at 1500x g and 4 °C and adjusted to 0.75% RBCs in NaCl, which was then used for the experiments.

The HA was performed as outlined in the World Organization for Animal Health (OIE) manual (World Organization for animal health, 2015). 50 µl of virus sample were serially diluted in rows of a U-bottomed 96-well plate using a 2-fold dilution series. 50 µl of the 0.75% guinea pig RBC suspension was added. Virus titers were expressed as HA units (HAU), corresponding to the reciprocal of the highest dilution causing complete erythrocyte agglutination.

### 3.2.8. Virus quantification in ferret tissue

Virus titers in ferret organs were determined via tissue titration. Towards this, lung, NT, or trachea tissue was homogenized and titrated in 10-fold dilutions in DMEM + 3x Pen/Strep. For homogenizing, tissue was placed into Lysing Matrix tubes with media and was homogenized using the following programs:

**Table 5** | Tissue homogenization programs.

| Organ | Time [s] | Cycles | Rpm |
|---|---|---|---|
| **Lungs** | 20 | 2 | 5500 |
| **Nasal turbinates** | 20 | 2 | 6500 |
| **Trachea** | 20 | 2 | 6500 |

Tissue homogenate was centrifuged at 1600x g and 4 °C for 3 min and the supernatant transferred into 1.5 ml Eppendorf tubes on ice Titrations were performed as described above (3.2.6) and the titer was expressed in $TCID_{50}$/g, to reflect the different tissue weights, using the following equation:

$$\frac{volume\ [ml]\ x \frac{TCID_{50}}{ml}\ x\ 1/1000}{tissue\ weight\ [g]} = TCID_{50}/g$$

### 3.2.9. Isolation of ferret PBMCs

Peripheral blood mononuclear cells (PBMCs) were isolated from fresh heparinized ferret blood through Histopaque density centrifugation method. Briefly, plasma was removed by centrifugation at 1800x g for 15 min. Remaining blood samples were diluted 1:1 with PBS and transferred onto room-temperature Histopaque. Samples were centrifuged at 400x g for 40 min with a medium acceleration and breaks turned off. The resulting layer containing mononuclear cells was removed and washed three times with Roswell

Park Memorial Institute (RPMI) 1640 medium, resuspended in 1 ml of $RPMI_{Elispot}$, and cells were counted using a Neubauer chamber.

### 3.2.10. Isolation of murine splenocytes

Spleens were mashed and filtered through a 70 µm cell strainer with 45 ml PBS. Cells were then centrifuged for 15 min at 800x g, and the cell pellet was resuspended in 5 ml red blood cell lysis buffer and incubated for 10 min at room temperature to lyse the red blood cells. Lysis was stopped by addition of 45 ml PBS and cells were pelleted at 300x g for 10 min. After repeating the cell lysis step once, the cell pellet was resuspended in 2 ml $RPMI_{Elispot}$, and cells were counted using a Neubauer chamber.

## 3.3. Animal Experiments

### 3.3.1. Immunization of mice and ferrets

All animal experiments were carried out in compliance with the regulations of German animal protection laws and were authorized by the responsible state authority. Balb/c and C57BL/6N mice were obtained from Janvier Labs, Le Genest-Saint-Isle, France. Six- to eight-week-old female mice were immunized twice intramuscularly four weeks apart with $1x10^6$ ffu of the respective VSV replicon particles diluted in 50 µl PBS or beta-propiolactone (BPL)-inactivated PR8 as a control.

Male and female ferrets (Mustela putorius furo) 16 weeks or older and seronegative for influenza viruses were provided by the breeding colony at Paul-Ehrlich-Institut, Langen. Males and Females were distributed evenly in all four groups. Groups of 4 animals were immunized twice intramuscularly 4 weeks apart with $1x10^8$ ffu of the respective VSV replicon particles or three times intranasally with $7.5x10^{12}$ genome equivalents of AAV vector, respectively. TIV from 2017/18 was administered two times i.n. and replaced by PBS for the third immunization.

### 3.3.2. Blood sampling and spleen isolation

To quantify the antibody responses on days 28, 35, and 56 after the initial immunization, 6 mice of each group were anesthetized by intraperitoneal injection with ketamine (100 mg/kg) and xylazine (10mg/kg) and exsanguinated by cardiac puncture. Serum tubes with gel separator were centrifuged at 14000x g for 10 min and serum was transferred into 1.5 ml Eppendorf tubes and stored at -20 °C for further analysis. For T cell responses, mice were sacrificed 7 days after the second immunization via cervical dislocation during ketamin/xylazin anesthesia. Mice were sterilized with 70% ethanol, before dissection of the spleen, which was directly transferred into 5 ml ELISpot medium.

Blood samples from ferrets were collected under medetomidine anesthesia via the cranial vena cava on day 0, and on the days of immunization and challenge infection. Serum Clot Activator Tubes with Gel Separator were centrifuged for 15 min at 1600x g and serum was transferred into 1.5 ml Eppendorf tubes and stored at -20 °C.

### 3.3.3. Intranasal influenza infection of mice

For virus challenge, mice were anesthetized by intraperitoneal injection with ketamine (100 mg/kg) and xylazine (10 mg/kg) and inoculated intranasally with $10^4$ $TCID_{50}$ of PR8 in 30 µl corresponding to 3x $LD_{100}$. Animals were monitored daily for clinical signs and body weight and euthanized as soon as the weight loss reached 25%. For T cell response analysis, spleens were harvested 7 days after the second immunization.

Four weeks after the last immunization, ferrets were anaesthetized with 0.1 ml ketamine (0.8 mg/kg)/medetomidine (0.125 mg/kg) and challenged intranasally with $10^5$ $TCID_{50}$ of A/Mexico/InDRE4487/2009 (H1N1) in 200 µl OptiMEM. Animals were monitored for signs of disease for 3 days post-challenge using a 0-1-2-3 scale for activity, respiratory (sneezing, nose exsudate, and congestion) and general clinical signs, with 0 representing the baseline physiological state (Kugel *et al.*, 2009). The assessed parameters were:

1) temperature (<38.5°C/38.5-39.0°C/39.0-39.5°C/>39.5°C),

2) weight loss (none/0-5%/5-10%/>10% loss of initial weight),

3) activity (normal/calm/depressed/inactive),

4) nasal exudate (none/serous/sero-mucous/muco-purulent),

5) congestion (none/mild/intermediate/severe),

6) sneezing (none/rarely/occasionally/frequently), and

7) assessment of labored breathing (none/occasional wheezing/continuous wheezing/labored breathing).

The scores were added together for each animal at each observation timepoint to obtain the cumulative clinical score. Changes in body temperature and body weight were also recorded. Nasal washes were collected daily and viral titers were determined. Towards this, 500 µl of PBS was instilled in one nostril and expectorate was collected in 50-ml centrifuge tubes. This procedure was repeated twice to obtain a minimum volume of 400 µl. Three days post-challenge, all animals were anesthetized with ketamine/medetomidine and sacrificed by intracardial injection of T61 at a dose of 0.3 ml/kg, and lung, nasal turbinates, and trachea were collected.

### 3.3.4. Passive serum transfer in C57BL/6 mice

To investigate the role of the antibodies in protection from infection, naïve animals were injected intraperitoneally with 500 µl of pooled sera collected on day 35 after initial immunization. The next day, mice were anesthetized by intraperitoneal injection with ketamine and xylazine, bled via the retrobulbar route, and infected intranasally with PR8 as outlined above. Recipient animals with total anti-PR8 antibody titers below 50% of the initial donor titer were considered a transfer failure and subsequently excluded from the study ($NA_{PR8}$ n=2, inactivated PR8 n=2).

## 3.4. Immunological Methods

### 3.4.1. Immunofluorescence analysis

Vero cells grown on 12-mm-diameter cover slips were inoculated with the respective VSV*ΔG replicons using a MOI of 1 ffu/cell and incubated at 37 °C for 12 h. Cells were washed with PBS and incubated with a 1:500 dilution of $NA_{H5N1}$ chicken antibody for 1 h. Subsequently, cells were washed three times and fixed with 3% paraformaldehyde for 30 min and then washed with PBS containing 0.1 M glycine. The cells were subsequently incubated with 1:500 goat anti-chicken IgG Alexa 546 for 1 h before three washing steps with distilled water. Finally, cells were embedded in DAPI Fluoromount-G and analyzed using a fluorescence microscope.

### 3.4.2. Biotinylation of cell surface proteins

To analyze cell surface protein expression, VeroE6 cells were seeded in 6-well plates and infected with the respective VSV replicons at a multiplicity of infection (MOI) of 10 in DMEM supplemented with 5% FBS and 1% L-glutamine. Non-infected BHK-21 cells were used as a control. 12 h post-infection, supernatant was removed, and cells were washed with ice-cold PBS three times for 5 min. Subsequently, cell surface proteins were biotinylated with 2mM EZ-Link sulfo-NHS-LC-LC-Biotin in PBS for 20 min. Three washing steps were performed using ice-cold PBS supplemented with 100 mM glycine to quench the reaction and remove all excess biotin. Cells were subsequently lysed with RIPA lysis buffer supplemented with HALT protease inhibitors according to the manufacturers' instructions for 15 min at 4 °C. Cell lysates were centrifuged at 14,000x g for 10 min at 4 °C to remove cell debris, and the supernatants were stored at –20 °C until further use. Protein concentration was determined using a BCA protein assay kit.

### 3.4.3. Immunoprecipitation

For immunoprecipitation 50 µg of total protein was co-incubated with 5 µl of homologous mouse serum from previously immunized mice. Total antibody titers of the

sera of previously immunized mice with the respective VSV replicons were adjusted to 3200. Samples were incubated under rotation at 4 °C for 3 h with the addition of protein G Plus agarose beads during the last h. Beads were then pelleted by centrifugation, washed 4 times with RIPA lysis buffer without protease inhibitors and resuspended in 30 µl of 4x SDS gel-loading buffer with 20% β-Mercaptoethanol.

### 3.4.4. Sodium Dodecyl Sulfate-Polyacrylamide Gel Electrophoresis (SDS-PAGE)

For verification of protein expression in target cells, the eluted immunoprecipitation samples were were incubated at 75 °C for 10 min to fully denature the proteins, and then separated by a 10% sodium dodecyl sulfate-polyacrylamide gel electrophoresis (SDS-PAGE) for 90 min at 160 V.

For quantification of the HA protein content of inactivated PR8 virus preparations, pre-determined concentrations of PR8 HA protein were 2-fold serially diluted in PBS and mixed with 2x SDS gel-loading buffer with 10% β-mercaptoethanol. Virus samples were diluted 1:10 in PBS and also mixed with 2x SDS gel-loading buffer. All samples were denatured at 75 °C for 10 min and four dilutions of known HA protein concentration and pre-diluted virus samples were separated on 10% SDS-PAGE and treated as described above. For Western blot analysis, proteins were transferred onto PVDF membranes as described below.

### 3.4.5. Western Blot analysis

For antibody-mediated detection of the respective protein, SDS-PAGE-separated samples were blotted onto Amersham Hybond-P PVDF membranes using the semi-dry method. The membrane was activated in methanol for 30 s and then washed in transfer buffer. Whatman filter papers, membranes and polyacrylamide gel were also soaked in transfer buffer and then arranged in layers in the transfer chamber. Proteins were blotted onto the membrane for 30 min at 12 V and unspecific binding was blocked using Tris-buffered saline with 0.1% Tween20 (TBS-T) and 5% skim milk powder (w/v) overnight at 4 °C.

For the specific detection of biotinylated influenza proteins, membranes were incubated with Pierce High Sensitivity Streptavidin-HRP diluted 1:4000 in TBS-T for 1 h at room temperature. After three washing steps with TBS-T for 5 min each, bands were visualized using Amersham ECL Prime Western blotting detection system with a MicroChemi 4.2 chemiluminescent imaging system, and the resulting bands were quantified from underexposed TIF images using ImageJ Analysis Software package.

For quantification of HA protein content in inactivated PR8 virus, membranes were incubated with a PR8 HA-specific primary antibody diluted 1:1000 in TBS-T for 2 h

at room-temperature to allow specific binding of proteins. Membranes were washed 3 times for 5 min with TBS-T, incubated for 1 h with 1:200,000 HRP-coupled anti-sheep secondary antibody in TBS-T. Membranes were washed again three times with TBS-T for 5 min before visualization with Amersham ECL Prime Western blotting detection system with a MicroChemi 4.2 chemiluminescent imaging system. The resulting bands were quantified from underexposed TIF images using ImageJ Analysis Software package, and HA concentration of vaccine samples were quantified by standard curve of known PR8 HA concentrations.

### 3.4.6. Neuraminidase activity assay

To quantify NA activity in VeroE6 cells infected with VSV replicons, $1x10^5$ cells were seeded in 96-well black polystyrene plates with clear bottom and infected at a MOI of 10 with the respective replicons. 12 h post-infection, supernatant was remove and replaced by 50 µl 0.2 mM 2'-(4-Methylumbelliferyl)-α-D-N-acetylneuraminate (MUNANA) diluted in NA assay buffer. Plates were sealed and incubated at 37 °C for 30 min. 100 µl NA assay stop buffer was added and plates were incubated for 30 min at room temperature. Free 4-methylumbelliferone (4-MU) was determined using a spectrofluorometer at an excitation of 365 nm and emission of 450 nm.

### 3.4.7. Enzyme-Linked ImmunoSpot (ELISpot) assay

To quantify the amount of antigen-reactive IFN-γ producing T cells in murine splenocytes or ferret PBMCs, the Mouse IFN-γ ELISPOT Ready-SET Go!® or equivalent reagents were used. The day before the isolation of the cells, a 96-well plate with PVDF-membrane bottom was activated with 70% ethanol and then washed with 200 µl sterile $H_2O$. Subsequently, plates were washed two times with 200 µl PBS, andcwells were coated with an IFN-γ capture antibody at a dilution of 1:250 for mouse assays and 1:100 for ferret assays in coating buffer or PBS, respectively. Plates were incubated overnight at 4 °C.

The next day, the plate was washed twice with 200 µl Sterile Azide-Free Coating Buffer or sterile RPMI per well, before blocking with 200 µl $RPMI_{Elispot}$ per well for 2 h or longer at room temperature. $2x10^5$ previously isolated splenocytes or PBMCs were seeded per well and incubated with 6 µg/ml Concanavalin A (ConA) for unspecific T cell activation as positive control, medium only as negative control, or 10 HAU pdmH1N1 or NDV for 36 h at 37 °C. Cells were then removed from the plate, and wells were washed with $H_2O$ for 10 min and three times with ELISpot washing buffer. The biotinylated detection antibody was diluted 1:250 in the provided assay diluent or PBS with 10% FBS, respectively and incubated for 2 h at room temperature. The plate was washed four times with ELISpot washing buffer, and wells were soaked for 1 min each time. Avidin-HRP or Pierce High

Sensitivity Streptavidin-HRP, respectively, was diluted 1:250 in ELISpot washing buffer and plates were incubated at room temperature for 45 min. After three wash steps with ELISpot washing buffer and two with PBS, wells were incubated with 100 µl 3-Amino-9-ethylcarbazole (AEC) substrate solution in the dark for 10 - 60 min. Development of spots was stopped by washing the wells three times with 200 µl H2O per well. The plates were dried in the dark overnight upside down with the rubber coating removed from the bottom. For detection of spots, plates were analyzed using the AID Elispot reader EL R04.

### 3.4.8. Immunoperoxidase-monolayer-assay (IPMA)

To visualize infected MDCK cells from virus titrations, heat-fixed titration plates (see 3.2.6) were stained by adding a matched ferret anti-H1N1 serum at a dilution of 1:500, followed by an incubation for 2 h at room temperature. The plates were then washed with PBS and incubated with a 1:750 dilution of a horseradish peroxidase-coupled anti-ferret secondary antibody for 1 h at room temperature. Following a final washing step, positive cells were visualized with AEC substrate solution as described in (3.4.7).

### 3.4.9. Total antibody quantification

Total influenza virus-specific antibody responses were quantified using an immuno-peroxidase monolayer assay with PR8- or pdmH1N1-infected MDCK cells as described previously (Direksin, Joo and Goyal, 2002). Briefly, MDCK cells were seeded in 96-well plates at 90% confluence and infected with PR8 at a MOI of 0.01. After 48 h, cells were washed once with PBS diluted 1:3 in double-distilled $H_2O$ and air-dried and fixed at 65 °C for 8 h. Serial two-fold dilutions of mouse or ferret sera were added to the fixed MDCK cells and antibody titers were detected by immunostaining as outlined above (3.4.8) and expressed as the reciprocal of the last serum dilution at which antibody-positive cells were detected.

### 3.4.10. Enzyme-linked lectin assay (ELLA)

To determine the amount of NI antibodies, an enzyme-linked lectin assay (ELLA) was performed as described previously (Couzens *et al.*, 2014). Briefly, flat-bottom, MaxiSorp polystyrene 96-well plates were coated with 100 µl fetuin (25 µg/ml) in 0.1 M PBS. Serum samples were heat-treated at 56 °C for 45 min prior to serial two-fold dilutions in PBS and subsequent co-incubation of duplicates with a predetermined 90% NA activity of PR8 at 37 °C for 16-18 h. After three wash steps with PBS containing 0.05% Tween-20 (PBS-T), peroxidase-labeled lectin from Arachis hypogaea was added and incubated for 2 h at room temperature. Plates were washed again before adding o-phenylenediamine dihydrochloride (OPD) substrate. The reaction was stopped with 1 N sulfuric acid

before reading the absorbance at 490 nm. The NI antibody titer was expressed as the reciprocal of the highest dilution that exhibited ≥50% inhibition of NA activity.

## 3.5. Bioinformatic Methods

### 3.5.1. Phylogenetic analysis

For construction of a phylogenetic tree, amino acid sequences of the NA proteins of IAV strains listed below were aligned using ClustalW standard settings on MEGA7 (Kumar, Stecher and Tamura, 2016). Alignments were subsequently used to construct a phylogenetic tree using neighbor-joining method and 1000 bootstrapped replications with observed amino acid differences as distance on the aligned sequences using MEGA7.

**Table 6** | Influenza A neuraminidase proteins with corresponding Genbank accession numbers used for phylogenetic analysis.

| **influenza A strain** | **Genbank accession number** |
|---|---|
| A/Puerto Rico/8/1934 | CY009446.1 |
| A/USSR/90/1977 | CY121880.1 |
| A/California/04/2009 | FJ969517.1 |
| A/chicken/Yamaguchi/7/2004 | AB166864.1 |
| A/Hangzhou/1/2013 | KC853765.1 |

### 3.5.2. Statistical analysis

Statistical analyses were performed using GraphPad Prism 6. Symbols represent the mean of each group and error bars indicate the standard deviation. In cases of negative standard deviation, error bars are not shown. Statistical analyses were performed on $\log_2$-transformed data using one-way or two-way ANOVA with Tukey post-test. All groups were compared and p-values ≤ 0.05 were considered significant.

# 4. OWN CONTRIBUTION

This PhD thesis involved two projects. My own contribution to each of these projects is detailed below:

## 4.1. Evaluating the extent of cross-protection conferred by the influenza neuraminidase

As part of my Master thesis I started working on the generation and evaluation of NA-expressing single-cycle VSV replicons. Under the supervision of Dr. Gert Zimmer at IVI in Mittelhäusern, Switzerland, I generated amongst others the VSV*ΔG replicons expressing NA proteins of the H1N1 viruses PR8, A/USSR/90/1977 and A/Mexico/InDRE4487/2009. The remaining replicons used in this study were kindly provided by Dr. Gert Zimmer. Furthermore, my Master thesis involved immunization of ferrets and subsequent evaluation of the resulting immune responses, including total antibody responses shown in this thesis and the contribution to protection. After I finished my Master thesis, we concluded that NA-based replicon vaccines merit further investigation. Towards this, I was responsible for the planning and execution of all experiments involved. With the help of Dr. Bevan Sawatsky and Dr. Kerstin Schott, I quantified antigen expression in target cells via cell surface biotinylation and immunoprecipitation. Together with Dr. Sarah-Katharina Kays and with the support of Dr. Theresa Enkrich, we set up the murine influenza model in our group, which I used throughout this study. Yvonne Krebs helped with the animal handling in the passive serum transfer experiment. I independently planned and performed total antibody response and IFNγ ELISpot assays. Dr. Hanna Sediri provided help in setting up and troubleshooting the NI antibody assay (ELLA), and Yvonne Krebs produced most of the ELLA data, including the analysis of the ferret sera. Finally, all bioinformatical methods were self-taught, including the analysis of molecular NA protein structures and phylogenetic analysis with initial support from Dr. Rebecca Schmidt.

As first author of the resulting manuscript published in Journal of Virology in June 2018, I wrote the first draft and prepared data analysis and figures. I finalized the manuscript together with Prof. Dr. von Messling and the help of Dr. Gert Zimmer:

*Neuraminidase-inhibiting antibody titers correlate with protection from heterologous influenza virus strains of the same neuraminidase subtype.* Lisa Walz, Sarah-Katharina Kays, Gert Zimmer, Veronika von Messling. Journal of Virology (2018) pp: JVI.01006-18. doi: 10.1128/JVI.01006-18

## 4.2. Comparing the efficacy of hemagglutinin stalk-induced immune responses in ferrets

In the context of his PhD thesis, Daniel Demminger at Robert Koch Institute in Berlin generated a set of AAV vectors expressing wild type or chimeric HA proteins, which aimed at broadening the specificity and functionality of the antibody response. Towards this, he immunized mice and showed that all constructs resulted in cross-reactive antibodies, including the wild type protein. However, only the AAV vector-based but not IIV vaccination protected mice against heterologous influenza virus challenge. He then initiated a collaboration with our group to confirm his results in the more clinically relevant ferret model. As the influenza ferret model is well established in our facility, Prof. Dr. von Messling, Daniel Demminger, Yvonne Krebs and I performed the experiment together, consisting of the immunizations, regular blood samplings, and the subsequent challenge. After challenge, clinical parameters had to be measured twice daily and nasal washes were taken once a day, which were given to Yvonne Krebs for titration. In addition, I was responsible for planning and conducting the ELISpot assay and the day of sacrifice. For that purpose, I performed preliminary experiments, setting up the ferret-specific IFNγ ELISpot assay, grew pdmH1N1 virus and performed HA titrations. The day of infection, I isolated splenocytes together with Daniel Demminger and performed the assay. With the help of Mareike Dörr and Kristin Pfeffermann, Daniel Demminger and I sacrificed the animals, took blood samples and harvested nasal turbinates, lungs and trachea, which I subsequently homogenized and titrated together with Yvonne Krebs. Furthermore, I performed all total antibody titrations and participated in data analysis of the respective experiments. As a first author, Daniel Demminger has prepared a first draft of the manuscript, which we are currently finalizing and are planning to submit in the near future:

*Adeno-associated virus-vector vaccines protect against influenza by eliciting neutralizing and Fcγ-receptor activating anitbodies.* Daniel E. Demminger, Lisa Walz, Kristina Dietert, Achim Gruber, Veronika von Messling, Thorsten Wolff. In preparation.

During the time of my PhD, I was involved in additional projects, one of which has just recently been submitted to Nature Medicine entitled: *Incomplete genetic reconstitution of B cell pools contributes to prolonged immune suppression after measles*. Velislava N. Petrova, Bevan Sawatsky, Alvin X. Han, Brigitta M. Laksono, Lisa Walz, Carl A. Anderson, Rory D. de Vries, Paul Kellam, Veronika von Messling, Rik L. de Swart, Colin A. Russell.

In this publication, B cell receptor sequencing of measles patients was performed to identify mechanisms, which underly prolonged measles-associated immune

suppression. To complement the findings from patients, Prof. Dr. von Messling and Dr. Bevan Sawatsky immunized ferrets with IIV or LAIV, and then infected the animals with the canine distemper virus (CDV), which is closely related to measles virus. To investigate the impact of Morillivirus infection of pre-existing immunity against influenza, the animals were then challenged with a matched H1N1 influenza strain. My role was to assist during blood sampling and immunization procedures and with the clinical assessment after IAV challenge infection. Furthermore, I evaluated IAV-specific neutralizing antibody titers throughout the experiment and performed nasal wash titrations together with Yvonne Krebs.

# 5. RESULTS

## 5.1. Neuraminidase-Inhibiting Antibody Titers Correlate with Protection from Heterologous Influenza Virus Strains of the Same Neuraminidase Subtype

### 5.1.1. Generation of single-cycle VSV replicon particles expressing the H1N1 PR8 HA or NA proteins

The majority of antibodies induced by IIVs are directed against the HA protein and act in a strain-specific manner (Air, Laver and Webster, 1987; Palese and Shaw, 2007; Scott E. Hensley *et al.*, 2009). To explore the protective potential of an immune response against the more conserved NA protein, we generated propagation-incompetent VSV by replacing the VSV G gene with either the HA or NA gene of H1N1 PR8, or with NA genes from a representative seasonal and pandemic H1N1 strain and a human H5N1 isolate with differing phylogenetic distances (Fig. 12). An additional transcription cassette encoding the enhanced green fluorescence protein (eGFP) gene was added downstream of the influenza antigen (Fig. 8A), in order to facilitate the monitoring of infected cells.

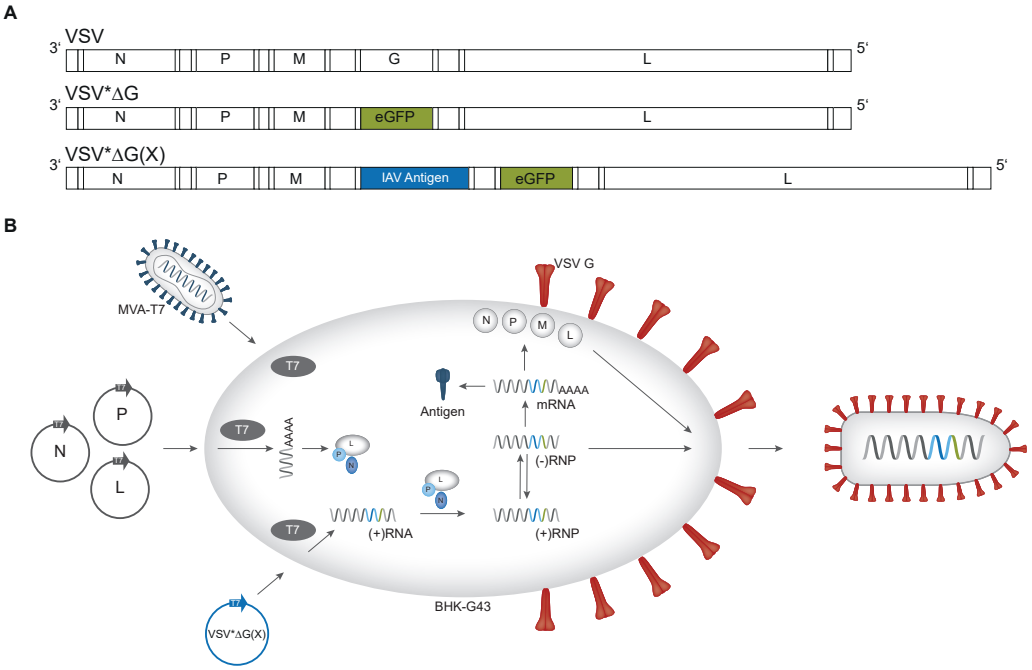


**Fig. 8 | Generation of influenza antigen-expressing VSV replicons. A** | Scheme of the genomes of the parental VSV and the recombinant VSV*ΔG replicons. VSV*ΔG lacks the gene enconding the VSV G protein and includes the eGFP gene in an additional transcription unit, depicted in green (the asterisk denotes for eGFP). VSV*ΔG(X) encode the respective heterologous influenza virus antigens, depicted in blue. **B** | Experimental design for recovery of the VSV*ΔG(X) replicon particles. T7 RNA polymerase is provided by a recombinant vaccinia virus vector (MVA-T7). Cotransfection of the recombinant VSV*ΔG(X) genome in anti-genomic orientation and three helper plasmids, encoding the viral RNA polymerase complex that are transcribed by the T7 RNA polymerase. Subsequently, the viral RNA polymerase complex binds to the anti-genomic RNA, resulting in a positive-stranded ribonucleoprotein (RNP) complex, a natural intermediate in the viral life cycle, which can autonomously perform replication and transcription. Adapted from (Zimmer, 2010, Walz *et al.*, 2018).

A replicon expressing GFP but no AIV antigens was also generated as a control. To rescue the VSV replicon particles, the helper cell line BHK-G43, genetically modified baby hamster kidney (BHK-21) cells that provide the VSV G protein *in trans*, were infected with a recombinant vaccinia virus expressing the T7 phage RNA polymerase (MVA-T7). Subsequently, cells were transfected with the plasmid encoding the respective VSV replicon genome in anti-genomic orientation together with three helper plasmids, driving the expression of the viral RNA polymerase complex all under control of the T7 promoter. After transcription by the T7 polymerase, the viral RNA polymerase complex binds to the anti-genomic recombinant RNA, resulting in a positive-stranded RNP complex, a natural intermediate in the viral life cycle, which can autonomously support replication and transcription (Fig. 8B). The resulting VSV replicon particles were successfully propagated on BHK-G43 cells, yielding virus titers of up to $5x10^8$ ffu/ml. Upon infection of parental BHK cells, no infectious particles were detected (data not shown), confirming that these vectors are only capable of performing a single round of replication (Zimmer *et al.*, 2014; Walz *et al.*, 2018).

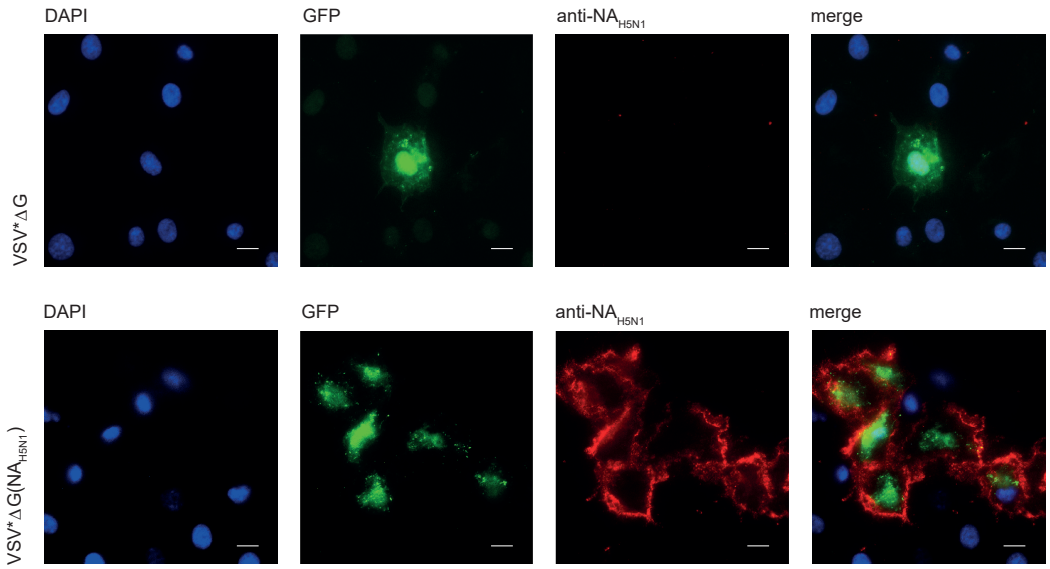


**Fig. 9 | Influenza antigen-expression by VSV replicons.** Immunofluorescence analysis of VeroE6 cells 12 hours post-infection. Cells were grown on cover slips and infected with either VSV*ΔG or VSV*ΔG(NAH5N1) at a MOI of 1. Immunofluorescence staining using a chicken anti-$NA_{H5NI}$ serum and goat anti-chicken IgG Alexa 546 secondary antibody. Subsequently, cells were fixed with 3% PFA and nuclei were stained with DAPI (blue fluorescence). Expression of eGFP indicates infected cells. Scale bar represents 10 µm.

Expression of the antigen on the surface of target cells could be confirmed by immunofluorescence staining. Towards this, VeroE6 cells were seeded on cover slips and subsequently infected with the respective replicons at MOI of 1. Twelve hours post-infection, cells were stained with a polyclonal anti-$NA_{H5NI}$ or anti-HA chicken serum, respectively, and goat anti-chicken IgG Alexa 546 secondary antibody. Subsequently, cells were fixed with 3% PFA and nuclei were stained with DAPI. Successful infection

of the cells was indicated by GFP expression. IAV antigens were detected on the cell surface, while GFP expression was detected in the cytoplasm (Fig. 9). Infection with the VSV*ΔG control vector resulted in GFP expression only and no binding of IAV-specific antibodies. This demonstrates that VSV-based replicon particles effectively infect mammalian cells and derive a surface expression of IAV antigens, here shown by $NA_{H5N1}$-expression, respectively.

### 5.1.2. Vaccination with VSV replicons induces sustainable antibody responses in C57BL/6 and Balb/c mice

Mice are extensively used for influenza research. Even though mice are not a natural host for influenza viruses, they can be infected with certain influenza viruses. The susceptibility of mice to influenza viruses depends both on the mouse strain and the influenza virus isolate. The majority of influenza virus research in mice employs either Balb/c or C57BL/6 strains in conjunction with the mouse-adapted PR8 or A/WSN/1933 (WSN) strains. Here, we used the PR8 virus as challenge strain and compared antibody responses induced by VSV replicons in Balb/c and C57BL/6 mice at different time points after immunization. Towards this, six- to eight-week old mice were immunized intramuscularly with $10^6$ ffu of VSV*ΔG($NA_{PR8}$) or VSV*ΔG($HA_{PR8}$) and boosted with the same dose 28 days later (Fig. 10A). A beta propiolactone (BPL)-inactivated PR8 preparation, representing currently licensed IIVs, and VSV*ΔG were included as controls. Intramuscular inoculation was chosen to reproduce the route of immunization of the seasonal IIV, and to allow the side-by-side comparison of the elicited immune

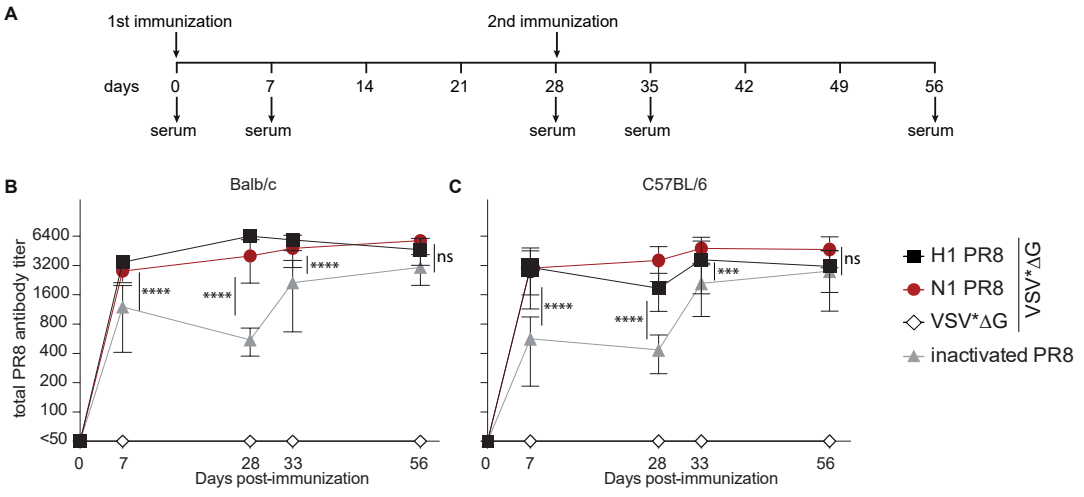


**Fig. 10 | Humoral immune responses in Balb/c and C57BL/6 mice induced by different vaccine candidates. A** | Schematic overview of the immunization strategy and blood and splenocyte sampling time points. Six- to eight-week-old naive Balb/c and C57BL/6 mice were immunized twice with $10^6$ ffu i.m. of the VSV*ΔG replicons or with 2.5 µg of BPL-inactivated PR8 virus and serum samples were taken at indicated time points. Kinetics of **B and C** | Total antibody titers against H1N1 PR8 virus. Symbols represent the mean of each group (n=6), and error bars indicate the standard deviation of the mean. Log2-transformed groups were compared using two-way ANOVA with Tukey post-test. Statistical significance is indicated by *p<0.05; **p<0.01; ***p<0.001; **** p<0.0001.

responses. Sera were collected before immunization as well as one and four weeks after the first and second immunization and total antibody titers directed against the homologous virus strain were quantified by immunoperoxidase monolayer assay (IPMA) with PR8-infected MDCK cells (Fig. 10B and C). Towards this, two-fold serial dilutions of serum were incubated on heat-fixed PR8-infected MDCK cells. The cells were subsequently stained with a horseradish-peroxidase (HRP)-coupled secondary antibody and total antibody titers were expressed as the reciprocal of the last dilution showing detectable staining of influenza-infected cells.

Mice immunized with the control replicon VSV*ΔG did not develop PR8-specific antibodies, irrespective of the mouse strain. All animals vaccinated with VSV*ΔG($HA_{PR8}$) or VSV*ΔG($NA_{PR8}$) produced comparable anti-PR8 virus titers of about 3200 as early as 7 days after the first immunization, which remained stable over the time course of the experiment. Compared to the VSV replicons, antibody titers elicited by the inactivated vaccine were significantly lower after the first immunization ($p \leq 0.0001$), with a higher titer in Balb/c mice after 7 days (ns, $p=0.1437$), which decreased to C57BL/6 titers at day 28 post-immunization. Vaccine-induced titers increased in both mouse strains after the second immunization, reaching similar levels as the VSV replicon vaccine groups. This demonstrates that Balb/c and C57BL/6 mice develop equal antibody levels after the immunization with different PR8-specific vaccines. Hence, C57BL/6 mice will be used for all upcoming experiments, as they provide the possibility of the characterization of not only humoral, but also cellular immune responses (Sellers *et al.*, 2012).

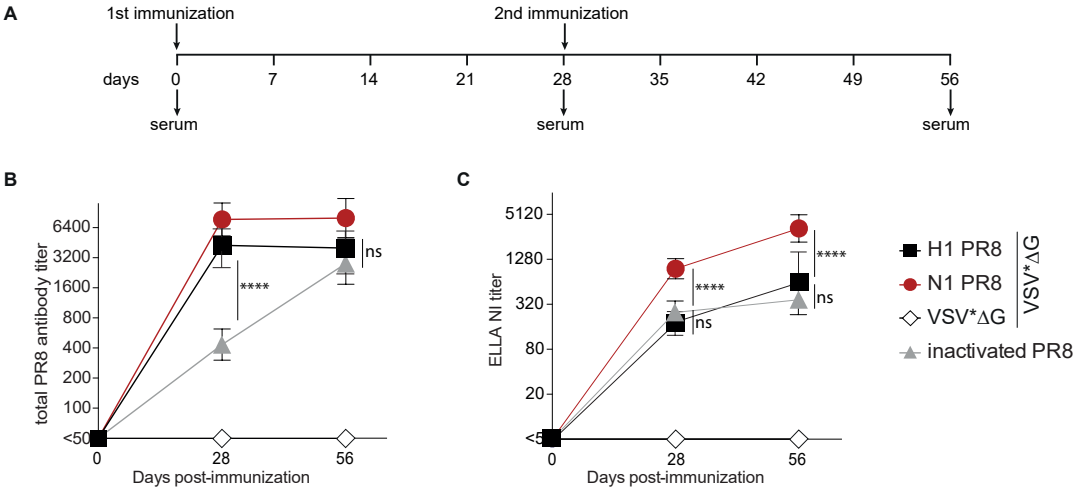


**Fig. 11 | Humoral immune responses in C57BL/6 mice induced by different vaccine candidates.** **A** | Schematic overview of the immunization strategy and blood and splenocyte sampling time points. Six- to eight-week-old female Balb/c and C57BL/6 mice were immunized twice with $10^6$ ffu i.m. of the VSV*ΔG replicons or with 2.5 µg of BPL-inactivated PR8 virus. Serum samples were taken before the immunization, as well as four weeks after the first and the second immunization. Kinetics of **B** | total antibody titers and **C** | 50% NI titer against H1N1 PR8 virus. Symbols represent the mean of each group (n=6), and error bars indicate the standard deviation of the mean. Log2-transformed groups were compared using two-way ANOVA with Tukey post-test. Statistical significance is indicated by *p<0.05; **p<0.01; ***p<0.001; **** p<0.0001. (Walz *et al.*, 2018).

### 5.1.3. HA and NA induce robust antibody responses against the homologous strain

To further evaluate the immunogenicity of NA-expressing VSV replicon particles, six- to eight-week old female C57BL/6 mice were immunized intramuscularly with $10^6$ ffu of VSV*ΔG($NA_{PR8}$) and boosted with the same dose 28 days later (Fig. 11A). VSV*ΔG, VSV*ΔG($HA_{PR8}$) and the inactivated PR8 preparation were included as controls. Sera were collected at the indicated times and total antibody titers directed against the homologous virus strain were quantified by IPMA with PR8-infected MDCK cells (Fig. 11B). Total antibody kinetics resembled the pattern observed previously (compare Fig. 10C). Mice immunized with the control replicon VSV*ΔG did not develop PR8-specific antibodies. Animals vaccinated with VSV*ΔG($HA_{PR8}$) or VSV*ΔG($NA_{PR8}$) produced comparable anti-influenza virus titers after the first immunization, which did not increase further after the boost. Antibody titers elicited by the inactivated vaccine were significantly lower after the first immunization ($p \leq 0.0001$), but increased after the second immunization, reaching similar levels as the VSV replicon vaccine groups (Walz *et al.*, 2018).

To assess the functionality of NA-specific antibodies, their sialidase-inhibiting activity was quantified using an ELLA with whole PR8 virus as sialidase source (Fig. 11C). VSV*ΔG($NA_{PR8}$) and the inactivated vaccine induced robust NA-inhibiting (NI) antibody titers after the first immunization, and titers increased in both groups after the second immunization. However, functional antibodies were significantly higher in the VSV*ΔG($NA_{PR8}$) group ($p \leq 0.0001$), demonstrating that the VSV replicon vaccine is more effective in inducing NI antibodies. The NI antibody titers of the group immunized with the HA-expressing VSV replicon were similar to the inactivated virus, illustrating the extent of sterical interference of HA-specific antibodies with NA access to SAs,

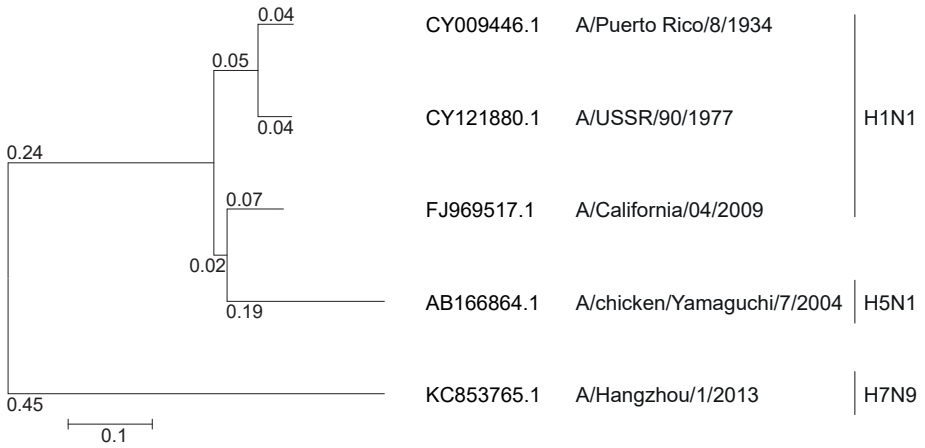


**Fig. 12 | Phylogenetic relationship of IAV NA genes included in this study.** Amino acid sequences were aligned using ClustalW and a phylogenetic tree constructed using neighbor-joining method and 1000 bootstrapped replications with observed amino acid differences as distance on the aligned sequences using MEGA7. (Walz *et al.,* 2018).

and suggesting that HA-specific antibodies also contribute to the NI titer detected in latter group. Taken together, this data illustrates the NA protein as a potential vaccine antigen, as it induces total antibody responses that are comparable to HA levels, with a functional activity that outperforms that of inactivated virus (Walz *et al.*, 2018).

### 5.1.4. NA proteins of increasing phylogenetic distance are expressed equally in host cells, but differ in their enzymatic activity

To explore the protective potential of an immune response against the more conserved NA protein, we generated VSV replicons expressing the NA protein of PR8, A/USSR/90/1977 (H1N1) as a prototypic seasonal H1N1 strain, pdmH1N1 A/California/04/2009 as a pandemic H1N1 strain, and A/chicken/Yamaguchi/7/2004 (H5N1) and A/Hangzhou/1/2013 (H7N9) as avian influenza viruses that cause severe disease in humans (Fig. 12) (Walz *et al.*, 2018).

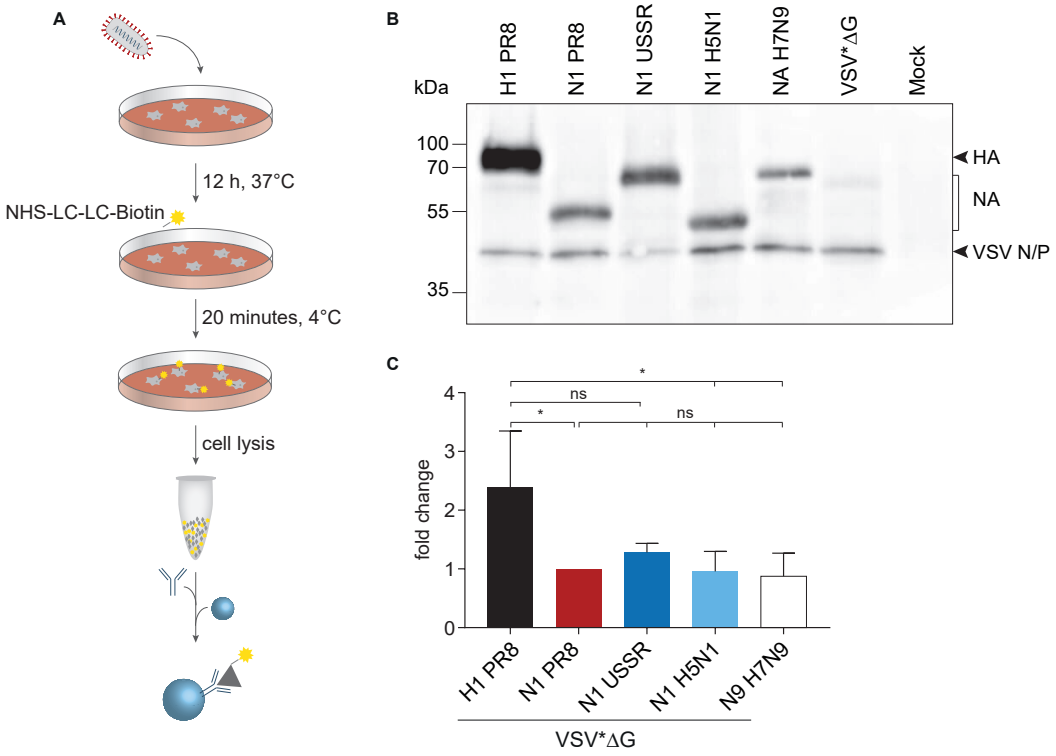


**Fig. 13 | Characterization of influenza antigen-expressing VSV replicons. A** | Schematic overview of the surface protein biotinylation and immunoprecipitation. VeroE6 cells were infected with the respective VSV*ΔG replicons at a MOI of 10. Twelve hours post-infection, cells were washed and surface proteins were labeled using EZ-Link Sulfo-NHS-LC-LC-Biotin at 4 °C. After subsequent quenching via PBS-glycine, cells were lysed in RIPA buffer and immunoprecipitated with the respective homologous mouse serum. **B** | Samples were thene separated via SDS PAGE, and biotin-labeled proteins were visualized using an avidin-HRP secondary antibody. **C** | Quantification of HA- or NA-specific protein bands relative to $NA_{PR8}$ protein. Bars represent the mean of three independent measurements and error bars indicate standard deviation of the mean. Groups were compared using one-way ANOVA with Tukey post-test. Statistical significance is indicated by *p<0.05; **p<0.01; ***p<0.001; **** p<0.0001. (Walz *et al.*, 2018).

To assess the surface expression levels of the different NA proteins, Vero E6 cells were infected with the respective replicons at a MOI of 10, followed by cell surface

biotinylation 12 hours post-infection. Subsequent immunoprecipitation was performed using the respective homologous mouse serum adjusted to the same antibody titer (Fig. 13A). Separation on SDS PAGE and staining with peroxidase-labeled streptavidin revealed that the $NA_{USSR}$ and $NA_{H7N9}$ proteins migrated at a molecular weight of about 75 kDa, whereas the $NA_{PR8}$ and $NA_{H5N1}$ protein were detected at around 55 kDa, reflecting the increased glycosylation of $NA_{USSR}$ and $NA_{H7N9}$ (Fig. 13B). An additional band at around 40 kDa was detectable in all lysates of VSV-infected cells, which represents sizes of VSV N and P proteins and is not present in Mock control lysates. Protein bands of four independent replicates were quantified and normalized relative to $NA_{PR8}$ for each blot (Fig. 13C). All NA proteins were expressed at comparable levels, suggesting similar antigen expression in vivo (Walz *et al.*, 2018).

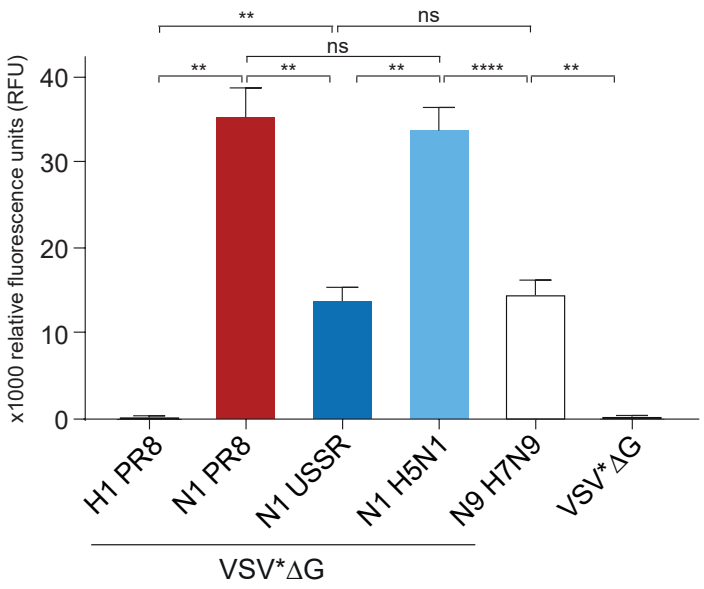


**Fig. 14 | Neuraminidase activity of VSV*ΔG-infected cells.** VeroE6 cells were infected with the respective replicons at a MOI of 10. Twelve hours post-infection, NA activity was measured for 30 minutes using 0,2 mM 2'-(4-Methylumbelliferyl)-α-D-N-acetylneuraminate (MUNANA) as substrate.

To evaluate the enzymatic activity of these antigens, a NA activity assay was performed, based on the NA enzyme cleaving the 2'-(4-Methylumbelliferyl)-α-D-N-acetylneuraminic acid (MUNANA) substrate to release the fluorescent product 4-methylumbelliferone (4-MU). Briefly, VeroE6 cells were infected with the respective replicons at a MOI of 10, simultaneously to the surface biotinylation approach, to allow a side-by-side comparison of antigen expression and enzymatic activity. Twelve hours post-infection, supernatant was removed and replaced by 5 µg MUNANA per well. After 30 minutes at 37 °C the reaction was stopped and fluorescence was measured. Negative controls $HA_{PR8}$ and VSV*ΔG remained negative for neuraminidase activity (Fig. 14). All NA proteins, in contrast, showed detectable NA activity. However, although surface expression was similar for NA proteins, their activity varied widely (compare Fig. 13C and 14). This suggests that enzymatic activity of NA-expressing VSV replicons is independent of their antigen expression levels.

### 5.1.5. VSV*ΔG(N1)s elicit functional subtype-specific antibodies

Data from several studies suggest an inverse correlation between high NI antibody titers and reduced morbidity (Rockman *et al.*, 2013; Monto *et al.*, 2015; Liu *et al.*, 2015). To systematically assess the breadth of NA-specific immune responses, mice were immunized twice with VSV replicons expressing $NA_{PR8}$, $NA_{USSR}$, $NA_{H5NI}$ and $NA_{H7N9}$ (Fig. 15A). For all NI carrying replicons, total and NI antibody titer against the homologous virus were within the same range (Fig. 15B and C), indicating similar NA expression *in vivo*. Immunization with $NA_{USSR}$ and $NA_{H5NI}$ resulted in NA-specific antibodies that reacted with PR8-infected MDCK cells as efficiently as antibodies that were obtained

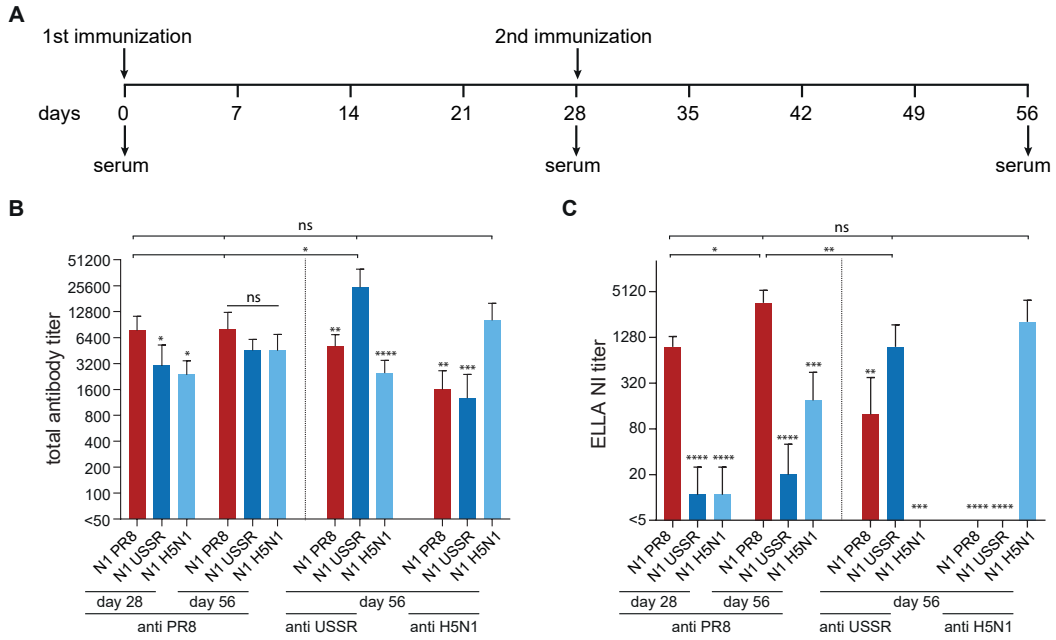


**Fig. 15 | Humoral immune responses in mice induced by the different NA proteins. A** | Schematic overview of the immunization strategy and blood sampling time points. Six- to eight-week-old female C57BL/6 mice were immunized twice with $10^6$ ffu i.m. of the VSV*ΔG replicons. Kinetics of **B** | total antibody titers and **C** | 50% NI titer against PR8, USSR and H5N1 viruses. Bars represent the mean of each group (n=6) and error bars indicate the standard deviation of the mean. Log2-transformed groups were compared using one-way ANOVA with Tukey post-test. Statistical significance is indicated by *p<0.05; **p<0.01; ***p<0.001; **** p<0.0001. (Walz *et al.*, 2018).

following immunization with $NA_{PR8}$ (Fig. 15B). In contrast, the matched antisera resulted in 5 – 10-fold higher total antibody titers for USSR and H5N1, respectively (Fig. 15B). The $NA_{USSR}$- and $NA_{H5NI}$-specific antisera also inhibited PR8 neuraminidase activity (Fig. 15C), but with lower efficacy than $NA_{PR8}$-specific antibodies ($p \leq 0.0001$). While the $NA_{PR8}$-specific antisera displayed NI activity against USSR, no cross-reactivity was observed for the $NA_{H5NI}$ group (Fig. 15C, anti-USSR), and none of the heterologous antisera were able to inhibit the $NA_{H5NI}$ neuraminidase activity (Fig. 15C, anti-H5N1). Interestingly, NI antibody titers were detected in groups with total antibody titers above 3200, suggesting that a correlation between total and NI antibodies could be established

(Walz *et al.*, 2018). No cross-reactive antibodies were detected after immunization with the heterologous N9 subtype (data not shown), illustrating that NA-specific antibodies only cross-react with NA proteins of the same subtype.

### 5.1.6. NA-expressing VSV replicons also induce influenza-specific cellular immune responses

In contrast to other vaccine platforms, VSV replicons elicit not only humoral but also cellular immune responses (Schulman, Khakpour and Kilbourne, 1968). To evaluate the extent of cellular immune responses after immunization with NA-specific VSV*ΔGs, splenocytes of animals vaccinated with the different N1 vaccine candidates were isolated 7 days after the second immunization and analyzed for antigen-specific IFNγ secretion by ELISpot assay using purified PR8 virus for restimulation (Fig. 16). In samples from mice sacrificed 7 days after intranasal infection with $1x10^4$ $TCID_{50}$ of PR8, 50-185 IFNγ-secreting cells per $1x10^6$ splenocytes were observed, while a background response below 3 IFNγ-secreting cells was seen in naïve control animals. PR8 stimulation of splenocytes from groups immunized with the inactivated vaccine or the VSV*ΔG control replicon resulted in IFNγ-secreting cell numbers close to background (0-5 positive cells). Following vaccination with the homologous VSV*ΔG($NA_{PR8}$) up to 65 spots per $1x10^6$ splenocytes were observed, while the heterologous N1 antigens were associated with lower but still positive responses ranging between 10 and 80 spots per $10^6$ splenocytes. However, these responses were not statistically different from background, indicating that the protective effect associated with the NA antigen in this context is primarily antibody-mediated (Walz *et al.*, 2018).

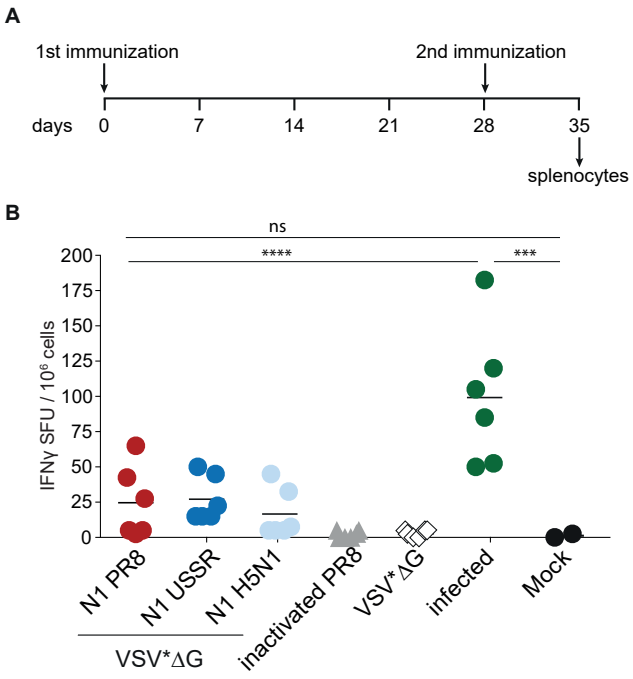


**Fig. 16 | Cellular immune responses in mice induced by the different VSV*ΔG replicons. A** | Schematic overview of the immunization strategy and splenocyte sampling time points. Six- to eight-week-old emale C57BL/6 mice were immunized twice with $10^6$ ffu i.m. of the VSV*ΔG replicons or with 2.5 µg of BPL-inactivated PR8 virus. **B** | IFNγ-ELISpot analysis results after restimulation with purified PR8 virus. H1N1 PR8-infected mice were used as positive and non-infected mice as negative controls. Groups were compared using one-way ANOVA with Tukey post-test. Symbols indicate individual animals and black bars represent respective mean. Statistical significance is indicated by *p<0.05; **p<0.01; ***p<0.001; **** p<0.0001. (Walz *et al.*, 2018).

### 5.1.7. N1-expressing VSV replicon particles partially protect mice from heterologous but not heterosubtypic virus challenge

NA-specific immune responses have previously been shown to protect from challenge with strains carrying homologous as well as heterologous HA proteins, as long as the NA protein is of the same subtype (Chen *et al.*, 2000; Sylte, Hubby and Suarez, 2007; Halbherr *et al.*, 2015; Wohlbold *et al.*, 2015). To evaluate the extent of protection and survival conferred by VSV replicon-based vaccines from challenge with heterologous virus strains, the 100% lethal dose of PR8 in C57BL/6 mice had to be determined. For this, groups of six- to eight-week old female mice were infected intranasally (i.n.) with $5x10^2$, $1x10^3$, $5x10^3$, $1x10^4$ or $5x10^4$ $TCID_{50}$ in a total volume of 30 µl. Mice were monitored daily for clinical signs and body weight change and euthanized as soon as weight loss reached 25%. All animals started losing weight on day one to three after the infection with a more rapid decrease the higher the infectious dose (Fig. 17A). Animals infected with $1x10^4$ and $5x10^4$ $TCID_{50}$ started dying on day 4 after infection (Fig. 17B) and 100% of animals infected with the highest dose reached humane endpoints one day later. In the two lowest dose groups, 20% and 25% of animals completely recovered from the infection. In order to ensure a 100% lethal infection of immunized mice, a dose of $1x10^4$ $TCID_{50}$ was used for further experiments.

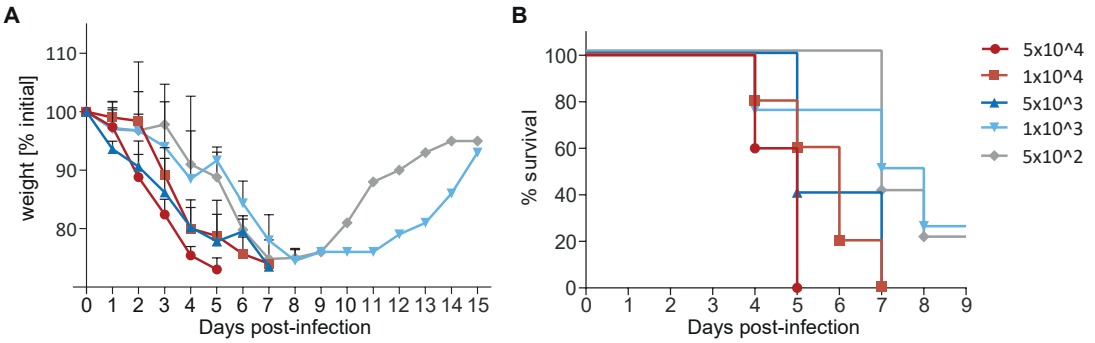


**Fig. 17 | Virus titration in C57BL/6 mice.** Mice were infected with different doses of H1N1 PR8 and were monitored daily for clinical signs and body weight. Animals were euthanized as soon as the weight loss reached 25%. **A** | Percent weight change after challenge and **B** | the respective percent survival (n=5).

To assess the extent of protection conferred by the different NA-expressing VSV replicons, we infected C57BL/6 mice intranasally with $1x10^4$ $TCID_{50}$ PR8 four weeks after the first and second immunization (Fig. 18A) (Walz *et al.*, 2018). Animals that received the homologous HA- or NA-expressing VSV*ΔG replicons or a matched inactivated vaccine were already fully protected from weight loss and mortality after a single immunization (Fig. 18B-E), while mice immunized with the VSV*ΔG control replicon or with VSV*ΔG($NA_{H7N9}$) reached humane end points within 6 to 7 days. A single immunization with the mismatched N1-expressing VSV*ΔG replicons resulted in partial protection from weight loss and mortality, specifically 50% for VSV*ΔG($NA_{USSR}$)

and 80% for VSV*ΔG($NA_{H5N1}$) (Fig. 18B and D), and a second immunization had no added beneficial effect (Fig. 18C and E).

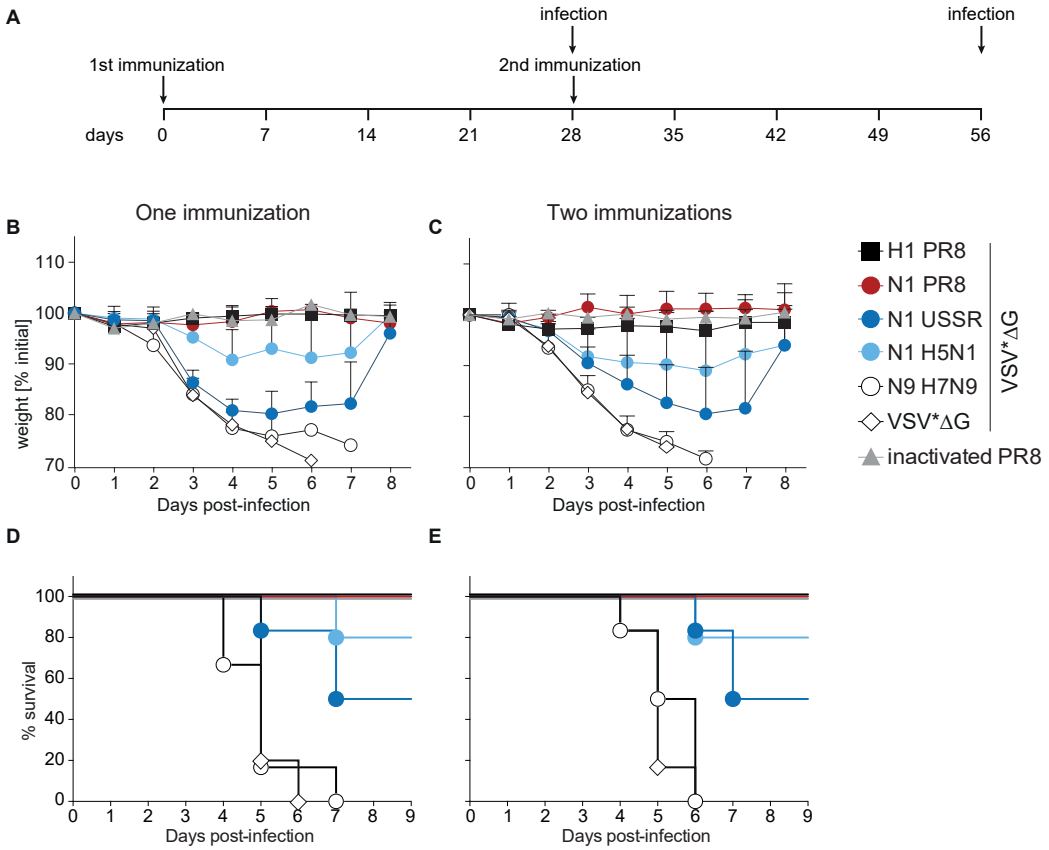


**Fig. 18 | Protective efficacy of the different vaccine candidates.** Mice were vaccinated once or twice in 4-week intervals and then challenged with 1x$10^4$ $TCID_{50}$ of H1N1 PR8 virus 4 weeks later. Upon challenge, animals were monitored daily for clinical signs and body weight and euthanized as soon as the weight loss reached 25%. Percent weight change after challenge following **A** | one or **B** | two immunizations (n=6, N1 H5N1 n=5) and **C and D** | the respective survival rate. (Walz *et al.,* 2018).

Interestingly, the level of cross-reaction did not correlate with the phylogenetic distance of the respective antigen to the H1N1 PR8 strain (compare Fig. 18D and E to Fig. 12). However, there was a clear correlation between mean NI antibody titers and percent survival for each group (Fig. 19A), and the correlation coefficient further improved after two immunizations (Fig. 19B), strengthening the link between NI antibodies and protection.

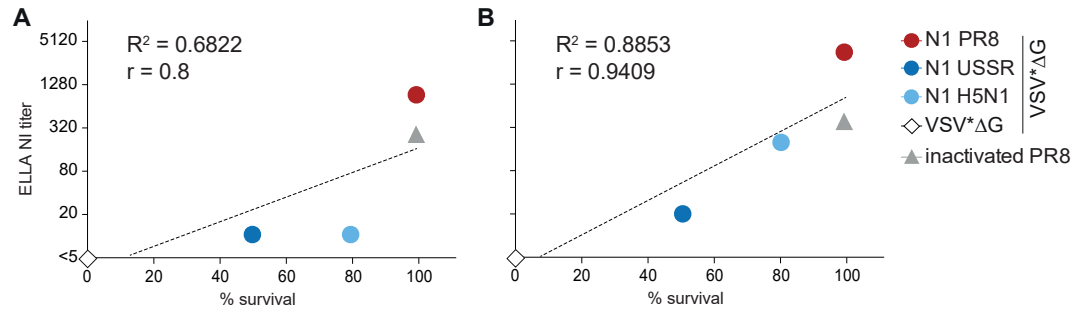


**Fig. 19 | Correlation between 50% NI titer and survival.** Correlation between mean 50% NI titer and percent survival at 4 weeks after **A** | the first or **B** | the second immunization. (Walz *et al.,* 2018).

### 5.1.8. Functional NA-specific antibodies are sufficient for cross-protection

To confirm that the observed cross-protection is due to functional NA-specific antibodies, passive antibody transfer experiments were performed. For this, sera from animals immunized twice with the respective VSV*ΔG replicons or inactivated PR8 were pooled on day 35 after initial immunization and total and NI antibody titers were measured (Fig. 20A). Antibody levels were similar to the previous experiment (compare Fig. 15 and Fig. 20B). However, the NI antibody titers were generally lower than previously, leading to titers below detection levels for VSV*ΔG($NA_{USSR}$).

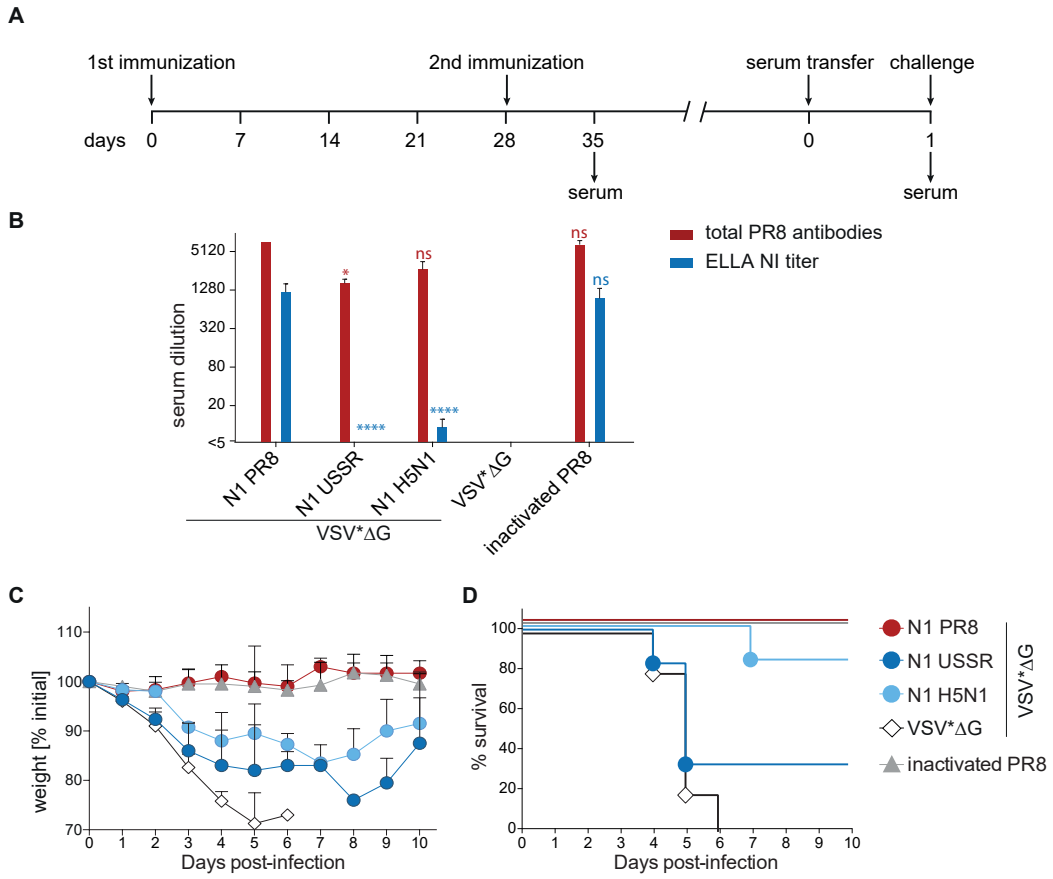


**Fig. 20 | Efficacy of passive serum transfer. A |** Schematic overview of the experimental design. Mice were vaccinated on days 0 and 28 with the respective VSV*ΔG replicons and serum was isolated 7 days after the boost immunization. Sera were subsequently transferred into naive mice. Blood samples were taken 24 h later and animals were challenged with 1x$10^4$ $TCID_{50}$ of H1N1 PR8 virus. **B |** Total antibody responses against PR8 (red) and 50% NI titers (blue) of donor mice. Bars represent the mean of three repeated measurements of pooled serum, and error bars indicate the standard deviation of the mean. Log2-transformed groups were compared to the $NA_{PR8}$ group using one-way ANOVA with Tukey post-test. Statistical significance is indicated by *p<0.05; **p<0.01; ***p<0.001; **** p<0.0001. **C |** Percent weight change and **D |** survival rate in recipient mice. Upon challenge, body weight was monitored and animals were euthanized as soon as the weight loss reached 25%. (Walz *et al.*, 2018).

Of the pooled serum, 500 µl was transferred into naïve six- to eight-week old female C57BL/6 mice (Fig. 20A), and total antibody titers were measured 24 h after transfer, before infection with 1x$10^4$ $TCID_{50}$ of PR8 (data not shown). Recipient animals with total anti-PR8 antibody titers below 50% of the initial donor titer were considered a

transfer failure and subsequently excluded from the study ($NA_{PR8}$ n=2, inactivated PR8 n=2). The weight loss and survival rates of the recipient animals mirrored that of the originally vaccinated groups, with antisera directed against $NA_{H5N1}$ being more protective than against $NA_{USSR}$ (compare Fig. 18C and E and Fig. 20C and D), demonstrating that subtype-specific cross-protection is largely antibody-mediated (Walz *et al.*, 2018).

### 5.1.9. Influenza HA or NA-expressing VSV replicon particles reduce spread to the lower respiratory tract in ferrets

Ferrets are frequently used to assess the immunogenicity and efficacy of influenza vaccines since they reproduce many of the clinical signs and overall course of disease seen in patients (Enkirch and von Messling, 2015). Following the same experimental design as before (Fig. 21A), immunization with VSV*ΔG replicons expressing the matched HA or NA proteins of pdmH1N1 A/California/04/2009 or VSV*ΔG($NA_{H5N1}$) elicited robust total antibody titers after the first immunization, which remained stable after a second immunization (Fig. 21B). While matched HA and NA proteins induced similar responses, levels in the $NA_{H5N1}$ group were slightly but not statistically significantly lower (Fig.21B). In contrast, both groups immunized with NA-expressing replicons induced similar NI antibody titers, with a slight increase after the second immunization (Fig. 21C), thereby reproducing the antibody response kinetics seen in mice (Walz *et al.*, 2018).

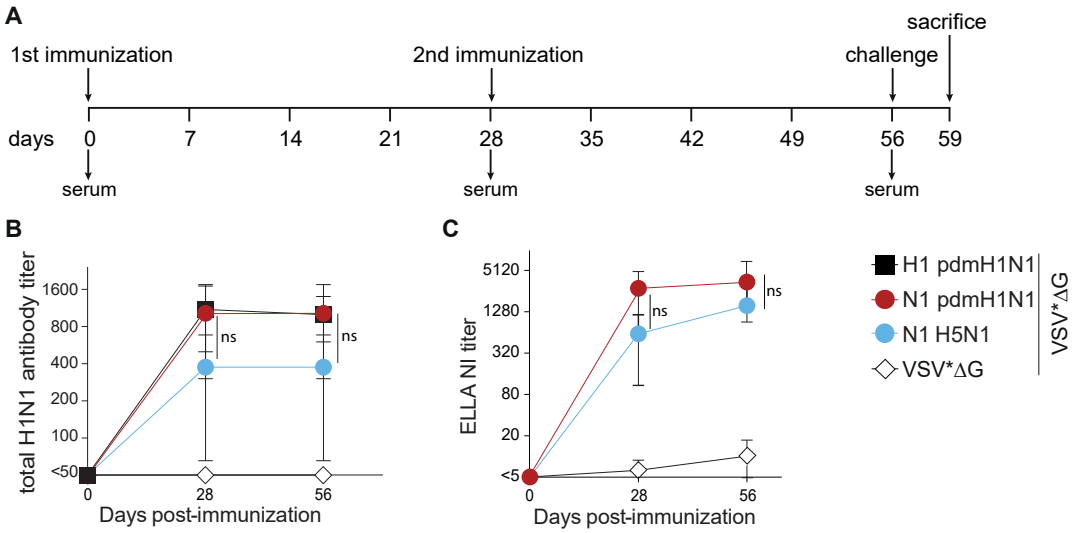


**Fig. 21 | Humoral immune responses in ferrets induced by the different VSV*ΔG replicons. A** | Schematic overview of the immunization and infection strategy and blood sampling time points. Naive ferrets were immunized twice with $10^8$ ffu VSV*ΔG replicons i.m.. All animals were challenged intranasally with $10^5$ $TCID_{50}$ A/Mexico/InDRE4487/2009 and sacrificed for virus titration on day 3 after infection. Kinetics of **B** | total antibody titers and **C** | 50% NI antibody titer against pdmH1N1 in animals immunized with matched or mismatched antigens. Log2-transformed groups were compared using two-way ANOVA with Tukey post-test. Statistical significance is indicated by *p<0.05; **p<0.01; ***p<0.001; **** p<0.0001. (Walz *et al.*, 2018).

Intranasal challenge of the animals with $10^5$ $TCID_{50}$ pdmH1N1 A/Mexico/InDRE4487/2009 resulted in weight loss from day 1 and gradually continued over the time course of the infection (Fig. 22A). Body temperature started to increase in all groups on day 2, peaking later that day (Fig. 22B). Animals developed a mild to moderate clinical disease, characterized by reduced activity, crusts around the nose and purulent nose exudate as early as day 1, which increased over time. Respiratory signs were predominant, including serous to mucopurulent nose exudate, congestion, wheezing and sneezing (Fig. 22C).

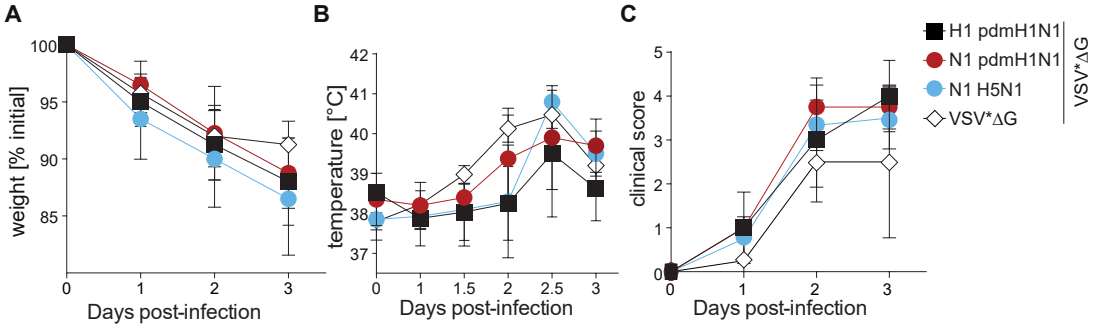


**Fig. 22 | Clinical signs in ferrets after infection.** All animals were challenged intranasally with $10^5$ $TCID_{50}$ A/Mexico/InDRE4487/2009 and clinical signs were monitored over 3 days after infection. **A** | Percent weight change, **B** | temperature change and **C** | clinical score over the course of infection. Symbols represent the mean of each group (n=4, post-infection N1 H5N1 n=2), and error bars indicate the standard deviation of the mean. (Walz *et al.,* 2018).

Unfortunately, two animals in the VSV*ΔG($NA_{H5N1}$) group succumbed to anesthesia immediately after challenge. All remaining animals were sacrificed on day 3 after infection, and viral load in NT and lungs as representatives of the upper and lower respiratory tract were quantified. NT titers were slightly lower in NA-immunized groups albeit not statistically different (Fig. 23A), and vaccination reduced spreading to the lung irrespective of the antigen used (Fig. 23B). It is of note that the two NA-immunized animals with detectable virus in the lung had the lowest NA-specific antibody titers in their respective groups. One of the two remaining animals in the VSV*ΔG($NA_{H5N1}$) group was completely protected from lower respiratory tract infection and the lung titer of the other one was around tenfold lower than the control group mean, suggesting an efficacy similar to the matched vaccines and providing further evidence for the correlation between functional NA-specific antibody responses and protection (Walz *et al.*, 2018).

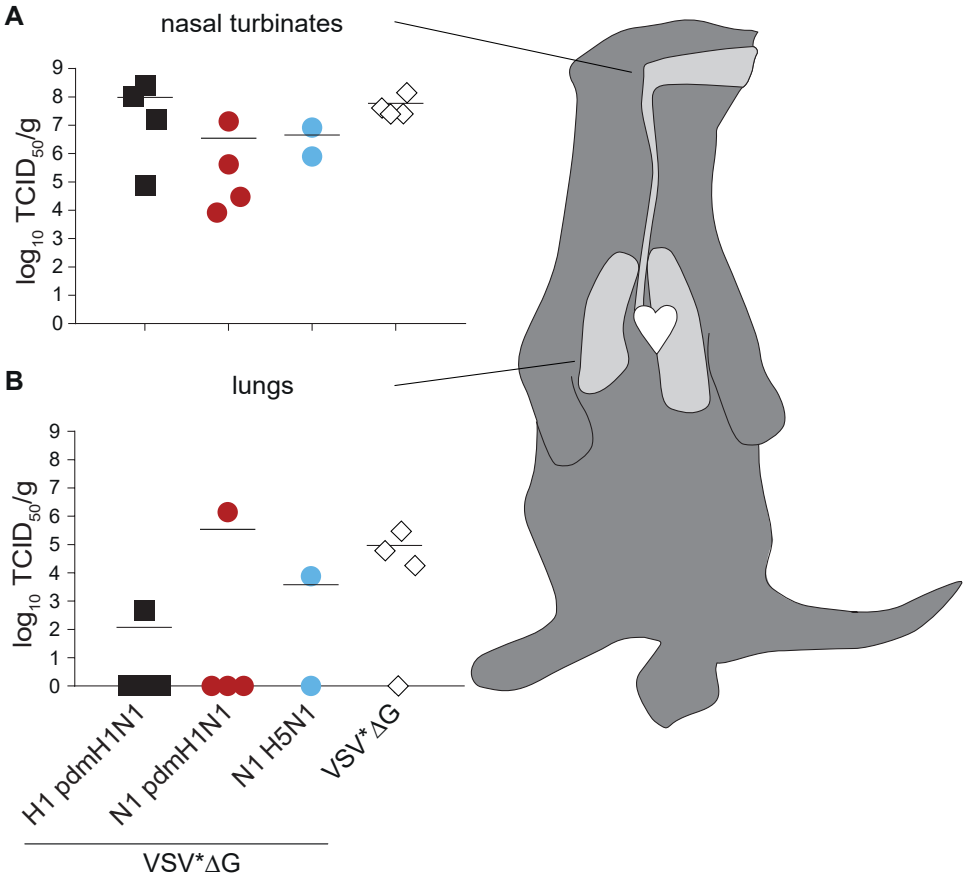


**Fig. 23 | Viral load in ferrets after infection.** All animals were challenged intranasally with $10^5$ $TCID_{50}$ A/Mexico/InDRE4487/2009 and sacrificed for virus titration on day 3 after infection. The virus titers were quantified in MDCK cells in **A** | nasal turbinates and **B** | lungs and expressed as $TCID_{50}$/g. Symbols indicate individual animals and black bars represent respective mean. (Walz et al., 2018).

## 5.2. HA-expressing AAV vector as vehicle for a broadly protective influenza vaccine

Aside of NA-based approaches towards a broadly protective influenza vaccine, the HA stem region has recently emerged as an attractive target for universal influenza vaccine development (Impagliazzo *et al.*, 2015; Valkenburg *et al.*, 2016; Ermler *et al.*, 2017). A novel approach to induce high levels of stalk-reactive antibodies is based cHAs. In these proteins, the stem region remains unchanged, while the globular head domains are replaced by differing "exotic" irrelevant subtypes, such as those of avian origin (Fig. 24A). AAV vectors have been generated to express the wild type HA protein of pdmH1N1 A/California/7/09 or three variable cHA, specifically cHA1, cHA2 and cHA3, consisting of the pdmH1N1 stem region combined with H2, H10 or H13 head domains, respectively (Fig. 24B). In a separate project, our collaborators found that these vectors broaden the specificity of functional antibody responses in mice, even after immunization with the wild type HA only. Here, we compared the immunogenicity and protective capacity of AAV vectors expressing wild type HA or cHA with the licensed inactivated vaccine in the more relevant ferret model.

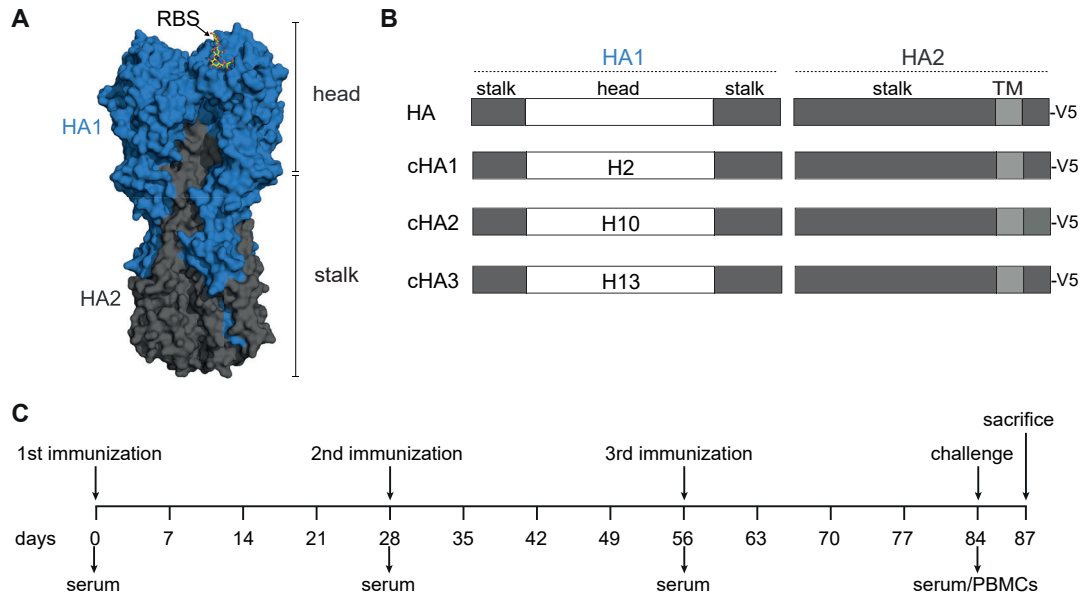


**Fig. 24 | Ferret immunization with AAV-HA vectors. A** | Side view of the HA trimer with the HA1 domain depicted in blue and the HA2 domain in dark grey. Atoms of the receptor binding site (RBS) are shown as sticks. **B** | Scheme of the of the parental HA of pdmH1N1 A/California/7/09 and the recombinant chimeric AAV-cHA constructs. Head domains of chimeric constructs were replaced by heterologous subtypes, i.e. H2, H10 or H13, respectively. **C** | Schematic overview of the immunization and infection strategy and blood and peripheral blood mononuclear cell (PBMC) sampling time points. Groups of four naive ferrets were immunized three times with 7.5 x$10^{12}$ genome equivalents with AAV-HA, heterologous prime/boost/boost with AAV-cHA3, AAV-cHA1 and AAV-cHA2, or with the control vector AAV-GFP. A control group was immunized twice with the quadrivalent IIV of season 2017/18 and a third time with PBS only. All animals were challenged intranasally with $10^5$ $TCID_{50}$ A/Mexico/InDRE4487/2009 on day 84 of the initial immunization and splenocytes were isolated the same day. Animals were sacrificed for virus titration on day 3 after infection.

To evaluate the immune response elicited by the different vectors, adult male ferrets were immunized intranasally (i.n.) a total of three times in 4-week intervals with the different replicons (Fig. 24C). An AAV-GFP vector, which expresses GFP only, but lacks influenza antigens and a season 2017/18 quadrivalent IIV were included as controls. Serum samples were collected at different time points to follow the antibody development, and peripheral blood mononuclear cells (PBMCs) were isolated at the day of challenge to evaluate T cell responses.

### 5.2.1. All vaccines mainly induce robust humoral immune responses

AAV vector-based candidate vaccines have been repeatedly shown to induce strong antibody responses after a single administration (McCarty, 2008; Sipo *et al.*, 2011; Ploquin *et al.*, 2013). To evaluate total pdmH1N1-specific antibody responses, an IPMA using pdmH1N1-infected MDCK cells was performed. All vaccinated animals developed IAV-specific antibodies after a single immunization (Fig. 25A). While antibody titers after AAV-HA and IIV vaccination continued to increase over time, AAV-cHA-specific titers remained stable (day 28 vs. 56 and 84, AAV-HA $p<0.01$, $p<0.0001$, respectively; LAIV ns; AAV-cHA ns). AAV-HA induced the strongest pdmH1N1-binding antibodies

after three immunizations (p<0.001). Interestingly, antibody titers elicited by the IIV control vaccine were significantly lower than AAV-cHA vectors after a single immunization (p<0.01), but increased to similar levels eight weeks after the second immunization.

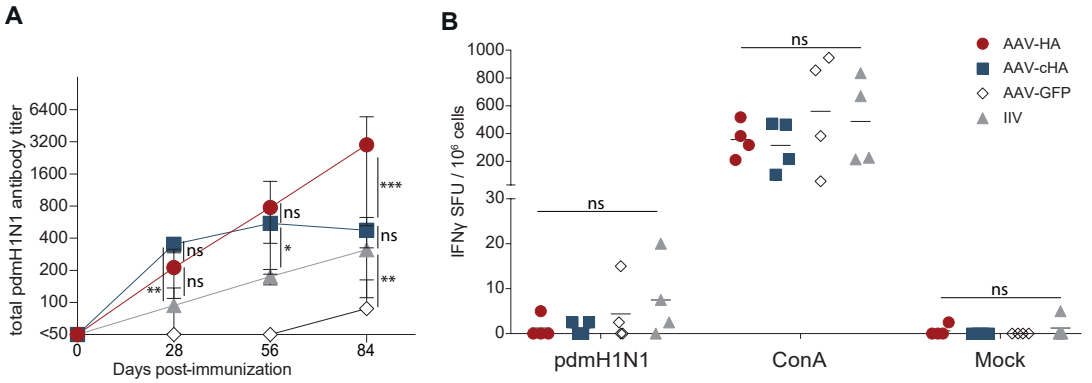


**Fig. 25 | Immune responses in ferrets induced by the different AAV vaccine candidates. A** | Total antibody titers against pdmH1N1 in animals immunized with AAV vectors expressing either wild type HA, various cHA or GFP only. IIV was used as a control. Log2-transformed groups were compared using two-way ANOVA with Tukey post-test. Statistical significance is indicated by *p<0.05; **p<0.01; ***p<0.001; **** p<0.0001. **B** | IFNγ-ELISpot analysis results after restimulation with purified pdmH1N1 virus. Concanavalin A (ConA) was used as positive and RPMI only as negative controls. Groups were compared using two-way ANOVA with Tukey post-test. Symbols indicate individual animals and black bars represent respective mean. No significant difference was observed within treatments.

Due to the *de novo* expression of target antigens, AAV vectors have been reported to induce not only B but also T cell responses (Kuck *et al.*, 2006; Sipo *et al.*, 2011). To evaluate the extent of cellular immune responses after immunization with HA-specific AAVs, PBMCs of animals vaccinated with the different vaccine candidates were isolated on day 84 and analyzed for antigen-specific IFNγ secretion by ELISpot assay using purified pdmH1N1 virus for restimulation (Fig. 24C). Treatment with cell culture medium (RPMI) only resulted in background responses of 0-5 IFNγ-secreting cells per $1x10^6$ PBMCs in all groups (Fig. 25B, RPMI). Unspecific T cell stimulation with Concanavalin A (Con A), a well-known T cell mitogen that can activate the immune system, recruit lymphocytes and elicit cytokine production (Dwyer and Johnson, 1981), resulted in levels of 50-900 positive cells per $1x10^6$ PBMCs, regardless of the immunization strategy (Fig. 25B, ConA). In samples from animals immunized with HA- or cHA-expressing AAVs, IFNγ-secreting cell numbers close to background were observed, while one animal of the AAV-GFP group and two IIV-immunized animals showed slightly higher responses of up to 20 positive cells per $1x10^6$ PBMCs. However, these responses were not statistically different from background, indicating that the protective effect associated with the HA antigen in this context is primarily antibody-mediated.

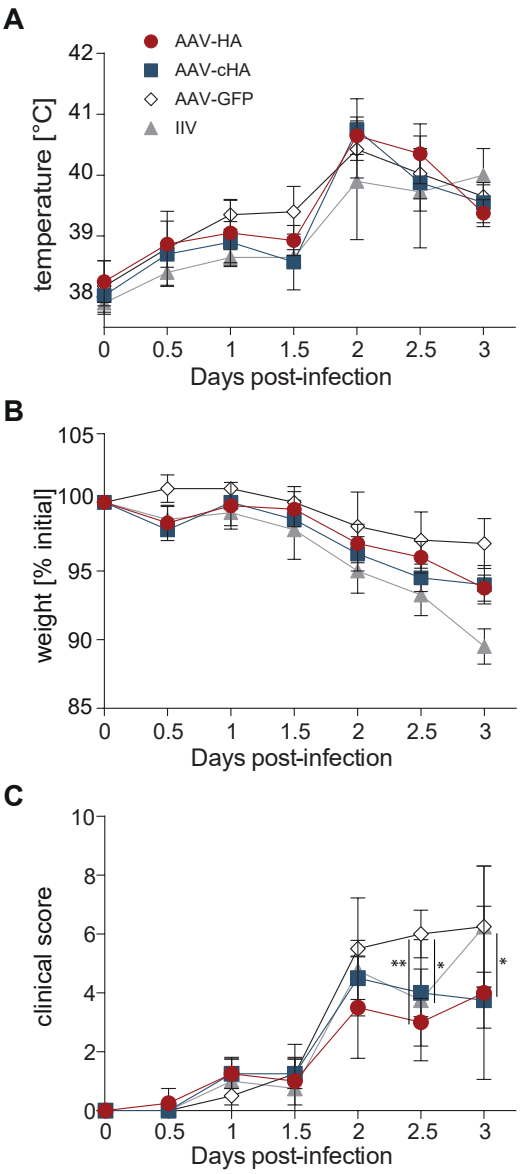


**Fig. 26 | Clinical signs in ferrets after infection.** All animals were challenged intranasally with $10^5$ $TCID_{50}$ A/Mexico/InDRE4487/2009 and clinical signs were monitored over 3 days after infection. **A** | Percent weight change, **B** | temperature change and **C** | clinical score over the course of infection. Symbols represent the mean of each group (n=4), and error bars indicate the standard deviation of the mean.

### 5.2.2. Disease Severity after homologous challenge is similar in all groups

Four weeks after the third immunization, all of animals were infected with $10^5$ $TCID_{50}$ of pdmH1N1 A/Mexico/InDRE4487/2009 via the intranasal route and the extent of nasal exudate, and respiratory, and general clinical signs were recorded until sacrifice 3 days later (Fig. 24C). Infection resulted in an elevated body temperature in all groups on day 1 with a peak on day 2 and no significant difference between the vaccine candidates. Notably, for two out of four animals in the IIV group the body temperature remained below 40 °C throughout the time course of infection (Fig. 26A). Similar results were observed for weight loss progression, with a continuous decrease until sacrifice in all groups (Fig. 26B).

The clinical course and disease severity were similar in all ferrets at the beginning of infection, as illustrated by the clinical scores (Fig. 26C). Animals developed first clinical signs, such as crusts around the nose and purulent nose exudate as early as day 1, increasing over time. Respiratory signs were predominant, including serous to mucopurulent nose exudate, congestion, wheezing and sneezing. However, significant differences between vaccinated animals and the AAV-GFP group were detectable starting on day 2. While clinical signs in the control animals continued to increase, vaccinated animals slowly started to recover from infection (Fig. 26C, day 2.5 and 3).

Nasal washes were collected daily after pdmH1N1 challenge infection for 3 days and virus titers were determined via titration on MDCK cells in order to determine the viral load (Fig. 27). Virus titers were similar in all four groups and reached a maximum of

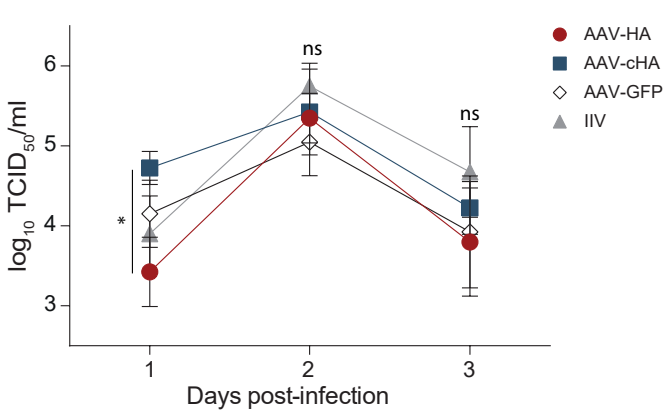


**Fig. 27 | Viral titers in nasal expectorate after challenge.** Nasal washes were collected daily for 3 days post-infection and titrated in MDCK cells. Titers were expressed as $TCID_{50}$/ml. Log2-transformed groups were compared using two-way ANOVA with Tukey post-test. Statistical significance is indicated by *p<0.05; **p<0.01; ***p<0.001; **** p<0.0001.

approximately $10^8$ $TCID_{50}$/ml on day 2 after infection. Subsequently, viral load decreased in the expectorate of all animals tested. Significant differences in the viral load of the different groups were only observed on day one between AAV-HA and AAV-cHA groups (p<0.05).

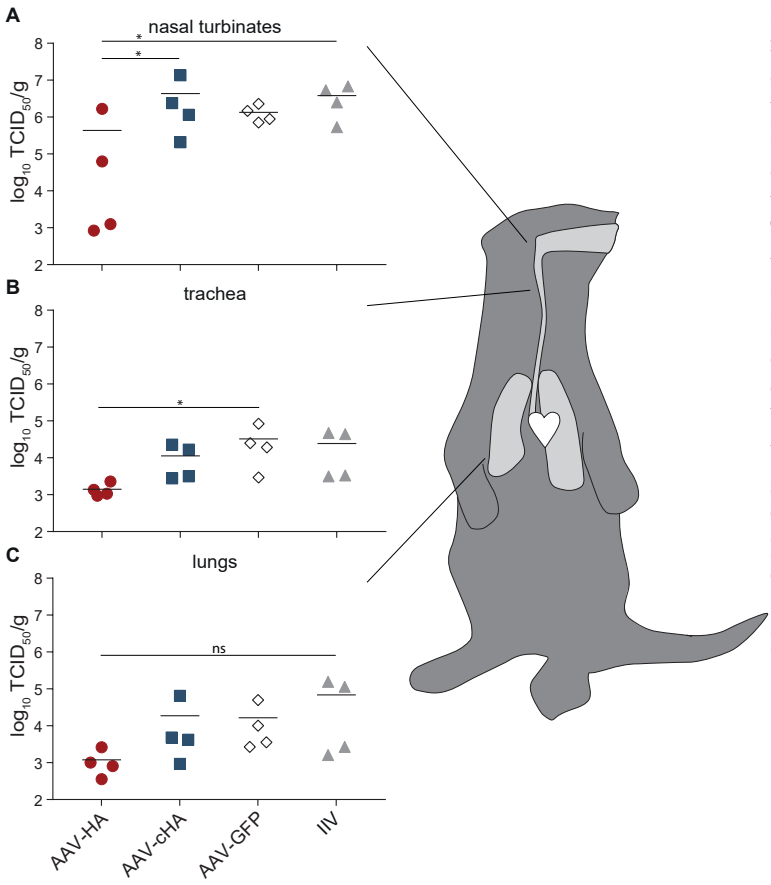


**Fig. 28 | Viral load in ferrets after infection.** All animals were challenged intranasally with $10^5$ $TCID_{50}$ A/Mexico/InDRE4487/2009 and sacrificed for virus titration on day 3 after infection. The virus titers in **A** | nasal turbinates, **B** | trachea, and **C** | lungs were quantified in MDCK cells and expressed as $TCID_{50}$/g. Symbols indicate individual animals and black bars represent respective mean. Log2-transformed groups were compared using one-way ANOVA with Tukey post-test. Statistical significance is indicated by *p<0.05; **p<0.01; ***p<0.001; **** p<0.0001.

Three days after challenge, animals were sacrificed, and the viral titers of the harvested nasal turbinates, trachea, and lung tissues were determined (Fig. 28). The viral load in nasal turbinates ranged around $10^3$ to $10^6$ $TCID_{50}$/g in AAV-HA vaccinated ferrets, while it ranged from $10^5$ to $10^8$ $TCID_{50}$/g in all other animals (p<0.05) (Fig. 28A). Similar results were obtained for trachea homogenates, where titers were significantly lower in the

AAV-HA group than in the AAV-GFP group ($P<0.05$). Viral titers in lung tissue varied from $10^3$ to $10^5$ $TCID_{50}$/g, whereas AAV-HA vaccination resulted in a more stable titer around $10^3$ $TCID_{50}$/g (Fig. 28C). Animals vaccinated with the licensed control vaccine developed viral titers in the upper and lower respiratory tract that were similar to AAV-GFP control animals. Thus, immunization with AAV-HA presumably protects ferrets from viral infection to a higher extent than cHA- or inactivated approaches. However, these results were not significantly different from the other immunization strategies.

# 6. DISCUSSION

Influenza viruses cause regular seasonal epidemics each winter as well as occasional pandemics that can have global impact on human health. Even though licensed vaccines are available, their efficacy varies, depending on the antigenic match between HA protein in the vaccine and in the actually circulating strains, resulting in the need for frequent strain updates and annual vaccination (Fleury et al., 1998; S E Hensley et al., 2009). This strain-specificity also results in limited efficacy of seasonal vaccines against newly emerging pandemic viruses. A "universal" influenza virus vaccine that induces long-term protection against all influenza virus strains would thus not only abolish the need for the annual flu shot, but also greatly improve pandemic preparedness. Using VSV*ΔG replicons encoding N1 proteins of the mouse-adapted PR8, a prototypic seasonal and pandemic H1N1, and a human H5N1 strain, we observed that in the absence of HA, NA induced robust humoral immune responses that protected mice and ferrets from challenge with a matched strain as efficiently as HA-specific immunity. For heterologous N1 proteins, the level of cross-reactive N1 antibodies correlated with protection, and antibodies alone were sufficient to confer this protection. These findings highlight the potential of NA as promising antigen to induce broader protection and demonstrate the potential of single cycle VSV replicons as vector platform for vaccine development. In a second approach, we were able to induce broadly reactive antibodies against a variety of IAV subtypes in C57BL/6 mice, using AAV vectors expressing wild type and cHA pdmH1N1 proteins and compared it to currently licensed IIV. Interestingly, neutralizing antibodies were found after AAV-HA immunization only and were not detectable after IIV vaccination. We were able to confirm those results in the ferret model, where vaccination with wild type HA resulted in highest and IIV in the lowest antibody response against homologous virus, whereas no cellular immune response was detectable in any of the vaccinated groups. Antibody responses correlated with protection from challenge infection, highlighting the great potential of the AAV platform expressing wild type HA as easily scalable influenza vaccine candidate. These findings indicate that a broadly specific and multifunctional antibody response can be induced by both influenza surface glycoproteins and demonstrate the potential of viral vector vaccines over IIV.

## 6.1. Different animal models are required at different stages of influenza vaccine research

As part of the humoral and cellular immune response against viral infections, T helper (Th) lymphocytes are divided into Th1 and Th2 cells. Th1 cells producing cytokines such as IFNγ and interleukin-2 (IL-2) and thereby evoking cell-mediated immunity and phagocyte-dependent inflammation. In contrast, Th2 lymphocytes are commonly associated with strong antibody responses and inhibition of phagocyte-dependent inflammation (Romagnani, 2000). C57BL/6 mice have been demonstrated to have a Th1-type bias to pathogens, whereas mice of other backgrounds, such as Balb/c, tend toward a Th2-predominant response (Mills *et al.*, 2000; Sellers *et al.*, 2012). We compared immune responses conferred by four different vaccine candidates in C57BL/6 and Balb/c mice. Surprisingly, both mouse strains developed similar antibody titers throughout the experiment. However, antibodies would have to be further characterized and classified into isotypes and subtypes to draw a definite conclusion. Nevertheless, based on those results, we chose the C57BL/6 mouse model for further experiments, retaining the opportunity of the evaluation of T cell responses.

Uncomplicated seasonal influenza virus infection in human patients is characterized by an acute onset of clinical signs within one or two days after the infection. They include upper respiratory infection characterized by congestion, sneezing, and coryza, lethargy and anorexia, and fever with a temperature peak of up to 41 °C, which gradually decrease over time (Bouvier and Lowen, 2010). In contrast, wild type mice are not naturally susceptible to influenza viruses, and infection with mouse-adapted influenza strains usually affect the lung and frequently result in a lethal outcome (Blazejewska *et al.*, 2011). Here, we found that disease in mice is primarily characterized by lethargy and weight loss, and that a humane end point defined by a 25% weight loss allowed a sensitive assessment of the level of protection from challenge infection. Comparing the cross-protection that is conferred by the different NA proteins, there was a clear correlation between functional antibody responses and protection. This correlation would have been much more difficult to quantify with a weaker readout than percent survival, highlighting a benefit of the mouse model for influenza vaccine research.

In both parts of the project, we also exploited the availability of a broad range of reagents and assays for this animal model, such as the IFNγ ELISpot assay. We first evaluated the different vaccine candidates and compared immunogenicity and efficacy in the mouse model, which allowed exploration of different experimental conditions. Based on these data, the clinically more relevant ferret model was then used to confirm our findings for the most promising vaccine candidates. For the NA-based approach, humoral and cellular immune responses as well as protection of the different NA proteins were

compared, and subsequently, cross-protection of the most potent $NA_{H5N1}$ protein could be evaluated in the ferret model, which thereupon enabled a more detailed analysis of differences in structure and epitopes of the proteins, further described below. Even though the nasal wash titers and overall clinical outcome was similar in all groups, taking into consideration the clinical score, temperature and weight change, we observed a reduction of lower respiratory tract infection that correlated with NI antibody titers – a correlate of protection identified in the mouse model.

Influenza virus infections usually start in the upper respiratory tract, but can spread to the lower respiratory tract and cause cough, dyspnea, and hypoxemia that can rapidly progress to pneumonia (Bouvier and Lowen, 2010). Like human patients, ferrets inoculated with human influenza viruses develop primarily an upper respiratory tract infection, with tissues lower in the respiratory tract being less frequently affected (Maher and DeStefano, 2004). The ferret model thus brought additional value to the study, by enabling a comparison of upper and lower respiratory tract infections, thereby further differentiating the levels of protection. Wild type HA, expressed from AAV even resulted in reduction of nasal turbinate titers, whereas the VSV-based approaches predominantly protected from virus spread into the lung.

Thus, our findings confirm that the mouse model is still the best choice for initial experiments, comparing different vaccine candidates and experimental conditions with a clear readout of protection. To then assess the potential for further clinical development of the most promising candidates, the ferret is the model of choice, as it more accurately reproduces the disease seen in human patients.

## 6.2. Similar efficacy of NA- and HA-specific immune responses against matched virus strains

While a recent study found HA- and NA-reactive T cells at similar frequencies after influenza infection (Chen *et al.*, 2018), an immunodominance of the wild type HA over the NA protein has been postulated based on the analysis of antibody prevalence in sera from individuals immunized with inactivated vaccines (Brett and Johansson, 2005). Since the NA content of currently licensed IIVs is not standardized, it is difficult to assess the contribution of NA-specific antibodies to vaccine efficacy (Kalbfuss *et al.*, 2008; Wohlbold *et al.*, 2015). However, after separate administration of purified HA and NA protein, comparable antibody levels have been observed in study participants (Johansson, Bucher and Kilbourne, 1989). Moreover, NA-based vaccines reduced clinical disease and viral shedding in patients (Couch *et al.*, 1974; Johansson, Matthews and Kilbourne, 1998; Sylte, Hubby and Suarez, 2007), and immunization of mice with purified NA protein resulted in lower lung titers and protection from lethal challenge

with the matched as well as heterologous strains carrying the same subtype (Liu *et al.*, 2015; Wohlbold *et al.*, 2015). Here we show that in the context of *de novo* protein expression, the protection conferred by NA-specific immune responses is similar to that of HA-specific responses against the matched strain, further strengthening the potential of the NA protein as vaccine antigen. Standardizing NA protein content and quality in existing vaccines might thus be a straightforward approach for inducing more broadly protective immune responses.

## 6.3. Neuraminidase-inhibiting antibody titers predict the extent of protection against heterologous strains

While HA-mediated protection is primarily strain-specific, the immune response elicited by NA proteins protects at least partially against heterologous strains carrying the same NA subtype (Johansson, Matthews and Kilbourne, 1998; Chen *et al.*, 2000; Rockman *et al.*, 2013; Wohlbold *et al.*, 2015). This aspect makes NA a promising candidate for the development of more broadly protective influenza vaccines. However, such development programs require robust correlates of protection to measure vaccine efficacy. Our study demonstrates that phylogenetic distance, which has been postulated to correlate with the extent of protection (Schulman, 1969; Marcelin *et al.*, 2010, 2011), may be only partially relevant. Instead, we observed a strong link between NI antibody titers and protection, irrespective of amino acid homology, phylogenetic distance, or HA subtype present. This is in agreement with previous reports showing that N1-specific NI antibody titers correlated with cross-protection against infection with LPAIV H5N1 infection (Rockman *et al.*, 2013; Monto *et al.*, 2015) and a recent study describing the levels of pre-existing NI antibodies as a better correlate of protection, when comparing it HI antibodies (Memoli *et al.*, 2016).

Yet, there is a need for better standardization of assays to measure NI antibody titers, as indicated in our study by the fact that steric hindrance by $HA_{PR8}$-specific antibodies result in detectable ELLA NI titers. However, many of these assays, such as the MUNANA assay used here, are usually based on small molecule substrates (Potier *et al.*, 1979), which unlike terminal SA attached to glycans on bulky proteins, have easy access to the active site of the NA. To show NI activity in those assays, an antibody has to bind very closely to the active site or inhibit the active site allosterically. To include NI titers resulting from steric hindrance of NA-specific antibodies, the ELLA uses fetuin, a highly sialylated glycoprotein, as a substrate (Couzens *et al.*, 2014; Gao, Couzens and Eichelberger, 2016). However, to distinguish between NA-specific and HA-specific steric hindrance, the NA protein has to be added as soluble protein. Alternatively, H6NX and/or H7NX reassortant viruses can be used to reduce the impact of anti-HA antibodies on the assays (Sandbulte *et al.*, 2009; Couzens *et al.*, 2014; Westgeest *et al.*, 2015). However,

it has to be noted that anti-stalk antibodies that broadly bind to HAs might still interfere with the assay in some cases (Rajendran *et al.*, 2017). VLPs with mismatched or without HA may also be used for NI assays (Gavrilov *et al.*, 2011) but only recombinant NA completely eliminates issues associated non-NA-specific inhibition (Prevato *et al.*, 2015). Thus, not only standardized ELLA assays, but also standardized quantification procedures for NA protein sources have to be developed. Furthermore, protective NI titers in vaccinees have to be evaluated to establish a protective threshold, as it is already available for hemagglutination inhibition, where a titer above 40 is considered protective (Hobson *et al.*, 1972). Notably, the fact that total antibody titers correlate with NI antibodies as reported previously (Rajendran *et al.*, 2017) and confirmed in our study, suggests that a standardized ELISA assay measuring total antibodies could ultimately be developed.

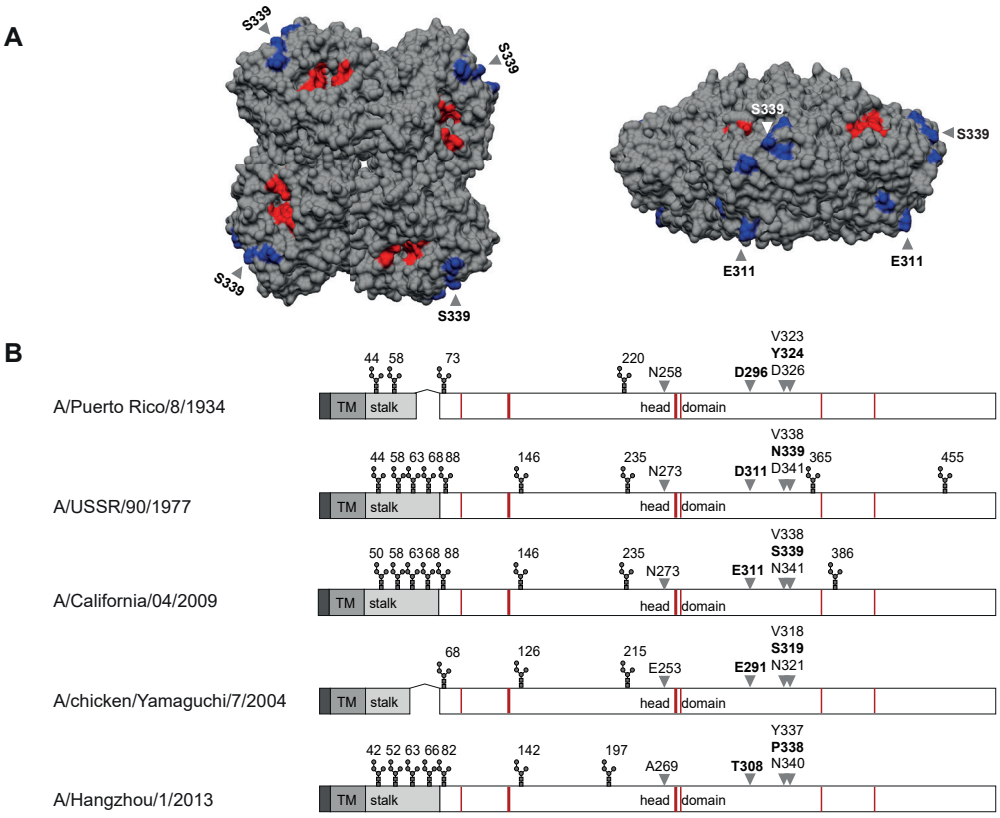


**Fig. 29 | Critical residues of NA proteins. A** | Top and side view of the NA tetramer, with active sites depicted in red and previously identified critical residues for cross-reactivity depicted in blue. **B** | Linear comparison of the NA proteins. The cytoplasmic domain, TM = transmembrane region, stalk region and head domain are depicted in dark, medium and light grey and white, respectively. Putative glycosylation sites are shown above, active sites in red and previously identified critical residues for inhibiting antibody binding are indicated by grey arrowheads and respective amino acid numbering. Adapted from (Walz *et al.*, 2018).

By measuring cleavage of the small NA substrate MUNANA by the respective VSV*ΔG replicons, we could show that NA proteins differ significantly in their enzymatic activity while maintaining similar expression levels. Proteins with more putative N-glycosylation

sites ($NA_{USSR}$ and $NA_{H7N9}$) showed lower neuraminidase activity. Comparing this to cross-reactive antibody levels, especially NI titers, NA proteins with higher activity seem to induce higher cross-reactive functional antibodies. This is consistent with previous publications, reporting a higher induction of NI antibody responses in cases of higher NA activity in influenza vaccines (Sultana *et al.*, 2014). It is also supported by the fact that several anti-NA monoclonal antibodies (MAbs) with protective efficacy in animal models often bind to conformational epitopes (Wohlbold *et al.*, 2017).

While numerous HA-specific epitopes and MAbs are characterized, little is known about NA epitopes. The extent of the cross-reactive antibodies and cross-protection observed in our study is in line with previous publications identifying critical residues for cross-reactivity of NA-specific antibodies (Khurana *et al.*, 2009; Wan *et al.*, 2013; Job *et al.*, 2017). Particularly, amino acids 311 and 339 located in a region associated with SA-binding and catalytic activity has been identified as essential for epitope recognition by antigenic mapping by mouse monoclonal antibodies to N1 domains (Wan *et al.*, 2013; Job *et al.*, 2017). These residues differ in $NA_{PR8}$, $NA_{USSR}$ and $NA_{H5N1}$, respectively, but turn out to be conserved between $NA_{pdmH1N1}$ and $NA_{H5N1}$, which may explain the high cross-reactivity observed in our ferret study (Fig. 29A). NA is a glycoprotein with several N-linked glycosylation sites, some of which are conserved, and others change over time. The role of this N-glycosylation in enzymatic activity and immunogenicity is poorly evaluated. Of note, the two NA proteins with stalk deletions characteristic of avian-origin viruses and the lowest number of potential N-glycosylation sites, $NA_{PR8}$ and $NA_{H5N1}$, elicited the highest NI antibody titers in our study, suggesting that stalk length and glycosylation pattern may also influence the extent of functional antibodies (Fig. 29B). However, our understanding of which epitopes are targeted by human antibodies is limited, and a causal connection between either characteristics and antigenicity would require validation involving a larger selection of proteins, similar to a recent Influenza B NA study (Wohlbold *et al.*, 2017). Furthermore, human monoclonal antibodies induced by both vaccination and infection should be isolated and characterized. Antigenic sites have to be better defined, and antibody footprints should be confirmed by structural biology analyses to better understand the potential for antigenic drift of NA proteins (Krammer *et al.*, 2018).

Quality and quantity of NA in currently licensed vaccines is not standardized, which results in a high variability between the different vaccine strains and manufacturers each season (Getie-Kebtie *et al.*, 2013; Wohlbold *et al.*, 2015). Very little is known about the stability of NA during the production process and over the shelf life of vaccines. A controlled human IAV virus challenge with the pdmH1N1 virus identified the levels of pre-existing NI antibodies as a better correlate of protection than HI antibodies, which

are currently the gold standard, highlighting the potential of NA as vaccine antigen (Memoli *et al.*, 2016). Together with the recent report that natural influenza infection, in contrast to immunization with inactivated vaccines, induces broadly cross-reactive NA-specific antibodies (Chen *et al.*, 2018), our study underlines the potential of NA-based vaccines and demonstrates that NI antibodies may serve as promising functional correlate of protection, if such vaccines are developed. Our understanding of NA immunogenicity would be greatly advanced if the NA protein content of seasonal and pandemic vaccines was standardized and part of the batch control and release process.

## 6.4. Wild type HA and cHA expressed by AAV vectors result in higher antibody responses compared to IIVs

A major obstacle in influenza vaccine development is the highly variable HA globular head that rapidly acquires mutations some of which can lead to antigenic changes. Most HA-head-specific antibodies are only protective against antigenically closely related viruses. In contrast, the stalk domain is more conserved. Anti-stalk antibodies are naturally induced by influenza infection, but in low levels compared to the immunodominant head domain (Corti *et al.*, 2011; Rajão and Pérez, 2018). Some of these antibodies can have broadly reactive activity (Ekiert *et al.*, 2009). Antibodies against the HA globular head neutralize infection by either preventing binding to cellular receptors or membrane fusion, and some have the ability to inhibit agglutination of erythrocytes *in vitro*. Functional stalk-specific antibodies are usually not measurable by standard assays, as they do not neutralize the virus or inhibit hemagglutination, but protect through inhibition of either entry, viral release, or by mediating ADCC or CDC (Rajão and Pérez, 2018). Daniel Demminger and Thorsten Wolff at the Robert Koch Institute explored an approach to induce broadly reactive antibodies against HA stem regions using AAV vectors expressing wild type HA or cHA, and compared them to IIVs based on the same pdmH1N1 virus. First results in C57BL/6 mice were in line with previous reports, as all vaccinated animals developed antibodies against the matched strain. However, only animals immunized with the AAV-HA vaccine developed neutralizing antibodies, which supports the hypothesis that HA head-specific antibodies neutralize infection of host cells. Based on literature, vaccination with cHAs was expected to show the broadest reactivity and highest HA stalk-reactive antibodies. Surprisingly, all groups developed broadly reactive antibodies, with the highest cross-reactivity in IIV serum, while only minor Fcγ receptor activation was detectable in this group. This correlates with previous data, reporting that IIV immunization does not prime ADCC in macaques (Jegaskanda *et al.*, 2013). Moreover, mice developed broadly neutralizing antibodies directed against the HA head region and accordingly, antibodies with broad reactivity against multiple subtypes were found in humans. This suggests a cross-reactive epitope

within the globular head domain of HA, most probably within or close to the conserved region of the receptor binding site (Ekiert and Wilson, 2012; Rajão and Pérez, 2018). Against our expectations, AAV vectors expressing wild type HA protein resulted not only in neutralizing antibody responses, but also in a high cross-reactivity of the antibodies within group 1 HAs. Those antibodies also mediated activation of the Fcγ receptor, indicating ADCC or other Fc-mediated mechanisms. Taken together, these results identify the wild type HA-expressing AAV vector as most promising vaccine candidate, since it acts through various humoral immune responses, inducing neutralizing and stalk-reactive antibodies.

Subsequently, the three different candidates were evaluated in this thesis in the clinically more relevant ferret model. Immunization of ferrets with the different vaccines confirmed the results obtained previously in mice, as all vaccines induced antibodies that bind to homologous virus after the first immunization. Repeated immunization with the matched AAV-HA vector resulted in highest and IIV in lowest total antibody responses. This could be confirmed by Daniel Demminger, who only detected HI antibodies in ferrets immunized with AAV-HA. Interestingly, immunization with the IIV did not induce any neutralizing antibodies in the mouse model and resulted in lowest total antibody responses in the ferret compared to the AAV-based vaccines. This effect has been observed previously, where no HI antibodies were detectable in ferrets after two immunizations with the IIV against homologous virus (Nachbagauer *et al.*, 2017).

Notably, protection correlated with antibody responses in mice and ferrets. Mice immunized with the AAV vectors were partially protected against homologous and heterologous challenge infection of the same subtype, with animals which developed neutralizing antibodies being completely protected against the matched virus, while cHA immunization did not induce neutralizing antibodies and resulted in 80% protection from homologous challenge. In ferrets AAV-HA immunization resulted in a reduction of disease severity and lower peak virus titer as well as shortened duration of replication, indicating an inhibition of the infection from the beginning. This is consistent with the viral load in different respiratory tissues, which were lowest in the animals immunized with wild type HA throughout the upper and lower respiratory tract. A recent study further supported these findings by correlating high levels of HA stalk-reactive antibodies measured by ELISA and high ADCC activity with protection against pdmH1N1 challenge in mice with passive transfer of sera from H5N1 vaccinees (Jacobsen *et al.*, 2017).

Thus, we could show that AAV-vectors expressing wild type and chimeric HA proteins outperformed commercially available IIVs in terms of the induced immune responses in

naïve animals, and the conferred protection from homologous as well as heterologous challenge. This underlines the potential of not only stalk-reactive antibodies, but also HA-immunization that induces neutralizing antibodies and Fcγ receptor activation. Moreover, we found that the traditional HAI assay did not accurately predict the protective effect of the vaccination, highlighting the need for new correlates of protection to accurately evaluate and predict the potential of new vaccine candidates.

## 6.5. VSV and AAV vectors are promising platforms for broadly protective influenza vaccines

The success of the propagation-competent VSV-based vaccine candidate against Ebola virus demonstrates the potential of VSV as a vaccine platform (Publicover, Ramsburg and Rose, 2005; Marzi *et al.*, 2015; Banadyga and Marzi, 2017). However, the benefit-risk profile of a propagation-competent viral vector may not be appropriate for all target pathogens. VSV replicons, which are limited to a single round of replication due to the lack of an essential viral gene in their genome, constitute an attractive alternative, as they maintain the high level protein expression capacity of the VSV replication machinery, but are unable to produce progeny virus (Publicover, Ramsburg and Rose, 2005; Zimmer *et al.*, 2014). A major advantage of VSV replicons and other RNA-based vaccines is that replication and transcription does not require any cDNA intermediates, precluding recombination with or integration in the chromosomal DNA of the vaccinee. Similar to LAIV, RNA-based vaccines result in intracellular antigen expression, which stimulates both, humoral and cellular immune responses (Zimmer, 2010). Consistent with the *de novo* protein synthesis, we were able to detect IFNγ secretion after stimulation of splenocytes from VSV*ΔG(N1)-immunized mice with influenza virus. However, the responses were low compared to previously influenza-infected animals, which may be due to the lack of strong T cell epitopes in the NA protein (Gutiérrez *et al.*, 2016). In contrast, we were able to demonstrate that NA proteins expressed with this system elicit robust functional antibody responses that exceed the titers induced by an inactivated vaccine. Repeated immunization resulted in an increase of these responses, and this effect might be improved further by including viral proteins with known conserved T cell epitopes such as the NP or M1 protein in the VSV replicon (Kreijtz, Fouchier and Rimmelzwaan, 2011), and by taking advantage of G proteins from heterologous, antigenically different VSV strains (Roberts *et al.*, 1999).

AAV vectors are well known and widely used in gene therapy (Nieto and Salvetti, 2014). The vectors are derived from a non-pathogenic virus family that is inherently replication-defective, which makes AAVs an attractive platform. Only after its capacity to induce strong humoral and cellular immune responses has been discovered in the context of a herpes simplex virus vaccine candidate, virologists have started to explore

the potential of AAV as vaccine platform (Manning *et al.*, 1997; Nieto and Salvetti, 2014). Regardless of the proposed T cell activation, we were not able to detect any pdmH1N1-specific IFNγ secretion after restimulation of splenocytes. However, analogous to the previous study, this may have been caused by the lack of strong T cell epitopes in the HA glycoprotein. In contrast, humoral immune responses significantly exceeded that of IIVs. An advantage of the AAV vector over VSV replicons is its potential for intranasal immunization, which mimics the natural infection. This provides protection at the pathogen at the initial site of infection, results in higher levels of local IgA antibodies, and allows for needle-free application (Rose, Zielen and Baumann, 2012). Furthermore, mucosal antibodies are thought to be more cross-reactive than IgG, thereby possibly mediating some protection against drift variants (Cerutti and Rescigno, 2008).

Taken together, we could show that influenza vaccines based on viral vectors are more efficient than currently licensed IIVs. However, in order to further increase cellular immune responses, other vectors such as MVA or measles could also be considered.

## 6.6. A "universal" influenza vaccine – a realistic goal?

Vaccination remains the most efficient and cost-effective tool to prevent influenza in humans. Current influenza virus vaccines primarily rely on the effective stimulation of the immune response against the surface glycoprotein HA and show efficacy when they are antigenically well matched to circulating strains. Seasonal influenza viruses undergo antigenic drift at a high rate, which results in a need of regular revision of the vaccine composition and annual revaccination. Antibodies against HA, predominantly the globular head domain, correlate with surrogate *in vitro* assays such as the HI or virus neutralizing assays, and are thus considered the major protective component. Thus, the high variability of the globular head of HA and the resulting antigenic changes are the primary weakness of these vaccines. A "universal" influenza virus vaccine that induces long-term protection against all influenza virus strains would abolish the need for annual vaccine updates, while increasing the breadth of immune responses and would significantly strengthen our pandemic preparedness. Such approaches attempt to overcome the constantly changing nature of influenza viruses, by inducing humoral and cellular immune responses against structurally conserved epitopes (Jang and Seong, 2014; Angeletti and Yewdell, 2018; Rajão and Pérez, 2018).

In this thesis, we show the potential of the more conserved NA protein and HA stalk-specific approaches, as well as the increased efficacy of the wild type HA expressed by a viral vector over conventional IIVs. The stalk domain of the HA protein, the NA protein, and also the highly conserved ion channel M2e are accessible for antibodies on the surface of virions and infected cells, which can then directly inhibit the virus or

eliminate infected cells via ADCC or CDC. The different approaches provide different modes of protection (Rajão and Pérez, 2018). For future vaccine candidates a targeted combination of different functional antibody responses might further improve cross-protection. Of note, an immunodominance of the wild type HA protein over the NA and M2 proteins has been postulated and will have to be taken into consideration for such newly generated vaccines.

Currently licensed IIVs do not stimulate cellular immune responses and are thus usually less effective against heterologous influenza infections (Bahadoran *et al.*, 2016; Mohn *et al.*, 2017). The cellular arm of the adaptive immune response plays an important role in influenza virus clearance and cross-protective immunity. These T cell responses are mainly directed against the relatively conserved internal proteins NP, M1, and the polymerase complex subunits, and thus have the potential to confer a high degree of cross-reactive immune response to various influenza strains (Rajão and Pérez, 2018). As shown in this study, viral vectors offer a platform that enables the stimulation of T cells. Yet, we could demonstrate that HA and NA proteins do not offer highly potent T cell epitopes. A vaccine candidate stimulating both arms should therefore contain a combination of broadly reactive B and T cell epitopes.

Finally, this PhD thesis demonstrates possible strategies towards such broadly protective influenza vaccines that could ultimately abolish the need for regular vaccine update and annual immunization campaigns. Combining new vaccine platforms such as viral vectors and highly conserved epitopes opens up new opportunities. Our study shows that VSV and AAV vectors are both promising candidates for such a vaccine. Nevertheless, further research is necessary to identify the most promising candidate. Regardless of the antigen that is finally used in future vaccines, this PhD thesis also highlights the need for surrogate assays to measure correlates of protection. Towards this, assays such as the ELLA, measuring functional NA-specific antibodies, have to be standardized worldwide and made accessible to all academic and commercial researchers involved. Lastly, the mechanisms underlying antigenic drift that results in escape from existing immunity to the respective antigens has to be characterized in more detail. Towards this, it will be important to further develop human challenge trials to test current and novel vaccination approaches while also collecting relevant information on antibody-mediated, cellular, and mucosal immunity.

# 7. REFERENCES

Air, G. M. (2012) 'Influenza neuraminidase', Influenza and Other Respiratory Viruses, 6(4), p. 245. Available at: http://dx.doi.org/10.1111/j.1750-2659.2011.00304.x.

Air, G. M., Laver, W. G. and Webster, R. G. (1987) 'Antigenic variation in influenza viruses.', Contributions to microbiology and immunology, 8, pp. 20–59. Available at: https://www.ncbi.nlm.nih.gov/pubmed?Db=pubmed&Cmd=Retrieve&list_uids=3304832&dopt=abstractplus.

Anderson, A. O. and Swearengen, J. R. (2012) 'Scientific and Ethical Importance of Animal Models in Biodefence Research', in Biodefense Research Methodology and Animal Models, pp. 27–43.

Angeletti, D. and Yewdell, J. W. (2018) 'Is It Possible to Develop a "Universal" Influenza Virus Vaccine?', Cold Spring Harbor Perspectives in Biology, 10(7), p. a028852. doi: 10.1101/cshperspect.a028852.

Bahadoran, A. et al. (2016) 'Immune responses to influenza virus and its correlation to age and inherited factors', Frontiers in Microbiology, 7, pp. 1–11. doi: 10.3389/fmicb.2016.01841.

Bahl, K. et al. (2017) 'Preclinical and Clinical Demonstration of Immunogenicity by mRNA Vaccines against H10N8 and H7N9 Influenza Viruses', Molecular Therapy, 25(6), pp. 1316–1327. doi: 10.1016/j.ymthe.2017.03.035.

Balazs, A. B. et al. (2013) 'Broad protection against influenza infection by vectored immunoprophylaxis in mice', Nature Biotechnology, 31(7), pp. 647–652. doi: 10.1038/nbt.2618.

Banadyga, L. and Marzi, A. (2017) 'Closer than ever to an Ebola virus vaccine', Expert Review of Vaccines, pp. 401–402. doi: 10.1080/14760584.2017.1309977.

Barberis, I. et al. (2016) 'History and evolution of influenza control through vaccination: From the first monovalent vaccine to universal vaccines', Journal of Preventive Medicine and Hygiene, 57(3), pp. E115–E120.

Basha, S. et al. (2011) 'Comparison of antibody and T-cell responses elicited by licensed inactivated- and live-attenuated influenza vaccines against H3N2 hemagglutinin', Human Immunology, 72(6), pp. 463–469. doi: 10.1016/j.humimm.2011.03.001.

Baxter, R. et al. (2011) 'Evaluation of the safety, reactogenicity and immunogenicity of FluBlok® trivalent recombinant baculovirus-expressed hemagglutinin influenza vaccine administered intramuscularly to healthy adults 50–64 years of age', Vaccine, 29(12), pp. 2272–2278. doi: 10.1016/j.vaccine.2011.01.039.

Blazejewska, P. et al. (2011) 'Pathogenicity of different PR8 influenza A virus variants in mice is determined by both viral and host factors', Virology, 412(1), pp. 36–45. doi: 10.1016/j.virol.2010.12.047.

Borggren, M. et al. (2016) 'A polyvalent influenza DNA vaccine applied by needle-free intradermal delivery induces cross-reactive humoral and cellular immune responses in pigs', Vaccine, 34(32), pp. 3634–3640. doi: 10.1016/j.vaccine.2016.05.030.

Bosch, F. X. et al. (1981) 'Proteolytic cleavage of influenza virus hemagglutinins: primary structure of the connecting peptide between HA1 and HA2 determines proteolytic

cleavability and pathogenicity of avian influenza viruses', Virology, 113(2), pp. 725–735. doi: 10.1016/0042-6822(81)90201-4.

Both, G. W. et al. (1983) 'Antigenic drift in influenza virus H3 hemagglutinin from 1968 to 1980: multiple evolutionary pathways and sequential amino acid changes at key antigenic sites.', Journal of virology, 48(1), pp. 52–60. Available at: http://www.ncbi.nlm.nih.gov/entrez/query.fcgi?db=pubmed&cmd=Retrieve&dopt=AbstractPlus&list_uids=6193288.

Bouvier, N. M. and Lowen, A. C. (2010) 'Animal models for influenza virus pathogenesis and transmission', Viruses, 2(8), pp. 1530–1563. doi: 10.3390/v20801530.

Boyd, A. C. et al. (2013) 'Towards a universal vaccine for avian influenza: Protective efficacy of modified Vaccinia virus Ankara and Adenovirus vaccines expressing conserved influenza antigens in chickens challenged with low pathogenic avian influenza virus', Vaccine, 31(4), pp. 670–675. doi: 10.1016/j.vaccine.2012.11.047.

Brett, I. C. and Johansson, B. E. (2005) 'Immunization against influenza A virus: Comparison of conventional inactivated, live-attenuated and recombinant baculovirus produced purified hemagglutinin and neuraminidase vaccines in a murine model system', Virology. Academic Press, 339(2), pp. 273–280. doi: 10.1016/J.VIROL.2005.06.006.

Bridges, C. B. et al. (2000) 'Risk of Influenza A (H5N1) Infection among Health Care Workers Exposed to Patients with Influenza A (H5N1), Hong Kong', The Journal of Infectious Diseases, 181(1), pp. 344–348. doi: 10.1086/315213.

Bucher, D. J. and Kilbourne, E. D. (1972) 'A 2 (N2) neuraminidase of the X-7 influenza virus recombinant: determination of molecular size and subunit composition of the active unit.', Journal of virology, 10(1), pp. 60–6. Available at: http://www.ncbi.nlm.nih.gov/pubmed/5040386.

Carrat, F. and Flahault, A. (2007) 'Influenza vaccine: The challenge of antigenic drift', Vaccine, 25(39–40), pp. 6852–6862. doi: 10.1016/j.vaccine.2007.07.027.

Carter, D. M. et al. (2016) 'Design and Characterization of a Computationally Optimized Broadly Reactive Hemagglutinin Vaccine for H1N1 Influenza Viruses', Journal of Virology. doi: 10.1128/JVI.03152-15.

Cerutti, A. and Rescigno, M. (2008) 'The Biology of Intestinal Immunoglobulin A Responses', Immunity, 28(6), pp. 740–750. doi: 10.1016/j.immuni.2008.05.001.

Chen, Y. Q. et al. (2018) 'Influenza Infection in Humans Induces Broadly Cross-Reactive and Protective Neuraminidase-Reactive Antibodies', Cell. Elsevier Inc., 173(2), p. 417–429.e10. doi: 10.1016/j.cell.2018.03.030.

Chen, Z. et al. (2000) 'Cross-protection against a lethal influenza virus infection by DNA vaccine to neuraminidase', Vaccine, 18(28), pp. 3214–3222. doi: 10.1016/S0264-410X(00)00149-3.

Cheng, X. et al. (2013) 'Evaluation of the Humoral and Cellular Immune Responses Elicited by the Live Attenuated and Inactivated Influenza Vaccines and Their Roles in Heterologous Protection in Ferrets', The Journal of Infectious Diseases, 208(4), pp. 594–602. doi: 10.1093/infdis/jit207.

Cohen, M. et al. (2013) 'Influenza A penetrates host mucus by cleaving sialic acids with neuraminidase', Virology Journal, 10(1), p. 321. doi: 10.1186/1743-422X-10-321.

Connole, M. D. et al. (2000) 'Natural pathogens of laboratory animals and their effects on research', Medical Mycology, 38(s1), pp. 59–65. doi: 10.1080/mmy.38.s1.59.65.

Corti, D. et al. (2011) 'A Neutralizing Antibody Selected from Plasma Cells That Binds to Group 1 and Group 2 Influenza A Hemagglutinins', Science, 333(6044), pp. 850–856. doi: 10.1126/science.1205669.

Couch, R. B. et al. (1974) 'Induction of partial immunity to influenza by a neuraminidase-specific vaccine.', The Journal of infectious diseases, 129(4), pp. 411–420. Available at: https://www.ncbi.nlm.nih.gov/pubmed?Db=pubmed&Cmd=Retrieve&list_uids=4593871&dopt=abstractplus.

Couzens, L. et al. (2014) 'An optimized enzyme-linked lectin assay to measure influenza A virus neuraminidase inhibition antibody titers in human sera', Journal of Virological Methods, 210, pp. 7–14. doi: 10.1016/j.jviromet.2014.09.003.

Cox, N. J. and Subbarao, K. (2000) 'Global Epidemiology of Influenza: Past and Present', Annual Review of Medicine, 51, pp. 407–21. doi: 10.1146/annurev.med.51.1.407.

Crank, M. C. et al. (2015) 'Phase 1 Study of Pandemic H1 DNA Vaccine in Healthy Adults', PLOS ONE. Edited by V. C. Huber, 10(4), p. e0123969. doi: 10.1371/journal.pone.0123969.

Crawford, J. et al. (1999) 'Baculovirus-derived hemagglutinin vaccines protect against lethal influenza infections by avian H5 and H7 subtypes', Vaccine, 17(18), pp. 2265–2274. doi: 10.1016/S0264-410X(98)00494-0.

Crevar, C. J. et al. (2015) 'Cocktail of H5N1 COBRA HA vaccines elicit protective antibodies against H5N1 viruses from multiple clades', Human Vaccines & Immunotherapeutics, 11(3), pp. 572–583. doi: 10.1080/21645515.2015.1012013.

Crosby, C. M. et al. (2017) 'Replicating Single-Cycle Adenovirus Vectors Generate Amplified Influenza Vaccine Responses', Journal of Virology. Edited by T. S. Dermody, 91(2). doi: 10.1128/JVI.00720-16.

Daya, S. and Berns, K. I. (2008) 'Gene Therapy Using Adeno-Associated Virus Vectors', Clinical Microbiology Reviews, 21(4), pp. 583–593. doi: 10.1128/CMR.00008-08.

Direksin, K., Joo, H. and Goyal, S. M. (2002) 'An Immunoperoxidase Monolayer Assay for the Detection of Antibodies against Swine Influenza Virus', Journal of Veterinary Diagnostic Investigation, 14(2), pp. 169–171. doi: 10.1177/104063870201400215.

Ducatez, M. F. et al. (2016) 'Low pathogenic avian influenza (H9N2) in chicken: Evaluation of an ancestral H9-MVA vaccine', Veterinary Microbiology, 189, pp. 59–67. doi: 10.1016/j.vetmic.2016.04.025.

Dwyer, J. M. and Johnson, C. (1981) 'The use of concanavalin A to study the immunoregulation of human T cells.', Clinical and experimental immunology, 46(2), pp. 237–49. Available at: http://www.pubmedcentral.nih.gov/articlerender.fcgi?artid=1536405&tool=pmcentrez&rendertype=abstract.

Ekiert, D. C. et al. (2009) 'Antibody Recognition of a Highly Conserved Influenza Virus Epitope', Science, 324(5924), pp. 246–251. doi: 10.1126/science.1171491.

Ekiert, D. C. et al. (2012) 'Cross-neutralization of influenza A viruses mediated by a single antibody loop', Nature, 489(7417), pp. 526–532. doi: 10.1038/nature11414.

Ekiert, D. C. and Wilson, I. A. (2012) 'Broadly neutralizing antibodies against influenza virus and prospects for universal therapies', Current Opinion in Virology, 2(2), pp. 134–141. doi: 10.1016/j.coviro.2012.02.005.

Enkirch, T. and von Messling, V. (2015) 'Ferret models of viral pathogenesis', Virology, 479–480, pp. 259–270. doi: 10.1016/j.virol.2015.03.017.

Ermler, M. E. et al. (2017) 'Chimeric Hemagglutinin Constructs Induce Broad Protection against Influenza B Virus Challenge in the Mouse Model', Journal of Virology. Edited by T. S. Dermody, 91(12). doi: 10.1128/JVI.00286-17.

FDA Information Regarding FluMist Quadrivalent Vaccine (2018). Available at: https://www.fda.gov/BiologicsBloodVaccines/Vaccines/ApprovedProducts/ucm508761.htm (Accessed: 30 May 2018).

Fields, B., Knipe, D. M. and Howley, P. M. (1996) Field's Virology, Lippincott Williams & Wilkins.

Finkelshtein, D. et al. (2013) 'LDL receptor and its family members serve as the cellular receptors for vesicular stomatitis virus', Proceedings of the National Academy of Sciences, 110(18), pp. 7306–7311. doi: 10.1073/pnas.1214441110.

Fiore, A. E., Bridges, C. B. and Cox, N. J. (2009) 'Seasonal Influenza Vaccines', in Current Topics in Microbiology and Immunology, pp. 43–82. doi: 10.1007/978-3-540-92165-3_3.

Fleury, D. et al. (1998) 'Antigen distortion allows influenza virus to escape neutralization', Nature Structural Biology, 5(2), pp. 119–124. doi: 10.1038/nsb0298-119.

Florek, N. W. et al. (2014) 'Modified Vaccinia Virus Ankara Encoding Influenza Virus Hemagglutinin Induces Heterosubtypic Immunity in Macaques', Journal of Virology, 88(22), pp. 13418–13428. doi: 10.1128/JVI.01219-14.

Fouchier, R. A. M. et al. (2005) 'Characterization of a Novel Influenza A Virus Hemagglutinin Subtype (H16) Obtained from Black-Headed Gulls', Journal of Virology, 79(5), pp. 2814–2822. doi: 10.1128/JVI.79.5.2814-2822.2005.

Francis, T. (1934) 'Transmission of influenza by filtrable virus', Science, 80, pp. 457–459.

Francis, T. (1937) 'Epidemiological Studies in Influenza', Am J Public Health Nations Health, 27(3), pp. 211–225. Available at: http://www.ncbi.nlm.nih.gov/pubmed/18014585.

Freidl, G. S. et al. (2015) 'Serological Evidence of Influenza A Viruses in Frugivorous Bats from Africa', PLOS ONE. Edited by M. L. Baker, 10(5), p. e0127035. doi: 10.1371/journal.pone.0127035.

Fujiyoshi, Y. et al. (1994) 'Fine structure of influenza A virus observed by electron cryo-microscopy.', The EMBO journal, 13(2), pp. 318–26. doi: 10.1093/embo-reports/kve234.

Gao, J., Couzens, L. and Eichelberger, M. C. (2016) 'Measuring Influenza Neuraminidase Inhibition Antibody Titers by Enzyme-linked Lectin Assay', Journal of Visualized Experiments, (115). doi: 10.3791/54573.

Gavrilov, V. et al. (2011) 'Influenza virus-like particles as a new tool for vaccine immunogenicity testing: Validation of a neuraminidase neutralizing antibody assay', Journal of Virological Methods, 173(2), pp. 364–373. doi: 10.1016/j.jviromet.2011.03.011.

Gerdil, C. (2003) 'The annual production cycle for influenza vaccine', Vaccine, 21(16), pp. 1776–1779. doi: 10.1016/S0264-410X(03)00071-9.

Getie-Kebtie, M. et al. (2013) 'Label-free mass spectrometry-based quantification of hemagglutinin and neuraminidase in influenza virus preparations and vaccines', Influenza and Other Respiratory Viruses, 7(4), pp. 521–530. doi: 10.1111/irv.12001.

Giles, B. M. and Ross, T. M. (2011) 'A computationally optimized broadly reactive antigen (COBRA) based H5N1 VLP vaccine elicits broadly reactive antibodies in mice and ferrets', Vaccine, 29(16), pp. 3043–3054. doi: 10.1016/j.vaccine.2011.01.100.

Goodman, A. G. et al. (2011) 'A Human Multi-Epitope Recombinant Vaccinia Virus as a Universal T Cell Vaccine Candidate against Influenza Virus', PLoS ONE. Edited by E. N. Miyaji, 6(10), p. e25938. doi: 10.1371/journal.pone.0025938.

Gutiérrez, A. H. et al. (2016) 'In vivo validation of predicted and conserved T cell epitopes in a swine influenza model', PLoS ONE, 11(7), pp. 1–19. doi: 10.1371/journal.pone.0159237.

Haff, R. F., Schriver, P. W. and Stewart, R. C. (1966) 'Pathogenesis of influenza in ferrets: nasal manifestations of disease.', British Journal of Experimental Pathology, 47(5), pp. 435–44. Available at: http://www.pubmedcentral.nih.gov/articlerender.fcgi?artid=2093728&tool=pmcentrez&rendertype=abstract.

Halbherr, S. J. et al. (2013) 'Vaccination with Recombinant RNA Replicon Particles Protects Chickens from H5N1 Highly Pathogenic Avian Influenza Virus', PLoS ONE, 8(6), p. e66059. doi: 10.1371/journal.pone.0066059.

Halbherr, S. J. et al. (2015) 'Biological and Protective Properties of Immune Sera Directed to the Influenza Virus Neuraminidase', Journal of Virology, 89(3), pp. 1550–1563. doi: 10.1128/JVI.02949-14.

Hanika, A. et al. (2005) 'Use of influenza C virus glycoprotein HEF for generation of vesicular stomatitis virus pseudotypes', Journal of General Virology, 86(5), pp. 1455–1465. doi: 10.1099/vir.0.80788-0.

Hashem, A. M. (2015) 'Prospects of HA-Based Universal Influenza Vaccine', BioMed Research International, 2015, pp. 1–12. doi: 10.1155/2015/414637.

Hensley, S. E. et al. (2009) 'Hemagglutinin receptor binding avidity drives influenza a virus antigenic drift', Science, 326(5953), pp. 734–736. doi: 10.1126/science.1178258.

Hensley, S. E. et al. (2009) 'Hemagglutinin receptor binding avidity drives influenza A virus antigenic drift', F1000 - Post-publication peer review of the biomedical literature. Available at: http://science.sciencemag.org/content/326/5953/734.short.

Herlocher, M. L. et al. (2001) 'Ferrets as a Transmission Model for Influenza: Sequence Changes in HA1 of Type A (H3N2) Virus', The Journal of Infectious Diseases, 184(5), pp. 542–546. doi: 10.1086/322801.

Hessel, A. et al. (2014) 'MVA Vectors Expressing Conserved Influenza Proteins Protect Mice against Lethal Challenge with H5N1, H9N2 and H7N1 Viruses', PLoS ONE. Edited by G. P. Kobinger, 9(2), p. e88340. doi: 10.1371/journal.pone.0088340.

Hilleman, M. R., Mason, R. P. and Buescher, E. L. (1950) 'Antigenic Pattern of Strains of Influenza A and B', Experimental Biology and Medicine, 75(3), pp. 829–834. doi: 10.3181/00379727-75-18361.

Hobson, D. et al. (1972) 'The role of serum haemagglutination-inhibiting antibody in protection against challenge infection with influenza A2 and B viruses', Journal of Hygiene, 70(04), pp. 767–777. doi: 10.1017/S0022172400022610.

Houser, K. and Subbarao, K. (2015) 'Influenza Vaccines: Challenges and Solutions', Cell Host & Microbe. Elsevier Inc., 17(3), pp. 295–300. doi: 10.1016/j.chom.2015.02.012.

Ibricevic, A. et al. (2006) 'Influenza Virus Receptor Specificity and Cell Tropism in Mouse and Human Airway Epithelial Cells', Journal of Virology, 80(15), pp. 7469–7480. doi: 10.1128/JVI.02677-05.

Impagliazzo, A. et al. (2015) 'A stable trimeric influenza hemagglutinin stem as a broadly protective immunogen', Science, 349(6254), pp. 1301–1306. doi: 10.1126/science.aac7263.

Jacobsen, H. et al. (2017) 'Influenza Virus Hemagglutinin Stalk-Specific Antibodies in Human Serum are a Surrogate Marker for In Vivo Protection in a Serum Transfer Mouse Challenge Model', mBio. Edited by R. Rappuoli, 8(5). doi: 10.1128/mBio.01463-17.

Jang, Y. and Seong, B. (2014) 'Options and Obstacles for Designing a Universal Influenza Vaccine', Viruses, 6(8), pp. 3159–3180. doi: 10.3390/v6083159.

Jegaskanda, S. et al. (2013) 'Standard Trivalent Influenza Virus Protein Vaccination Does Not Prime Antibody-Dependent Cellular Cytotoxicity in Macaques', Journal of Virology, 87(24), pp. 13706–13718. doi: 10.1128/JVI.01666-13.

Jin, H. et al. (2003) 'Multiple amino acid residues confer temperature sensitivity to human influenza virus vaccine strains (flumist) derived from cold-adapted a/ann arbor/6/60', Virology, 306(1), pp. 18–24. doi: 10.1016/S0042-6822(02)00035-1.

Jin, H. and Chen, Z. (2014) 'Production of live attenuated influenza vaccines against seasonal and potential pandemic influenza viruses', Current Opinion in Virology. Elsevier B.V., 6(1), pp. 34–39. doi: 10.1016/j.coviro.2014.02.008.

Job, E. R. et al. (2017) 'Antibodies directed towards neuraminidase N1 control disease in a mouse model of influenza', Journal of Virology, (November), p. JVI.01584-17. doi: 10.1128/JVI.01584-17.

Johansson, B. E. et al. (1987) 'Immunologic response to influenza virus neuraminidase is influenced by prior experience with the associated viral hemagglutinin. III. Reduced generation of neuraminidase-specific helper T cells in hemagglutinin-primed mice.', Journal of immunology (Baltimore, Md. : 1950), 139(6), pp. 2015–9. Available at: http://www.ncbi.nlm.nih.gov/pubmed/2957444.

Johansson, B. E., Bucher, D. J. and Kilbourne, E. D. (1989) 'Purified influenza virus hemagglutinin and neuraminidase are equivalent in stimulation of antibody response but induce contrasting types of immunity to infection.', Journal of

virology. American Society for Microbiology, 63(3), pp. 1239–46. Available at: https://www.ncbi.nlm.nih.gov/labs/articles/2915381/%5Cnhttp://jvi.asm.org/cgi/content/long/63/3/1239.

Johansson, B. E., Matthews, J. T. and Kilbourne, E. D. (1998) 'Supplementation of conventional influenza A vaccine with purified viral neuraminidase results in a balanced and broadened immune response', Vaccine, 16(9–10), pp. 1009–1015. doi: 10.1016/S0264-410X(97)00279-X.

Johnson, N. P. A. S. and Mueller, J. (2002) 'Updating the accounts: global mortality of the 1918-1920 "Spanish" influenza pandemic.', Bulletin of the history of medicine, 76(1), pp. 105–15. doi: 10.1353/bhm.2002.0022.

Kalbfuss, B. et al. (2008) 'Monitoring influenza virus content in vaccine production: Precise assays for the quantitation of hemagglutination and neuraminidase activity', Biologicals, 36(3), pp. 145–161. doi: 10.1016/j.biologicals.2007.10.002.

Kalhoro, N. H. et al. (2009) 'A recombinant vesicular stomatitis virus replicon vaccine protects chickens from highly pathogenic avian influenza virus (H7N1)', Vaccine. Available at: http://www.sciencedirect.com/science/article/pii/S0264410X08017519.

Kärber, G. (1931) 'Beitrag zur kollektiven Behandlung pharmakologischer Reihenversuche', Naunyn-Schmiedebergs Archiv für Experimentelle Pathologie und Pharmakologie, 162(4), pp. 480–483. doi: 10.1007/BF01863914.

Kay, M. A. et al. (2000) 'Evidence for gene transfer and expression of factor IX in haemophilia B patients treated with an AAV vector', Nature Genetics, 24(3), pp. 257–261. doi: 10.1038/73464.

Kendal, A. P., Bozeman, F. M. and Ennis, F. A. (1980) 'Further studies of the neuraminidase content of inactivated influenza vaccines and the neuraminidase antibody responses after vaccination of immunologically primed and unprimed populations', Infection and Immunity. American Society for Microbiology, 29(3), pp. 966–971. doi: 10.1093/infdis/136.Supplement_3.S415.

Khurana, S. et al. (2009) 'Antigenic Fingerprinting of H5N1 Avian Influenza Using Convalescent Sera and Monoclonal Antibodies Reveals Potential Vaccine and Diagnostic Targets', PLoS Medicine. Edited by M. Peiris, 6(4), p. e1000049. doi: 10.1371/journal.pmed.1000049.

Kilbourne, E. D. et al. (1971) 'Correlated Studies of a Recombinant Influenza-Virus Vaccine. I. Derivation and Characterization of Virus and Vaccine', Journal of Infectious Diseases, 124(5), pp. 449–462. doi: 10.1093/infdis/124.5.449.

King, J. C. et al. (2009) 'Evaluation of the safety, reactogenicity and immunogenicity of FluBlok® trivalent recombinant baculovirus-expressed hemagglutinin influenza vaccine administered intramuscularly to healthy children aged 6–59 months', Vaccine, 27(47), pp. 6589–6594. doi: 10.1016/j.vaccine.2009.08.032.

Kirchenbaum, G. A., Carter, D. M. and Ross, T. M. (2016) 'Sequential Infection in Ferrets with Antigenically Distinct Seasonal H1N1 Influenza Viruses Boosts Hemagglutinin Stalk-Specific Antibodies', Journal of Virology. Edited by A. García-Sastre, 90(2), pp. 1116–1128. doi: 10.1128/JVI.02372-15.

Kolpe, A. et al. (2017) 'M2-based influenza vaccines: recent advances and clinical potential', Expert Review of Vaccines, 16(2), pp. 123–136. doi: 10.1080/14760584.2017.1240041.

Krammer, F. et al. (2013) 'Chimeric Hemagglutinin Influenza Virus Vaccine Constructs Elicit Broadly Protective Stalk-Specific Antibodies', Journal of Virology, 87(12), pp. 6542–6550. doi: 10.1128/JVI.00641-13.

Krammer, F. et al. (2018) 'NAction! How Can Neuraminidase-Based Immunity Contribute to Better Influenza Virus Vaccines?', MBio., 9(2).(pii), p. mBio.02332-17. doi: 10.1128/mBio.02332-17. doi: 10.1128/mBio.02332-17.

Krammer, F. and Palese, P. (2013) 'Influenza virus hemagglutinin stalk-based antibodies and vaccines', Current Opinion in Virology, 3(5), pp. 521–530. doi: 10.1016/j.coviro.2013.07.007.

Kreijtz, J. H. C. M., Fouchier, R. A. M. and Rimmelzwaan, G. F. (2011) 'Immune responses to influenza virus infection', Virus Research, pp. 19–30. doi: 10.1016/j.virusres.2011.09.022.

Krug, R. M. et al. (1989) 'Expression and replication of the influenza virus genome', in The Influenza viruses, pp. 89–152. doi: 10.1007/978-1-4613-0811-9_2.

Kuck, D. et al. (2006) 'Intranasal vaccination with recombinant adeno-associated virus type 5 against human papillomavirus type 16 L1', J Virol, 80(6), pp. 2621–2630. doi: 80/6/2621 [pii]\r10.1128/JVI.80.6.2621-2630.2006.

Kugel, D. et al. (2009) 'Intranasal Administration of Alpha Interferon Reduces Seasonal Influenza A Virus Morbidity in Ferrets', Journal of Virology, 83(8), pp. 3843–3851. doi: 10.1128/JVI.02453-08.

Kumar, S., Stecher, G. and Tamura, K. (2016) 'MEGA7: Molecular Evolutionary Genetics Analysis Version 7.0 for Bigger Datasets', Molecular biology and evolution, 33(7), pp. 1870–1874. doi: 10.1093/molbev/msw054.

Lambert, L. C. and Fauci, A. S. (2010) 'Influenza Vaccines for the Future', New England Journal of Medicine, 363(21), pp. 2036–2044. doi: 10.1056/NEJMra1002842.

Lazniewski, M. et al. (2017) 'The structural variability of the influenza A hemagglutinin receptor-binding site.', Briefings in functional genomics. doi: 10.1093/bfgp/elx042.

Ledgerwood, J. E. et al. (2012) 'Influenza virus H5 DNA vaccination is immunogenic by intramuscular and intradermal routes in humans', Clinical and Vaccine Immunology, 19(11), pp. 1792–1797. doi: 10.1128/CVI.05663-11.

Lee, P. S. et al. (2012) 'Heterosubtypic antibody recognition of the influenza virus hemagglutinin receptor binding site enhanced by avidity', Proceedings of the National Academy of Sciences, 109(42), pp. 17040–17045. doi: 10.1073/pnas.1212371109.

Lee, P. S. et al. (2014) 'Receptor mimicry by antibody F045–092 facilitates universal binding to the H3 subtype of influenza virus', Nature Communications, 5(1), p. 3614. doi: 10.1038/ncomms4614.

Lee, Y.-N. et al. (2015) 'Co-immunization with tandem repeat heterologous M2 extracellular proteins overcomes strain-specific protection of split vaccine

against influenza A virus', Antiviral Research, 122, pp. 82–90. doi: 10.1016/j.antiviral.2015.08.001.

Leigh, M. W. et al. (1995) 'Receptor specificity of influenza virus influences severity of illness in ferrets', Vaccine, 13(15), pp. 1468–1473. doi: 10.1016/0264-410X(95)00004-K.

Leigh, M. W., Cheng, P. W. and Boat, T. F. (1989) 'Developmental Changes of Ferret Tracheal Mucin Composition and Biosynthesis', Biochemistry, 28(24), pp. 9440–9446. doi: 10.1021/bi00450a029.

Li, J. and Zhang, Y. (2012) 'Messenger RNA Cap Methylation in Vesicular Stomatitis Virus, a Prototype of Non-Segmented Negative-Sense RNA Virus', in Methylation - From DNA, RNA and Histones to Diseases and Treatment. InTech. doi: 10.5772/54598.

Li, Q. et al. (2014) 'Epidemiology of Human Infections with Avian Influenza A(H7N9) Virus in China', New England Journal of Medicine, 370(6), pp. 520–532. doi: 10.1056/NEJMoa1304617.

Li, X. et al. (2012) 'Novel AAV-based genetic vaccines encoding truncated dengue virus envelope proteins elicit humoral immune responses in mice', Microbes and Infection, 14(11), pp. 1000–1007. doi: 10.1016/j.micinf.2012.05.002.

Li, Z. et al. (2015) 'Efficacy of a parainfluenza virus 5 (PIV5)- Based H7N9 vaccine in mice and guinea pigs: Antibody titer towards ha was not a good indicator for protection', PLoS ONE, 10(3). doi: 10.1371/journal.pone.0120355.

Lichty, B. D. et al. (2004) 'Vesicular Stomatitis Virus: A Potential Therapeutic Virus for the Treatment of Hematologic Malignancy', Human Gene Therapy, 15(9), pp. 821–831. doi: 10.1089/hum.2004.15.821.

Lillie, P. J. et al. (2012) 'Preliminary assessment of the efficacy of a T-cell-based influenza vaccine, MVA-NP+M1, in humans', Clinical Infectious Diseases, 55(1), pp. 19–25. doi: 10.1093/cid/cis327.

Linden, R. M. et al. (1996) 'Site-specific integration by adeno-associated virus.', Proceedings of the National Academy of Sciences, 93(21), pp. 11288–11294. doi: 10.1073/pnas.93.21.11288.

Liu, C. et al. (1995) 'Influenza type A virus neuraminidase does not play a role in viral entry, replication, assembly, or budding.', Journal of virology, 69(2), pp. 1099–106. Available at: http://jvi.asm.org/content/69/2/1099.abstract.

Liu, W.-C. et al. (2015) 'Cross-Reactive Neuraminidase-Inhibiting Antibodies Elicited by Immunization with Recombinant Neuraminidase Proteins of H5N1 and Pandemic H1N1 Influenza A Viruses', Journal of Virology. Edited by S. Perlman, 89(14), pp. 7224–7234. doi: 10.1128/JVI.00585-15.

López-Macías, C. et al. (2011) 'Safety and immunogenicity of a virus-like particle pandemic influenza A (H1N1) 2009 vaccine in a blinded, randomized, placebo-controlled trial of adults in Mexico', Vaccine, 29(44), pp. 7826–7834. doi: 10.1016/j.vaccine.2011.07.099.

Low, J. G. H. et al. (2014) 'Safety and immunogenicity of a virus-like particle pandemic influenza A (H1N1) 2009 vaccine: Results from a double-blinded, randomized

Phase I clinical trial in healthy Asian volunteers', Vaccine, 32(39), pp. 5041–5048. doi: 10.1016/j.vaccine.2014.07.011.

Luke, C. J. and Subbarao, K. (2006) 'Vaccines for pandemic influenza', Emerging Infectious Diseases, 12(1), pp. 66–72. doi: 10.3201/eid1201.051147.

Maher, J. A. and DeStefano, J. (2004) 'The ferret: An animal model to study influenza virus', Lab Animal, 33(9), pp. 50–53. doi: 10.1038/laban1004-50.

Manning, W. C. et al. (1997) 'Genetic immunization with adeno-associated virus vectors expressing herpes simplex virus type 2 glycoproteins B and D.', Journal of virology, 71(10), pp. 7960–2. Available at: http://www.pubmedcentral.nih.gov/articlerender.fcgi?artid=192154&tool=pmcentrez&rendertype=abstract.

Marcelin, G. et al. (2010) 'Inactivated Seasonal Influenza Vaccines Increase Serum Antibodies to the Neuraminidase of Pandemic Influenza A(H1N1) 2009 Virus in an Age-Dependent Manner', The Journal of Infectious Diseases, 202(11), pp. 1634–1638. doi: 10.1086/657084.

Marcelin, G. et al. (2011) 'A contributing role for anti-neuraminidase antibodies on immunity to pandemic h1n1 2009 influenza a virus', PLoS ONE, 6(10), p. e26335. doi: 10.1371/journal.pone.0026335.

Marcelin, G., Sandbulte, M. R. and Webby, R. J. (2012) 'Contribution of antibody production against neuraminidase to the protection afforded by influenza vaccines', Reviews in Medical Virology, 22(4), pp. 267–279. doi: 10.1002/rmv.1713.

Margine, I. and Krammer, F. (2014) 'Animal Models for Influenza Viruses: Implications for Universal Vaccine Development', Pathogens, 3(4), pp. 845–874. doi: 10.3390/pathogens3040845.

Marzi, A. et al. (2015) 'VSV-EBOV rapidly protects macaques against infection with the 2014/15 Ebola virus outbreak strain', Science, 349(6249), pp. 739–742. doi: 10.1126/science.aab3920.

Matrosovich, M. N. et al. (1997) 'Avian influenza A viruses differ from human viruses by recognition of sialyloligosaccharides and gangliosides and by a higher conservation of the HA receptor-binding site', Virology, 233(1), pp. 224–234. doi: 10.1006/viro.1997.8580.

Matrosovich, M. N. et al. (2004a) 'Human and avian influenza viruses target different cell types in cultures of human airway epithelium', Proceedings of the National Academy of Sciences, 101(13), pp. 4620–4624. doi: 10.1073/pnas.0308001101.

Matrosovich, M. N. et al. (2004b) 'Neuraminidase Is Important for the Initiation of Influenza Virus Infection in Human Airway Epithelium', Journal of Virology, 78(22), pp. 12665–12667. doi: 10.1128/JVI.78.22.12665-12667.2004.

Matsuoka, Y., Lamirande, E. W. and Subbarao, K. (2009) 'The Mouse Model for Influenza', in Current Protocols in Microbiology. Hoboken, NJ, USA: John Wiley & Sons, Inc., p. 15G.3.1-15G.3.30. doi: 10.1002/9780471729259.mc15g03s13.

McCarty, D. M. (2008) 'Self-complementary AAV Vectors; Advances and Applications', Molecular Therapy, 16(10), pp. 1648–1656. doi: 10.1038/mt.2008.171.

Memoli, M. J. et al. (2016) 'Evaluation of antihemagglutinin and antineuraminidase antibodies as correlates of protection in an influenza A/H1N1 virus healthy human challenge model', mBio, 7(2). doi: 10.1128/mBio.00417-16.

Mills, C. D. et al. (2000) 'M-1/M-2 Macrophages and the Th1/Th2 Paradigm', The Journal of Immunology, 164(12), pp. 6166–6173. doi: 10.4049/jimmunol.164.12.6166.

Mohn, K. G.-I. et al. (2017) 'Immune responses after live attenuated influenza vaccination', Human Vaccines & Immunotherapeutics. Taylor & Francis, 14(3), pp. 00–00. doi: 10.1080/21645515.2017.1377376.

Monto, A. S. et al. (2015) 'Antibody to influenza virus neuraminidase: An independent correlate of protection', Journal of Infectious Diseases, 212(8), pp. 1191–1199. doi: 10.1093/infdis/jiv195.

Nachbagauer, R. et al. (2014) 'Induction of Broadly Reactive Anti-Hemagglutinin Stalk Antibodies by an H5N1 Vaccine in Humans', Journal of Virology, 88(22), pp. 13260–13268. doi: 10.1128/JVI.02133-14.

Nachbagauer, R. et al. (2017) 'A universal influenza virus vaccine candidate confers protection against pandemic H1N1 infection in preclinical ferret studies', npj Vaccines. Springer US, 2(1), p. 26. doi: 10.1038/s41541-017-0026-4.

Narasaraju, T. et al. (2009) 'Adaptation of human influenza H3N2 virus in a mouse pneumonitis model: insights into viral virulence, tissue tropism and host pathogenesis', Microbes and Infection, 11(1), pp. 2–11. doi: 10.1016/j.micinf.2008.09.013.

Nieto, K. et al. (2009) 'Combined prophylactic and therapeutic intranasal vaccination against human papillomavirus type-16 using different adeno-associated virus serotype vectors', Antiviral Therapy, 14(8), pp. 1125–1137. doi: 10.3851/IMP1469.

Nieto, K. and Salvetti, A. (2014) 'AAV vectors vaccines against infectious diseases', Frontiers in Immunology, 5(JAN), pp. 1–9. doi: 10.3389/fimmu.2014.00005.

Novak, M. et al. (1993) 'Murine model for evaluation of protective immunity to influenza virus', Vaccine, 11(1), pp. 55–60. doi: 10.1016/0264-410X(93)90339-Y.

Organisation, W. H. (2015) Recommended composition of influenza virus vaccines for use in the 2015–2016 northern hemisphere influenza season., http://www.euro.who.int/__data/assets/pdf_file/0011/290954/WHO-Euro-recommendations-influenza-vaccination-2015-2016.pdf?ua=1]. Available at: http://eutils.ncbi.nlm.nih.gov/entrez/eutils/elink.fcgi?dbfrom=pubmed&id=25771542&retmode=ref&cmd=prlinks%5Cnpapers3://publication/uuid/D5A5FF30-19E1-45F0-A209-809291D78F8F (Accessed: 29 May 2018).

Palese, P. et al. (1974) 'Characterization of temperature sensitive influenza virus mutants defective in neuraminidase', Virology, 61(2), pp. 397–410. doi: 10.1016/0042-6822(74)90276-1.

Palese, P. and Shaw, M. L. (2007) 'Orthomyxoviridae: The Viruses and Their Replication', in Fields virology. 5th edn. Philadelphia, PA: Lippincott Williams & Wilkins, Wolters Kluwer Business, pp. 1647–1689.

Paterson, R. G. and Lamb, R. A. (1990) 'Conversion of a class II integral membrane protein into a soluble and efficiently secreted protein: Multiple intracellular and

extracellular oligomeric and conformational forms', Journal of Cell Biology, 110(4), pp. 999–1011. doi: 10.1083/jcb.110.4.999.

Petsch, B. et al. (2012) 'Protective efficacy of in vitro synthesized, specific mRNA vaccines against influenza A virus infection', Nature Biotechnology, 30(12), pp. 1210–1216. doi: 10.1038/nbt.2436.

Pillet, S. et al. (2016) 'A plant-derived quadrivalent virus like particle influenza vaccine induces cross-reactive antibody and T cell response in healthy adults', Clinical Immunology, 168, pp. 72–87. doi: 10.1016/j.clim.2016.03.008.

Ploquin, A. et al. (2013) 'Protection against henipavirus infection by use of recombinant adeno-associated virus-vector vaccines', Journal of Infectious Diseases, 207(3), pp. 469–478. doi: 10.1093/infdis/jis699.

Potier, M. et al. (1979) 'Fluorometric assay of neuraminidase with a sodium (4-methylumbelliferyl-α-d-N-acetylneuraminate) substrate', Analytical Biochemistry, 94(2), pp. 287–296. doi: 10.1016/0003-2697(79)90362-2.

Prevato, M. et al. (2015) 'Expression and Characterization of Recombinant, Tetrameric and Enzymatically Active Influenza Neuraminidase for the Setup of an Enzyme-Linked Lectin-Based Assay', PLOS ONE. Edited by Z. Ye, 10(8), p. e0135474. doi: 10.1371/journal.pone.0135474.

Publicover, J., Ramsburg, E. and Rose, J. K. (2005) 'A Single-Cycle Vaccine Vector Based on Vesicular Stomatitis Virus Can Induce Immune Responses Comparable to Those Generated by a Replication-Competent Vector', Journal of Virology, 79(21), pp. 13231–13238. doi: 10.1128/JVI.79.21.13231-13238.2005.

Rajão, D. S. and Pérez, D. R. (2018) 'Universal vaccines and vaccine platforms to protect against influenza viruses in humans and agriculture', Frontiers in Microbiology, 9(FEB), pp. 1–21. doi: 10.3389/fmicb.2018.00123.

Rajendran, M. et al. (2017) 'Analysis of anti-influenza virus neuraminidase antibodies in children, adults, and the elderly by ELISA and enzyme inhibition: Evidence for original antigenic sin', mBio, 8(2), pp. 1–12. doi: 10.1128/mBio.02281-16.

Van Reeth, K. et al. (2009) 'Prior infection with an H1N1 swine influenza virus partially protects pigs against a low pathogenic H5N1 avian influenza virus', Vaccine, 27(45), pp. 6330–6339. doi: 10.1016/j.vaccine.2009.03.021.

Remacle, A. G. et al. (2008) 'Substrate cleavage analysis of furin and related proprotein convertases: A comparative study', Journal of Biological Chemistry, 283(30), pp. 20897–20906. doi: 10.1074/jbc.M803762200.

Renegar, K. B. (1992) 'Influenza virus infections and immunity: a review of human and animal models.', Laboratory animal science, 42(3), pp. 222–32. Available at: http://www.ncbi.nlm.nih.gov/pubmed/1320150.

Rentsch, M. B. and Zimmer, G. (2011) 'A vesicular stomatitis virus replicon-based bioassay for the rapid and sensitive determination of multi-species type I interferon', PLoS ONE, 6(10), p. e25858. doi: 10.1371/journal.pone.0025858.

Rimmelzwaan, G. F. and McElhaney, J. E. (2008) 'Correlates of protection: Novel generations of influenza vaccines', Vaccine, 26(SUPPL. 4), pp. D41–D44. doi: 10.1016/j.vaccine.2008.07.043.

Roberts, A. et al. (1999) 'Attenuated vesicular stomatitis viruses as vaccine vectors.', Journal of virology. American Society for Microbiology, 73(5), pp. 3723–3732. Available at: http://eutils.ncbi.nlm.nih.gov/entrez/eutils/elink.fcgi?dbfrom=pubmed&id=10196265&retmode=ref&cmd=prlinks%5Cnpapers2://publication/uuid/8A0A05DE-7A35-4FB4-B549-DC29EA1973B6.

Rockman, S. et al. (2013) 'Neuraminidase-Inhibiting Antibody Is a Correlate of Cross-Protection against Lethal H5N1 Influenza Virus in Ferrets Immunized with Seasonal Influenza Vaccine', Journal of Virology, 87(6), pp. 3053–3061. doi: 10.1128/JVI.02434-12.

Rogers, G. N. et al. (1983) 'Single amino acid substitutions in influenza haemagglutinin change receptor binding specificity', Nature, 304(5921), pp. 76–78. doi: 10.1038/304076a0.

Romagnani, S. (2000) 'T-cell subsets (Th1 versus Th2)', Annals of Allergy, Asthma and Immunology, pp. 9–21. doi: 10.1016/S1081-1206(10)62426-X.

Rose, M. A., Zielen, S. and Baumann, U. (2012) 'Mucosal immunity and nasal influenza vaccination', Expert Review of Vaccines, pp. 595–607. doi: 10.1586/erv.12.31.

Rott, R., Becht, H. and Orlich, M. (1974) 'The significance of influenza virus neuraminidase in immunity', Journal of General Virology, 22(1), pp. 35–41. doi: 10.1099/0022-1317-22-1-35.

Russell, R. J. et al. (2004) 'H1 and H7 influenza haemagglutinin structures extend a structural classification of haemagglutinin subtypes', Virology, 325(2), pp. 287–296. doi: 10.1016/j.virol.2004.04.040.

Ryder, A. B. et al. (2016) 'Vaccination with Vesicular Stomatitis Virus-Vectored Chimeric Hemagglutinins Protects Mice against Divergent Influenza Virus Challenge Strains', Journal of Virology, 90(5), pp. 2544–2550. doi: 10.1128/JVI.02598-15.

Sakabe, S. et al. (2011) 'Mutations in PA, NP, and HA of a pandemic (H1N1) 2009 influenza virus contribute to its adaptation to mice', Virus Research, 158(1–2), pp. 124–129. doi: 10.1016/j.virusres.2011.03.022.

Sandbulte, M. et al. (2015) 'Optimal Use of Vaccines for Control of Influenza A Virus in Swine', Vaccines, 3(1), pp. 22–73. doi: 10.3390/vaccines3010022.

Sandbulte, M. R. et al. (2009) 'A miniaturized assay for influenza neuraminidase-inhibiting antibodies utilizing reverse genetics-derived antigens', Influenza and other Respiratory Viruses, 3(5), pp. 233–240. doi: 10.1111/j.1750-2659.2009.00094.x.

Santos, J. J. et al. (2017) 'Development of an alternative modified live Influenza B virus vaccine', J Virol, 91(12), pp. e00056-17. doi: 10.1128/JVI.00056-17.

Schild, G. C., Wood, J. M. and Newman, R. W. (1975) 'A single radial immunodiffusion technique for the assay of influenza haemagglutinin antigen. Proposals for an assay method for the haemagglutinin content of influenza vaccines', Bulletin of the World Health Organization, 52(2), pp. 223–231.

Schulman, J. L. (1969) 'The role of antineuraminidase antibody in immunity to influenza virus infection.', Bulletin of the World Health Organization, 41(3), pp. 647–50. Available at: https://www.ncbi.nlm.nih.gov/pubmed?Db=pubmed&Cmd=Retrieve&list_uids=5309490&dopt=abstractplus.

Schulman, J. L., Khakpour, M. and Kilbourne, E. D. (1968) 'Protective effects of specific immunity to viral neuraminidase on influenza virus infection of mice', J Virol. American Society for Microbiology, 2(8), pp. 778–786. Available at: http://www.ncbi.nlm.nih.gov/pubmed/5701819.

Sellers, R. S. et al. (2012) 'Immunological variation between inbred laboratory mouse strains: Points to consider in phenotyping genetically immunomodified mice', Veterinary Pathology, 49(1), pp. 32–43. doi: 10.1177/0300985811429314.

Shi, Y. et al. (2014) 'Enabling the "host jump": Structural determinants of receptor-binding specificity in influenza A viruses', Nature Reviews Microbiology, pp. 822–831. doi: 10.1038/nrmicro3362.

Shinya, K. et al. (2006) 'Influenza virus receptors in the human airway', Nature, 440(7083), pp. 435–436. doi: 10.1038/440435a.

Simonsen, L. et al. (2013) 'Global Mortality Estimates for the 2009 Influenza Pandemic from the GLaMOR Project: A Modeling Study', PLoS Medicine. Edited by S. I. Hay, 10(11), p. e1001558. doi: 10.1371/journal.pmed.1001558.

Sipo, I. et al. (2011) 'Vaccine protection against lethal homologous and heterologous challenge using recombinant AAV vectors expressing codon-optimized genes from pandemic swine origin influenza virus (SOIV)', Vaccine, 29(8), pp. 1690–1699. doi: 10.1016/j.vaccine.2010.12.037.

Skehel, J. J. and Wiley, D. C. (2000) 'Receptor Binding and Membrane Fusion in Virus Entry: The Influenza Hemagglutinin', Annual Review of Biochemistry, 69(1), pp. 531–569. doi: 10.1146/annurev.biochem.69.1.531.

Smith, W., Andrewes, C. H. and Laidlaw, P. P. (1933) 'A Virus Obtained From Influenza Patients', The Lancet, 222(5732), pp. 66–68. doi: 10.1016/S0140-6736(00)78541-2.

Spearman, C. (1908) 'The Method of "Right and Wrong Cases" ("Constant Stimuli") Without Gauss'S Formulae', British Journal of Psychology, 1904-1920, 2(3), pp. 227–242. doi: 10.1111/j.2044-8295.1908.tb00176.x.

Stachyra, A. et al. (2017) 'A prime/boost vaccination with HA DNA and Pichia-produced HA protein elicits a strong humoral response in chickens against H5N1.', Virus research, 232, pp. 41–47. doi: 10.1016/j.virusres.2017.01.025.

Steel, J. et al. (2010) 'Influenza virus vaccine based on the conserved hemagglutinin stalk domain', mBio, 1(1). doi: 10.1128/mBio.00018-10.

Subbarao, K. and Joseph, T. (2007) 'Scientific barriers to developing vaccines against avian influenza viruses', Nature Reviews Immunology, 7(4), pp. 267–278. doi: 10.1038/nri2054.

Sultana, I. et al. (2014) 'Stability of neuraminidase in inactivated influenza vaccines', Vaccine. Elsevier Ltd, 32(19), pp. 2225–2230. doi: 10.1016/j.vaccine.2014.01.078.

Sutter, G., Ohlmann, M. and Erfle, V. (1995) 'Non-replicating vaccinia vector efficiently expresses bacteriophage T7 RNA polymerase', FEBS Letters, 371(1), pp. 9–12. doi: 10.1016/0014-5793(95)00843-X.

Swayne, D. E. (2007) 'Understanding the Complex Pathobiology of High Pathogenicity Avian Influenza Viruses in Birds', Avian Diseases, 51(s1), pp. 242–249. doi: 10.1637/7763-110706-REGR.1.

Swayne, D. E. and Suarez, D. L. (2000) 'Highly pathogenic avian influenza.', Revue scientifique et technique (International Office of Epizootics), 19(2), pp. 463–82. Available at: http://www.ncbi.nlm.nih.gov/pubmed/10935274.

Sylte D. L., M. J. . S. (2009) 'Influenza neuraminidase as a vaccine antigen', Curr Top Microbiol Immunol, 333, pp. 227–241. doi: 10.1007/978-3-540-92165-3_12.

Sylte, M. J., Hubby, B. and Suarez, D. L. (2007) 'Influenza neuraminidase antibodies provide partial protection for chickens against high pathogenic avian influenza infection', Vaccine, 25(19), pp. 3763–3772. doi: 10.1016/j.vaccine.2007.02.011.

Tang, X. et al. (2017) 'Recombinant Adenoviruses Displaying Matrix 2 Ectodomain Epitopes on Their Fiber Proteins as Universal Influenza Vaccines', Journal of Virology, 91(7), pp. e02462-16. doi: 10.1128/JVI.02462-16.

Tao, W. et al. (2017) 'Consensus M2e peptide conjugated to gold nanoparticles confers protection against H1N1, H3N2 and H5N1 influenza A viruses', Antiviral Research, 141, pp. 62–72. doi: 10.1016/j.antiviral.2017.01.021.

Tong, S. et al. (2012) 'A distinct lineage of influenza A virus from bats', Proceedings of the National Academy of Sciences, 109(11), pp. 4269–4274. doi: 10.1073/pnas.1116200109.

Tong, S. et al. (2013) 'New World Bats Harbor Diverse Influenza A Viruses', PLoS Pathogens. doi: 10.1371/journal.ppat.1003657.

Turley, C. B. et al. (2011) 'Safety and immunogenicity of a recombinant M2e-flagellin influenza vaccine (STF2.4xM2e) in healthy adults', Vaccine, 29(32), pp. 5145–5152. doi: 10.1016/j.vaccine.2011.05.041.

Ungchusak, K. et al. (2005) 'Probable Person-to-Person Transmission of Avian Influenza A (H5N1)', New England Journal of Medicine, 352(4), pp. 333–340. doi: 10.1056/NEJMoa044021.

Valero-Pacheco, N. et al. (2016) 'Antibody Persistence in Adults Two Years after Vaccination with an H1N1 2009 Pandemic Influenza Virus-Like Particle Vaccine', PLOS ONE. Edited by F. Krammer, 11(2), p. e0150146. doi: 10.1371/journal.pone.0150146.

Valkenburg, S. A. et al. (2016) 'Stalking influenza by vaccination with pre-fusion headless HA mini-stem', Scientific Reports, 6(1), p. 22666. doi: 10.1038/srep22666.

Vander Veen, R. L. et al. (2012) 'Safety, immunogenicity, and efficacy of an alphavirus replicon-based swine influenza virus hemagglutinin vaccine', Vaccine, 30(11), pp. 1944–1950. doi: 10.1016/j.vaccine.2012.01.030.

Vander Veen, R. L. et al. (2013) 'Haemagglutinin and nucleoprotein replicon particle vaccination of swine protects against the pandemic H1N1 2009 virus', Veterinary Record, 173(14), p. 344. doi: 10.1136/vr.101741.

Walz, L. et al. (2018) 'Sialidase-Inhibiting Antibody Titers Correlate with Protection from Heterologous Influenza Virus Strains of the Same Neuraminidase Subtype.', Journal of virology. American Society for Microbiology, p. JVI.01006-18. doi: 10.1128/JVI.01006-18.

Wan, H. et al. (2013) 'Molecular Basis for Broad Neuraminidase Immunity: Conserved Epitopes in Seasonal and Pandemic H1N1 as Well as H5N1 Influenza Viruses', Journal of Virology, 87(16), pp. 9290–9300. doi: 10.1128/JVI.01203-13.

Wan, H. et al. (2015) 'Structural characterization of a protective epitope spanning A(H1N1)pdm09 influenza virus neuraminidase monomers', Nature Communications, 6(1). doi: 10.1038/ncomms7114.

Webster, R. G. et al. (1992) 'Evolution and ecology of influenza A viruses.', Microbiological reviews, 56(1), pp. 152–79. doi: 10.1111/j.1541-0420.2008.01180.x.

Wesley, R. D., Tang, M. and Lager, K. M. (2004) 'Protection of weaned pigs by vaccination with human adenovirus 5 recombinant viruses expressing the hemagglutinin and the nucleoprotein of H3N2 swine influenza virus', Vaccine, 22(25–26), pp. 3427–3434. doi: 10.1016/j.vaccine.2004.02.040.

Westgeest, K. B. et al. (2015) 'Optimization of an enzyme-linked lectin assay suitable for rapid antigenic characterization of the neuraminidase of human influenza A(H3N2) viruses.', Journal of virological methods, 217, pp. 55–63. doi: 10.1016/j.jviromet.2015.02.014.

Whittle, J. R. R. et al. (2011) 'Broadly neutralizing human antibody that recognizes the receptor-binding pocket of influenza virus hemagglutinin', Proceedings of the National Academy of Sciences, 108(34), pp. 14216–14221. doi: 10.1073/pnas.1111497108.

Wiley, D. (1987) 'The Structure And Function Of The Hemagglutinin Membrane Glycoprotein Of Influenza Virus', Annual Review of Biochemistry, 56(1), pp. 365–394. doi: 10.1146/annurev.biochem.56.1.365.

Wilson, J. R. et al. (2016) 'An influenza A virus (H7N9) anti-neuraminidase monoclonal antibody with prophylactic and therapeutic activity in vivo', Antiviral Research, 135, p. 48. doi: 10.1016/j.antiviral.2016.10.001.

Wohlbold, T. J. et al. (2015) 'Vaccination with Adjuvanted Recombinant Neuraminidase Induces Broad Heterologous, but Not Heterosubtypic, Cross-Protection against Influenza Virus Infection in Mice', mBio, 6(2), p. e02556. doi: 10.1128/mBio.02556-14.

Wohlbold, T. J. et al. (2016) 'Hemagglutinin Stalk- and Neuraminidase-Specific Monoclonal Antibodies Protect against Lethal H10N8 Influenza Virus Infection in Mice.', Journal of virology, 90(2), pp. 851–61. doi: 10.1128/JVI.02275-15.

Wohlbold, T. J. et al. (2017) 'Broadly protective murine monoclonal antibodies neuraminidase epitopes', Nature Microbiology, 2(October), p. 1415. doi: 10.1038/s41564-017-0011-8.

Wohlbold, T. J. and Krammer, F. (2014) 'In the shadow of hemagglutinin: A growing interest in influenza viral neuraminidase and its role as a vaccine antigen', Viruses, 6(6), pp. 2465–2494. doi: 10.3390/v6062465.

Wood, J. M. and Levandowski, R. A. (2003) 'The influenza vaccine licensing process', Vaccine, pp. 1786–1788. doi: 10.1016/S0264-410X(03)00073-2.

World Organization for animal health (2015) Manual of Diagnostic Tests and Vaccines for Terrestrial Animals. Available at: http://www.oie.int/standard-setting/terrestrial-manual/access-online/ (Accessed: 23 July 2018).

Wright, P. F., Neumann, G. and Kawaoka, Y. (2007) 'Orthomyxoviruses', in Fields Virology 5th Edition.

Wu, Y. Y. et al. (2014) 'Bat-derived influenza-like viruses H17N10 and H18N11', Trends in Microbiology. Elsevier Ltd, 22(4), pp. 183–191. doi: 10.1016/j.tim.2014.01.010.

Xu, L. et al. (2013) 'The mouse and ferret models for studying the novel avian-origin human influenza A (H7N9) virus', Virology Journal, 10(1), p. 253. doi: 10.1186/1743-422X-10-253.

Yang, S. gui et al. (2009) 'Construction and cellular immune response induction of HA-based alphavirus replicon vaccines against human-avian influenza (H5N1)', Vaccine, 27(52), pp. 7451–7458. doi: 10.1016/j.vaccine.2009.05.014.

Yoshida, R. et al. (2009) 'Cross-Protective Potential of a Novel Monoclonal Antibody Directed against Antigenic Site B of the Hemagglutinin of Influenza A Viruses', PLoS Pathogens. Edited by P. Palese, 5(3), p. e1000350. doi: 10.1371/journal.ppat.1000350.

Zimmer, G. (2010) 'RNA replicons - A new approach for influenza virus immunoprophylaxis', Viruses, 2(2), pp. 413–434. doi: 10.3390/v2020413.

Zimmer, G. et al. (2014) 'Pseudotyping of vesicular stomatitis virus with the envelope glycoproteins of highly pathogenic avian influenza viruses.', The Journal of general virology, 95(Pt 8), pp. 1634–9. doi: 10.1099/vir.0.065201-0.

Zimmerman, R. K. et al. (2016) '2014-2015 Influenza Vaccine Effectiveness in the United States by Vaccine Type', Clinical infectious diseases : an official publication of the Infectious Diseases Society of America, 63(12), pp. 1564–1573. doi: 10.1093/cid/ciw635.

# ABBREVIATIONS

| | |
|---|---|
| 4-MU | 4-methylumbelliferone |
| AAV | Adeno-associated virus |
| Ab | antibody |
| ADCC | antibody-dependent cell-mediated cytotoxicity |
| AS | anti-sense |
| BHK G43 | genetically modified BHK-21 cells that provide the VSV G protein in trans |
| BHK-21 | baby hamster kidney cells |
| BPL | beta propiolactone |
| CDC | complement-dependent cytotoxicity |
| CDV | canine distemper virus |
| cHA | chimeric HA |
| COBRA | Computationally Optimized Broadly Reactive Antigen |
| ConA | Concanavalin A |
| DNA | deoxyribonucleic acid |
| eGFP | enhanced green fluorescence protein |
| ELISpot | Enzyme-Linked ImmunoSpot |
| ELLA | Enzyme-linked lectin assay |
| EMA | European Medicines Agency |
| EMEA | European Medicines Evaluation Agency |
| FBS | fetal bovine serum |
| HA/H | hemagglutinin |
| HA/HI | hemagglutination/ hemagglutination inhibition assay |
| HAU | hemagglutination units |
| HPAI | highly pathogenic avian influenza |
| HRP | horseradish peroxidase |
| i.m. | intramuscularly |
| i.n. | intranasally |
| IAV | influenza A virus |
| IFNγ | interferon gamma |
| IIV | inactivated influenza vaccine |
| IL-2 | interleukin-2 |
| IPMA | immunoperoxidase monolayer assay |
| IPMA | Immunoperoxidase-monolayer-assay |
| LAIV | live-attenuated influenza vaccine |
| LDL | low density lipoprotein |
| LPAI | low pathogenic avian influenza |
| M1/M2 | matrix portein 1/2 |
| M2e | extracellular domain of M2 |
| MAb | monoclonal antibodies |
| MDCK | Madin-Darby canine kidney |
| MOI | multiplicity of infection |
| MUNANA | 2'-(4-Methylumbelliferyl)-α-D-N-acetylneuraminic acid (MUNANA) |
| MVA | modified vaccinia virus Ankara |
| MVA-T7 | recombinant vaccinia virus expressing the T7 phage RNA polymerase |
| NA/N | neuraminidase |
| NDV | Newcastle Disease Virus |
| NEP | nuclear export protein |

| | |
|---|---|
| NI | neuraminidase-inhibiting |
| NP | nucleoprotein |
| NS1/NS2 | non-structural protein ½ |
| NT | nasal turbinates |
| NT | nasal turbinates |
| OPD | o-phenylenediamine dihydrochloride |
| p.i. | post-infection |
| PA | polymerase acid |
| PB1 | polymerase basic 1 |
| PB2 | polymerase basic 2 |
| PBMC | Peripheral blood mononuclear cell |
| PBS | Phosphate-buffered saline |
| PCR | polymerase chain reaction |
| pdmH1N1 | pandemic H1N1 from 2009 |
| PR8 | A/Puerto Rico/8/34 (H1N1) |
| RBC | red blood cell |
| RNA | ribonucleic acid |
| S | sense |
| SA | sialic acid |
| SDS-PAGE | Sodium Dodecyl Sulfate-Polyacrylamide Gel Electrophoresis |
| SeV | Sendai virus |
| ss | single-stranded |
| TBS | Tris-buffered saline |
| TCID50 | |
| Th | T helper cells |
| TPCK-trypsin | tosylsulfonyl phenylalanyl chloromethyl ketone-treated trypsin |
| U | unit |
| VLP | virus-like particle |
| VN | virus neutralizing |
| vRNP | viral ribonucleoprotein |
| VSV | vesicular stomatitis virus |
| VSV G | VSV glycoprotein |
| VSV L | VSV large polymerase |
| VSV M | VSV matrix protein |
| VSV N | VSV nucleoprotein |
| VSV P | VSV phosphoprotein |
| WHO | World Health Organization |

# LIST OF FIGURES AND TABLES

# DECLARATION OF AUTHORSHIP

I hereby certify that I have written the present dissertation with the topic:

Generation and Evaluation of

universal influenza vaccine candidates

independently, using no other aids then those I have cited. I have clearly mentioned the source of the passages that are taken word for word or paraphrased from other works.

The presented thesis has not been submitted in this or any other form to another faculty or examination institution.

## Eidesstattliche Versicherung

Hiermit versichere ich, dass ich die vorgelegte Dissertation mit dem Titel

Generation and Evaluation of

universal influenza vaccine candidates

selbstständig verfasst habe und keine anderen als die angegebenen Quellen und Hilfsmittel verwendet habe. Die Stellen der Dissertation, die anderen Werken und Veröffentlichungen dem Wortlaut oder dem Sinn nach entnommen wurden, sind durch Quellenangaben gekennzeichnet.

Diese Dissertation wurde in der jetzigen oder in ähnlicher Form noch an keiner anderen Hochschule eingereicht und hat noch keinen sonstigen Prüfungszwecken gedient.

Mainz, 27.07.2018

# ACKNOWLEDGEMENTS

# CURRICULUM VITAE

*...I'm still confused, but on a higher level.*

— Enrico Fermi —